MURDOCH
UNIVERSITY
PERTH, WESTERN AUSTRALIA

School of Veterinary and Life Science

Honours Thesis

Characterisation of miR-494 in coagulation

Wing Lui (32039827)

Supervisor:

Dr. Jasmine Tay

Associate Professor Robert J. Mead

Examiners:

Associate Professor Mark Watson

Dr. Dave Berryman

Table of Contents

Chapter 2: Materials

Chapter 3: Methods

Declaration

I declare this thesis is my own account of my research and contains as its main content work which has not been previously submitted for a degree at any tertiary education institution.

…….

Wing Lui

Acknowledgements:

Frist of all, I cannot imagine how much I have done this year. However, I would like to acknowledge these people who have helped me a lot throughout the year. I definitely cannot finish this thesis without their help and advice.

Firstly, I would like to thank my supervisor, Dr. Jasmine Tay, for providing support in my study and research. She gave me a lot of advice on writing the literature review, this thesis and also the presentation in HAA 2015 (Haematology Society of Australia and New Zealand, the Australian & New Zealand Society of Blood Transfusion and the Australasian Society of Thrombosis and Haemostasis). I apologise that I made some silly mistakes in the beginning of the year but she remained very patient, therefore, she is a very good supervisor. Also, thank you for all the encouragement and support throughout the year.

Besides my supervisor, I would like to thank the members in the WACTH team, Dr. Jim Tiao, Dr. Quintin Hughes and Prof. Ross Baker. They also gave me a lot of valuable comments in my thesis and oral presentation in HAA. Thanks for giving me an opportunity to go to the HAA conference (also thanks to ASTH) and it is a very nice experience. I am glad that I can be one of the members in the WACTH team.

Also, I thank the staff working in IIID, Prof. Mark Watson, Prof. Abha Chopra, Ms. Geraldine Lau and Mr. John Blinco. They gave me some advice in my research and also answered some technical questions that I had.

Special thanks to my lecturers and chairs in my university life, Prof. Robert Mead, Dr. Wayne Greene, Dr. Garth Maker and Dr. Jason Terpoilli. Without their encouragement, I would not have considered studying Honours. I would like to say I have learnt a lot in this year and thanks for all your hard work in my university life.

Last but not least, I would like to thank my parents and my brother for supporting me throughout this year and all your hard work to send me to Perth.

List of figures

List of tables

Abbreviations

h	hours
α	Alpha
α2AP	alpha 2 antiplasmin
β	Beta
ɣ	Gamma
20α-HSD	20α-hydroxsteroid dehydrogenase
ACTB	Beta-Actin
ADAMTS13	A Disintegrin and Metalloproteinase with a ThromboSpondin Type 1 motif, member 13
ADP	Adenosine diphosphate
AKT	Protein kinase B
AP1	Activator protein 1
C4BP	C4b-binding protein
C4BPA	C4b-binding protein α
CCP	Complement control protein
DGCR8	DiGeorge critical region 8
DMEM	Dulbecco's Modified Eagle Medium
E_2	oestrogen
ECL	Enhanced chemiluminescence
EGF-like	Epidermal growth factor-like
ERα	Estrogen receptor alpha
F3	Tissue factor gene
FCS	Fetal calf serum
FV	Factor V
FVII	Factor VII
FVIII	Factor VIII
FIX	Factor IX

FX	Factor X
FXI	Factor XI
FXII	Factor XII
FXIII	Factor XIII
GAPDH	Glyceraldehyde 3-phosphate dehydrogenase
GLA	Gamma- carboxyglutamic acid
GP	Glycoprotein
JNK	Jun NH_2-terminal kinase
JUN	Activator protein 1 gene
LB	Lysogeny broth
miRNA	Micro-ribonucleic acid
miR-NC	Negative control micro-ribonucleic acid
miR-494	Micro-ribonucleic acid 494
NaPyr	Sodium pyruvate
NEAA	Non-essential amino acids solution
PAI-1	Plasminogen activator inhibitor-1
PCI	Protein C inhibitor
PLG	Plasminogen
pre-miRNA	Precursor-miRNA
PROS1	Protein S gene
PS	Protein S
PTM	Post-translational modification
RISC	RNA-induced silencing complex
RT-qPCR	Real-time Quantitative Polymerase Chain Reaction
SHBG	Sex hormone binding globulin
SDS-PAGE	Sodium dodecyl sulphate polyacrylamide gel electrophoresis
SP1	Specificity protein 1

STAT	Signal transducer and activator of transcription
t-PA	Tissue-type plasminogen activator
TAFI	Thrombin activatable fibrinolysis inhibitor
TF	Tissue factor
TFPI	Tissue factor pathway inhibitor
TFPI2	Tissue factor pathway inhibitor 2
THBS1	Thrombospondin 1
TM	Thrombomodulin
TSR	Thrombin-sensitive region
TXA_2	Thromboxane A2
u-PA	urokinase-type plasminogen activator
VWF	Von Willebrand Factor

Abstract:

Micro-ribonucleic acids (miRNAs) are non-coding RNAs that, in the majority of cases, regulate gene expression by binding to the 3' untranslated region (UTR) sequence of target mRNAs to cause decreased mRNA levels. Recently, several studies showed that selected miRNAs also target important genes in coagulation and haemostasis. The miRNA, miR-494, downregulates Protein S (PS) mRNA levels by binding to the 3'UTR sequence of *PROS1* mRNA transcript. Further study demonstrated that some coagulation factors without predicted miR-494 binding sites in their 3'UTR sequences showed significant changes in their mRNA levels, including plasminogen (*PLG*), tissue factor (*F3*) and C4BPα (*C4BPA*). It is possible that miR-494 directly targets transcriptional activators or repressors to indirectly regulate the expression of those coagulation factors lacking predicted miR-494 binding sites. This current study hypothesised that miR-494 has an important role in regulating coagulation pathways and haemostasis by targeting multiple coagulation factor genes via direct and indirect mechanisms. HuH-7 cells were transfected with miR-494 for 48h and 72h followed by mRNA and protein analysis. Direct interaction between miR-494 and transcription factor 3'UTRs (*JUN, SP1* and *STAT5B* 3'UTRs) was determined using dual-luciferase reporter assays. The mRNA and protein levels of PS and PLG was significantly downregulated, and the C4BPA mRNA and protein levels were upregulated with the presence of miR-494. Moreover, the protein level of tissue factor (TF) was decreased at 72h post-transfection but no changes were found in its mRNA levels. Computational analyses showed that predicted miR-494 binding sites were found in the *JUN, SP1* and *STAT5B* 3'UTRs. Dual luciferase reporter assay confirmed the presence of functional miR-494 binding sites in the 3'UTR sequence of *SP1* and *STAT5B*. The *SP1* and *STAT5B* mRNA levels were significantly downregulated with the presence of miR-494 but no change was observed for the *JUN* mRNA levels. Computational analysis showed that a predicted Sp1 binding site was found in the promoter region of human *PLG* gene. A report by Gutierrez-Fernandez *et. al.* (2007) suggested that Sp1 acts as a transcriptional activator in the murine *PLG* promoter. These suggested that miR-494 may indirectly downregulate PLG expression by targeting Sp1. Taken together, miR-494 directly downregulates PS expression, and

indirectly downregulates PLG expression through Sp1 repression and upregulates C4BPA expression. These results suggested that miR-494 has a prothrombotic effect.

Chapter 1: Introduction

1.1 Introduction:

The average life-expectancy together with the world population has increased dramatically during the 20th century (Hunter and Fineberg, 2014). Non-communicable diseases, including cancer, chronic respiratory disease and liver disease, are major contributors to the fatal burden and disability worldwide, with cardiovascular disease being the leading cause of death (GBD 2013 Mortality and Causes of Death Collaborators, 2015). Cardiovascular diseases, such as ischaemic stroke and venous thromboembolism, are caused by imbalances in haemostasis (blood coagulation) leading to thrombosis, which is the formation of a blood clot (thrombus) in the blood vessel obstructing blood flow through the circulation.

Platelet activation and activation of the coagulation cascade are complex haemostatic mechanisms that are tightly regulated by different coagulation activators and inhibitors. Under normal physiological conditions, haemostasis acts in response to vascular injury to prevent unnecessary blood loss from damaged vessels. Thrombosis prevention, however, involves careful control of preventing excessive clot formation and clot dissolution. Increasingly, evidence suggests additional layers of complexity in the regulation of blood clotting and development of thrombotic disease to involve new players, such as microparticles and micro-ribonucleic acids.

1.2 Haemostasis:

Haemostasis is a normal physiological response for preventing blood loss from injured blood vessels and repairing the damaged endothelium. Aberrant blood clotting and disturbed platelet activity can cause uncontrolled blood loss leading to severe haemorrhage or increased clotting resulting in thrombosis. Haemostasis consists of two major phases, primary (platelet activation) and secondary (coagulation cascade) haemostasis. Platelets are involved in both phases of the haematological response.

Platelets are blood circulating anucleate discoid cells (~4μm diameter and ~1μm thick) responsible for blood clot formation. They are generated from the cytoplasm of their precursor cells, mature megakaryocytes, which are enormous cells (50-100μm in diameter) with large nuclei produced in the bone marrow. Platelets are continuously replaced and the average normal platelet lifespan is about 9 to 12 days (Martini and Nath, 2009). The formation of platelets and the rate of megakaryocyte activity are stimulated by (1) thrombopoietin, a peptide hormone generated in the kidneys; (2) interleukin-6, a hormone that stimulates platelet formation; and (3) multi-CSF, a cytokine that promotes the growth of megakaryocytes. Platelets have three important glycoprotein receptors, glycoprotein (GP) Ib-V-IX complex, GPVI and GPIIb/IIIa. These receptors are responsible for the detection of exposed subendothelial matrix to activate platelets in response to endothelial injury (Clemetson, 2012).

1.2.1 Primary haemostasis: Platelet Activation and aggregation

Platelet activation and aggregation constitutes primary haemostasis (Figure 1.1). The first phase of primary haemostasis, also known as adhesion, acts to slow down moving platelets in the plasma which enables interaction with the exposed matrix. The major molecular response to this process includes Von Willebrand Factor (VWF) and the platelet receptors – GPIb-V-IX, GPIIb-IIIa and GPVI (Adams and Bird, 2009). VWF is another important component in haemostasis, which participates in platelet adhesion, aggregation and coagulation. VWF is a large multimeric glycoprotein consisting 2-80 subunits linked by disulphide bridges. The larger multimeric glycoproteins are stored in Weibel-Palade bodies (endothelial cells) or alpha granules (platelets). The smaller multimeric glycoproteins are constitutively secreted by megakaryocytes and endothelial cells. In the coagulation cascade, binding sites for VWF are present in collagen, GPIb, GPIIb/IIIa and Factor VIII. Multimeric VWFs enhance platelet aggregation and the large VWF multimer is regulated through continuous cleavage by A Disintegrin and Metalloproteinase with a ThromboSpondin Type 1

motif, member 13 (ADAMTS13); an important process in preventing aberrant thrombosis (Sadler, 1998).

In adhesion, VWF circulating in plasma binds to specific sites on the exposed matrix. This allows the GPIb-V-IX receptor complex on platelets to interact with the A1 domains within VWF, inducing platelet activation (Ruggeri, 1997; Ruggeri, 2003). This is achieved through platelet GPVI receptors binding to collagen and the direct interaction to the exposed matrix (Sugiyama *et. al.*, 1987). Activated platelets then release a coagulation factor, thrombin, which has an important role in secondary haemostasis. In addition, activated platelets also secrete multiple molecules, including thromboxane A2 (TXA_2); fibrinogen, VWF and Factor V (FV) from alpha granules; and adenosine diphosphate (ADP) from dense granules, to recruit more platelets and accelerate the aggregation process (Weiss, 1975; Hamberg *et. al.*, 1975; Harrison and Cramer, 1993).

Platelet aggregation constitutes an important step in platelet plug formation and haemostasis. The release of TXA_2, and molecules from alpha and dense granules creates a positive feedback loop to activate other platelets nearby; the ADP molecules bind to both $P2Y_1$ and $P2Y_{12}$ receptors and the TXA_2 molecules bind to thromboxane receptors (TPα) on the platelet membrane (Cattaneo *et. al.*, 2002). Thrombin also binds to proteinase-activated receptor (PAR) 1 and PAR4 receptors on the platelet membrane to activate other platelets (Ramakrishnan *et. al.*, 2001). Platelet activation induces morphological changes, from biconvex discoid to irregular with multiple filopodial extensions caused by increased intracellular calcium ions. The morphological change in activated platelets increases their ability to interact and adhere to neighbouring platelets due to the increased surface area (Clemetson, 2012). During aggregation, platelet activation changes the GPIIb/IIIa receptors from an inactive to active state. Fibrinogen and VWF act as bridges between two GPIIb/IIIa receptors on neighbouring activated platelets. The interaction between fibrinogen, VWF and

GPIIb/IIIa receptors, as well as the shape changes in activated platelets, results in the formation of a stable platelet plug (Bennett, 2005).

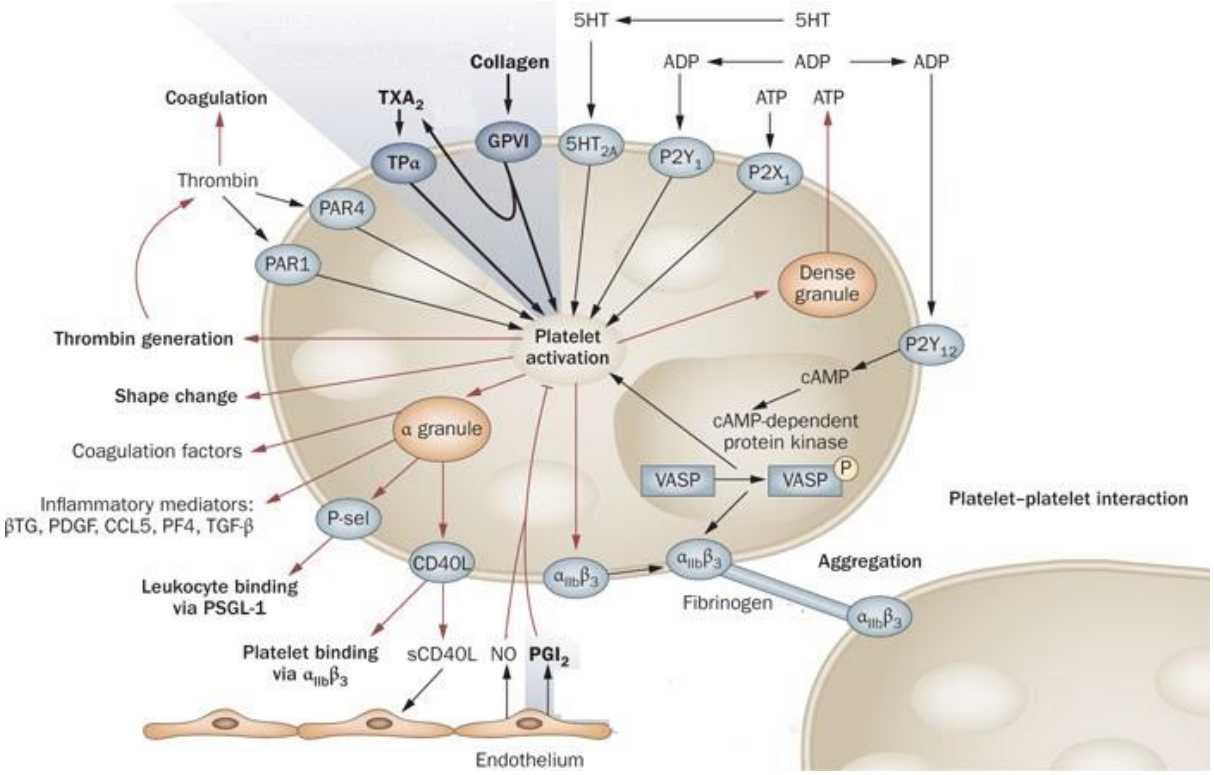

Figure 1.1. Factors and receptors involved in platelet activation (Pignone and Williams, 2010).

1.2.2 Secondary haemostasis: coagulation cascade

The coagulation cascade was first described in 1964 (Davie and Ratnoff, 1964; Macfarlane, 1964), which highlighted the stepwise activation of zymogens that ultimately results in the conversion of fibrinogen into fibrin to form a clot. This traditional model indicated that these series of reactions followed either intrinsic (initiated by contact system) or extrinsic (initiated by tissue factor) pathway. These two pathways result in the activation of Factor X (FX) and the conversion of prothrombin into thrombin. However, this traditional model is no longer deemed to be the most accurate model in physiology. Østerud and Raparort (1977) argued that the intrinsic and extrinsic pathways of the coagulation cascade are not separate because the TF/FVIIa complex is able to activate Factor IX (FIX) in the intrinsic pathway. Clinical studies have found that patients with Factor XII (FXII) deficiency do not suffer severe haemorrhage in

comparison to patients with FIX deficiency (Hoffbrand and Pettit, 1993). As such, the coagulation cascade is a far more complex process than the simple pathway that was originally described. More anticoagulant proteins, such as Protein C and tissue factor pathway inhibitor (TFPI), and the fibrinolysis pathway were discovered after the description of the traditional model. Currently, the contemporary model of coagulation cascade includes initiation, amplification and propagation phases. Compared to the traditional model, the contemporary model suggests that the coagulation cascade is initiated by tissue factor (TF) and acts to further enhance the effects of TF in the amplification phase (Camerer *et. al.*, 1996).

1.2.2.1 Initiation and amplification phases

TF is a transmembrane glycoprotein and a member of the class II cytokine receptor family. It is constitutively expressed in the vascular adventitia and membrane exposed after vessel injury. It is also highly expressed in heart, lungs, kidneys and brain. It has important roles in inflammation, apoptosis, embryonic development, cell migration and coagulation. The coagulation cascade is initiated by the release of TF from the vascular adventitia, known as initiation phase or TF pathway or extrinsic pathway (Figure 1.2). TF also functions as a cofactor for Factor VII (FVII) to activate FVII and cause the TF/FVIIa complex formation. The TF/VIIa complex activates FX. FXa and thrombin activate FV to cause the formation of prothrombinase complex through the interaction of FXa and FVa (Monkovict and Tracy, 1990; Schuijt *et. al*., 2013). The prothrombinase complex activates prothrombin, however, this can only produce small amounts of thrombin. Compared to the initiation phase, the amplification phase, which is also known as contact activation or intrinsic pathway, can increase FXa production by 50 to 100 times to accelerate thrombin production (Lawson and Mann, 1991; Ahmad *et. al.*, 1992; Mann *et. al.*, 1992). In the amplification phase, the TF/FVIIa complex activates Factor IX (FIX); while thrombin activates FV, FIX and Factor VIII (FVIII). The formation of FIXa/FVIIIa complex by the binding of FIXa and FVIIIa activates FX and produces

more thrombin (Camerer *et. al.*, 1996). These activated coagulation factors create a positive feedback loop and results in a rapid generation of thrombin and platelet activation.

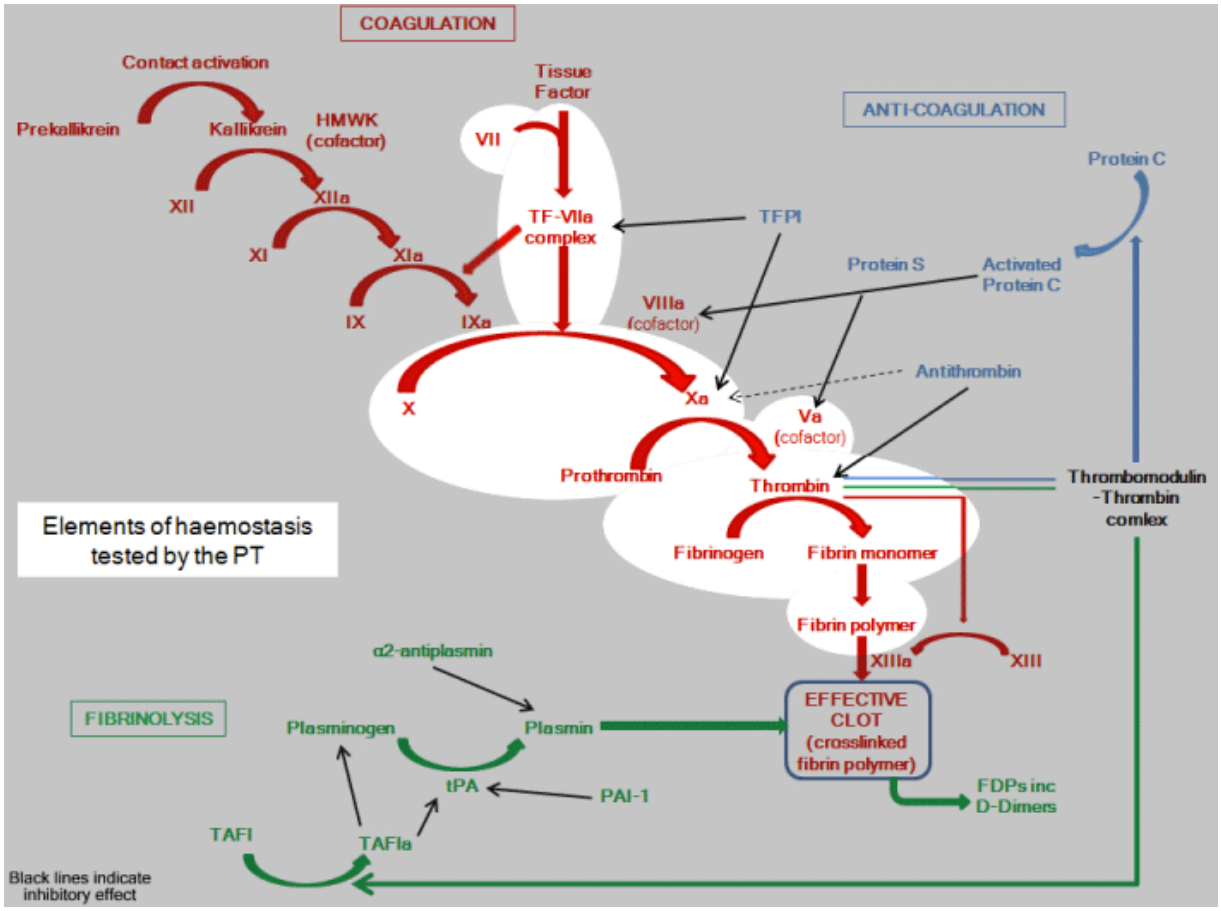

Figure 1.2. Coagulation cascade and its regulatory proteins (Long Road Graphics Inc, 2012).

1.2.2.2 Propagation phase

The propagation phase, also known as the final common pathway, is the last phase of the coagulation cascade for blood clot formation. Fibrinogen is a hexamer composed of two sets of three polypeptides (Aα, Bβ and γ), encoded by *FGA, FGB* and *FGG* genes, respectively, and linked together by disulphide bonds (Fish and Neerman-Arbez, 2012). It is the precursor of fibrin, and a key component of blood clot formation by acting as bridges for platelets. The efficiency of blood clot depends on optimum thrombin generation by (1) activated platelets; (2) other essential components in coagulation, such as calcium; (3) coagulation factors involved

in the amplification phase; (4) and the prothrombinase complex. The result of the “thrombin burst” generated from the amplification phase results in a large amount of fibrinogen converted into fibrin and the activation of Factor XIII (FXIII). An effective, stable clot requires coalescing a large amount of fibrin monomers to form fibrin polymers, which are generated from the interactions between cross-linked fibrin polymers and active FXIII (FXIIIa). The clot stability can be affected by various factors, including pH, calcium concentration, thrombin concentration, platelet numbers and the density of the fibrin network (Adams and Bird, 2009).

1.2.2.3 Fibrinolysis

Fibrinolysis is essential for removing the blood clot produced by activated coagulation (Figure 1.2). It is highly regulated to ensure haemostasis is maintained. Plasmin is activated by plasminogen, a circulating proenzyme, which is activated by either tissue-type plasminogen activator (t-PA) or urokinase-type plasminogen activator (u-PA) (Hoylaerts *et. al.*, 1982). These two serine proteases have a very short half-life because of high concentration of plasminogen activator inhibitor-1 (PAI-1), an inhibitor of t-PA and u-PA, presented in the circulation. t-PA is synthesised and secreted by endothelial cells; and u-PA is secreted from various cell types, such as monocytes, macrophages and urinary epithelium. The activation of plasmin results in cleavage of cross-linked fibrin and production of fibrin degradation products, such as, D-dimer. In addition to PAI-1, alpha 2 antiplasmin (α2AP) and Thrombin Activatable Fibrinolysis Inhibitor (TAFI) also negatively regulate the fibrinolysis. α2AP inhibits plasmin under normal physiological conditions, however, α2AP is unable to bind to plasmin while plasmin is bound to fibrin in fibrinolysis. Moreover, thrombin activates TAFI to protect the clot from being removed by plasmin. TAFI downregulates fibrinolysis by removing an important binding site in plasminogen, fibrin C-terminal residues, and reduces the effectiveness of plasmin-mediated clot lysis (Chapin and Hajjar, 2015).

1.2.3 Regulation of coagulation cascade

Regulation of the coagulation cascade is essential for preventing excessive thrombin and fibrin production. At least four major regulatory proteins have been described in the coagulation cascade, including antithrombin, TFPI, Protein C and Protein S (PS) (Figure 1.2).

1.2.3.1 Anticoagulation factors

Antithrombin, also known as antithrombin III, is a serine protease inhibitor and is an important inhibitor of coagulation. It is constitutively activated to degrade multiple procoagulation factors, including thrombin, FVIIa, FIXa, FXa and FXIa. Another inhibitor in the coagulation cascade is TFPI, a single chain polypeptide. TFPI is an endogenous inhibitor of the coagulation cascade, which inactivates both the TF/FVIIa complex and FXa (Sandset and Abildgaard, 1991). It circulates in the blood stream by binding to low-density lipoprotein, and is generated by endothelium and platelets. Therefore, antithrombin and TFPI are the regulators in coagulation and prevent the development of thrombosis (Adams and Bird, 2009).

1.2.3.2 Anticoagulation Protein C Pathway

Anticoagulation Protein C pathway is important for regulating coagulation and preventing thrombosis. Thrombin is activated through a series of reactions in the initiation and amplification phases of coagulation (Figure 1.3I). Thrombin binds to epidermal growth factor (EGF) domains 5 and 6 of thrombomodulin (TM). This allows the interaction between endothelial Protein C receptor (EPCR) and Protein C. EPCR binds to the Gla domain of Protein C and stimulates Protein C activation (APC) (Figure 1.3II). Protein S (PS) acts as a cofactor of APC and degrades FVa and by cleaving FVa heavy chains, where FVIIIa is degraded by APC through the stimulation of FV and PS (Figure 1.3III) (Dahlback, 1991; Dahlback and Villoutreix, 2005).

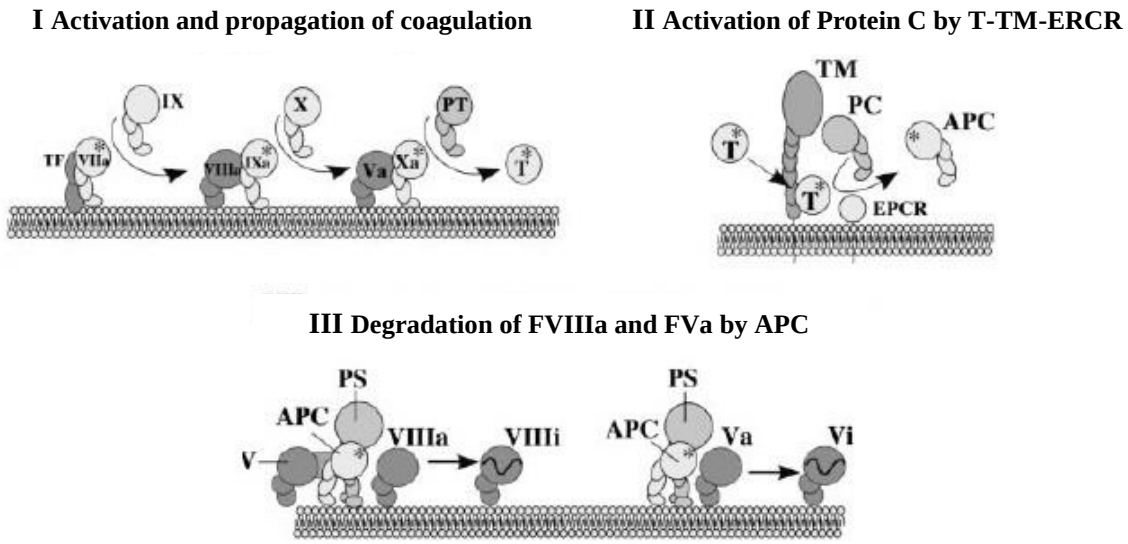

Figure 1.3. The anticoagulation Protein C pathway (Dahlback and Villoutreix, 2005).

Protein S (PS), encoded by *PROS1* gene, is a non-enzymatic vitamin K-dependent plasma protein and is primarily synthesised by hepatocytes (Fair and Marlar, 1986). It acts as a cofactor of APC to degrade FVa and FVIIIa, and inhibit thrombin formation (Figure 1.3III) (Fay and Walker, 1989). PS is a mosaic protein with four different functional domains, including a gamma-carboxyglutamic acid (GLA), a thrombin-sensitive region (TSR), four epidermal growth factor-like (EGF-like) modules and a sex hormone binding globulin (SHBG)-like domain (Vehar and Davie, 1980).

C4b-binding protein (C4BP), encoded by *C4BPA* and *C4BPB* genes, is a large, spider-like structured glycoprotein which contains seven α chains, an unique β chain and a central core to hold these chains together by disulphide bonds. Each α chain consists of eight complement control protein (CCP) domains, whereas the β chain contains three CCP domains and a PS binding site (Goldsby *et. al.*, 2000). Approximately 30% to 40% of PS in plasma is free circulating PS, and the remaining PS is bound to the C4BP β-chain to generate the C4BP-PS complex (Goldsby *et. al.*, 2000). When in the complex with C4BP, PS is not functional in the

anticoagulation Protein C pathway and loses its ability to interact with tyrosine kinase receptors (Evenas *et. al.*, 2000). However, the C4BP-PS complex remains functional in the complement system because the α-chains are not affected by PS. Therefore, a very strong interaction between PS and the β-chain of C4BP allows indirect regulation of the coagulation cascade (Figure 1.4) (Taylor *et. al.*, 1995; Linse *et. al.*, 1997).

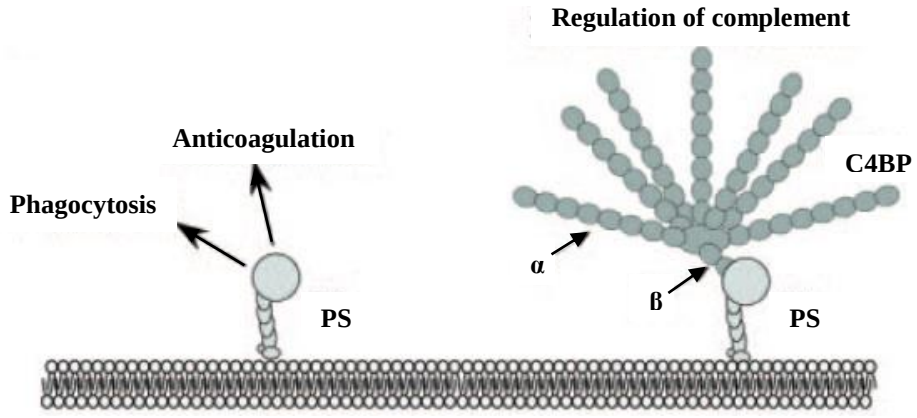

Figure 1.4. The C4BP and PS interaction regulates coagulation (Dahlback and Villoutreix, 2005). C4b-binding protein (C4BP) contains seven α chains and an unique β chain. Protein S (PS) binds to C4BP β-chain and causes loss of PS function. Therefore, C4BP can indirectly regulate the coagulation cascade through binding to PS.

1.3 Protein S deficiency

PS deficiency is divided into hereditary and acquired PS deficiency. Hereditary PS deficiency is a serious autosomal dominant disorder caused by mutations in the *PROS1* gene. It can be categorised into three types: patients with type I PS deficiency have reduced PS activity with low total and free PS levels, type II patients have reduced PS activity with normal total and free PS levels; and type III patients have both low PS activity and low free PS levels but normal total PS levels (Bertina, 1990). Approximately 200 different *PROS1* mutations have been characterised (Garcia de Frutos *et. al.*, 2007). Using copy number variation analysis, Pintao *et al.* (2009) reported that 6 out of 18 (33%) probands with PS deficiency had duplications or deletions in the *PROS1* gene. From these 6 cases, 3 probands with type I PS deficiency were found to have complete deletion of *PROS1* gene. Partial deletions of *PROS1* from exons 4 to 9 and exons 9 to 11 were detected in probands with type I and type III deficiency, respectively. Genetic analysis of the family shown thrombotic conditions over three generations shows that a novel nonsense mutation was identified in the *PROS1* gene (Cho *et. al.*, 2012). A transition (AAG $\rightarrow$ TAG) detected in the exon 10 of the *PROS1* gene. The nonsense mutation in the *PROS1* gene causes vascular access thrombosis (Cho *et. al.*, 2012).

Individuals with no alterations of *PROS1* gene can cause acquire PS deficiency under various conditions, including chronic inflammation, vitamin-K deficiency, liver diseases and especially increased circulating oestrogen levels during pregnancy and contraceptive pill use (Ten Kate and Van Der Meer, 2008). Both hereditary and acquired PS deficiency are associated with a significant increased risk of venous thrombosis (Pintao *et. al.*, 2009; Castoldi *et. al.*, 2010). Unfortunately, the underlying mechanisms that cause acquired PS deficiency are poorly understood.

1.4 Micro-ribonucleic acids:

Micro-ribonucleic acids (miRNAs) are small regulatory, non-coding RNAs, ~22 -25 nucleotides in length, which regulate gene expression by binding to the 3' untranslated region (UTR) sequence of target mRNAs to cause mRNA degradation or repress mRNA translation (Teruel-Montoya *et. al.*, 2015). The first miRNA, *lin-4*, was discovered in *Caenorhabditis elegans* in 1993 (Lee *et. al.*, 1993). The expression of *lin-4* was found to be induced at the beginning of the larval development stages of *C. elegans* and occurred in association with the downregulation of the *lin-14* gene, however, *lin-4* did not code for any functional protein (Lee *et. al.*, 1993). Through further investigation, Lee *et al.* (1993) found that *lin-4* bound via complementary base pairing at multiple locations within the 3'UTR of *lin-14* gene leading to inhibition of *lin-14* mRNA and protein expression. This discovery demonstrated a novel posttranscriptional gene regulation mechanism that has since revolutionised the study of functional non-coding RNAs. miRNAs have been reported to play important roles in cell growth, apoptosis, gene regulation and the maintenance of cell differentiation. Recently, several miRNAs have been reported to target genes that regulate different stages in the coagulation system (Teruel-Montoya *et. al.*, 2015). Research from our laboratory have reported that the miRNA, miR-494, directly targets the anticoagulant, Protein S, and regulates the expression of different coagulation factors, postulating an important role for miR-494 in the coagulation (Dr. Jasmine Tay, personal communication).

1.4.1 miRNA biogenesis

miRNA genes are transcribed from DNA by RNA polymerase II to form primary miRNAs (pri-miRNAs), which are about 60-100 nt in length (Figure 1.5) (Lee *et. al.*, 2002; Lee *et. al.*, 2004). The pri-miRNA transcripts are subsequently processed by a number of enzymes, first by the Drosha complex, a nucleic RNAse III endonuclease – along with DiGeorge critical region 8 (DGCR8), which is a Drosha cofactor. DGCR8 is a double-stranded RNA binding domain

protein with the function of cleaving longer pri-miRNAs into short single hairpin precursor-miRNAs (pre-miRNA) (Lee *et. al.*, 2003; Han *et. al.*, 2004). Then, pre-miRNAs are exported out of the nucleus by exportin-5 and Ran-GTP for further processing (Rui Yi *et. al.*, 2003).

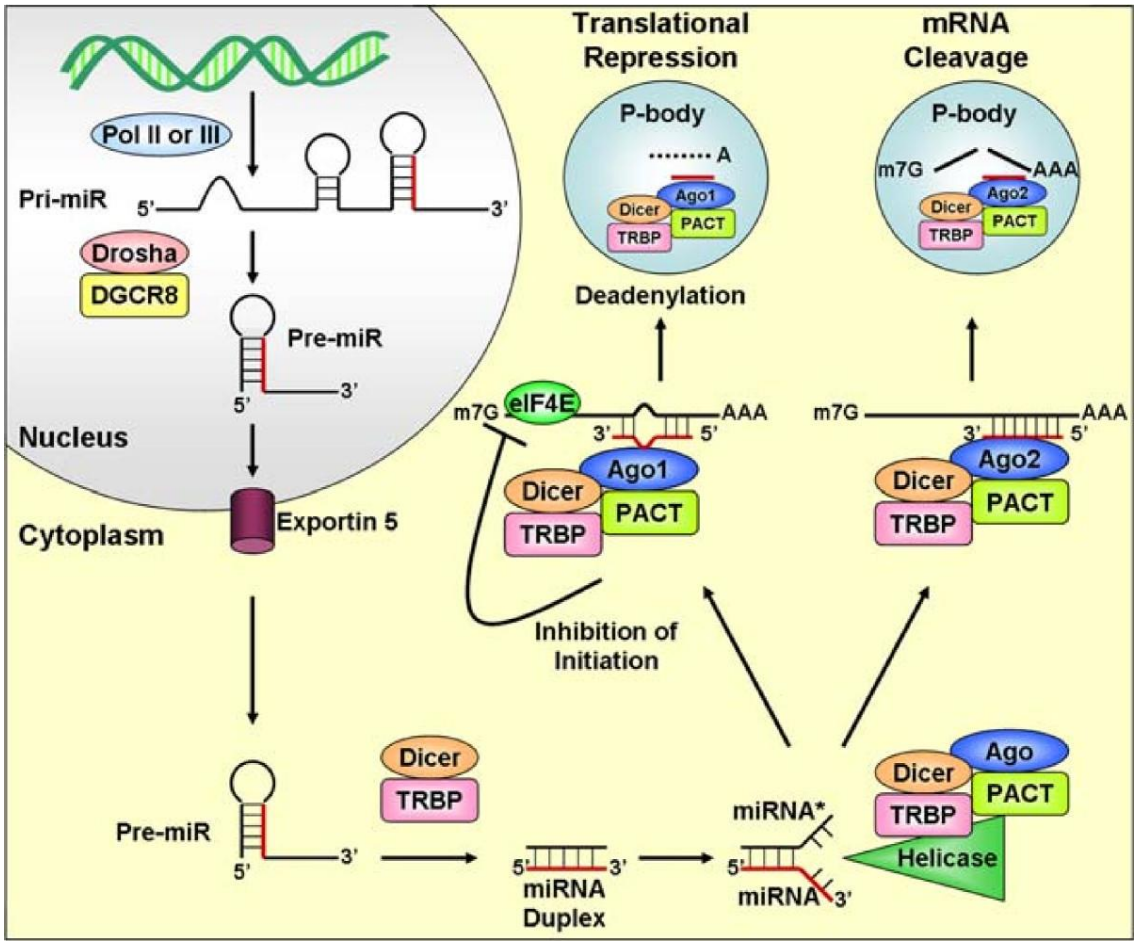

Figure 1.5. miRNA biogenesis and regulation of its target genes (Kapinas and Delany, 2011).

Once in the cytoplasm, pre-miRNAs are cleaved by the Dicer enzyme complex, a cytoplasmic RNAse III, which removes the loop structure of pre-miRNA molecules to generate double stranded miRNAs ~22 nt in length (Carmell and Hannon, 2004). Mature miRNAs are then transferred by the Dicer complex to the RNA-induced silencing complex (RISC) which consists of Argonaute proteins (Ago1, Ago2, Ago3 and Ago4). RISC is a key component of miRNA and small interfering RNA (siRNA) biogenesis, as well as initiating gene silencing to protect cells from viral infections. Argonaute proteins in RISC unwind the miRNA duplexes to form a mature single-stranded miRNA products (Landthaler *et. al.*, 2008). The passenger strand will usually

be degraded by RISC. After the formation of mature miRNA in RISC, the RISC incorporated miRNA causes mRNA degradation or translational repression by binding to the 3'UTR sequence of miRNA's target genes (Kapinas and Delany, 2011).

1.4.2 miRNA target recognition

miRNAs are able to recognise their targets through total and partial complementarity. Target recognition is highly dependent on base-pairing between the miRNA seed region, which is made up of 2-8 nucleotides from the 5'-end of the miRNA, and the target mRNA to repress protein expression. miRNAs, which bind with partial complementarity, accelerate the processes of deadenylation and cause mRNA decapping leading to general translational repression (Eulalio *et. al.*, 2009). A perfect complementary miRNA-mRNA interaction results in the destabilisation of the target mRNA where it is cleaved by Ago proteins in RISC. Different seed binding types affect the functional capacity of miRNAs. The seed types are divided into three main groups: 5' dominant seed, 5'-dominant canonical and 3' compensatory (Figure 1.6). In 5'-dominant seed sites, minimal additional base pair with canonical seed sequence is initially described as strong target regulation. With 5'-dominant canonical sites, the 5' and 3' ends of miRNAs can pair well to their targets. The supplementary 3'-base pairing in the 5'-dominant canonical site allows increased binding effectiveness. The 3'-compensatory sites, which contain disrupted seed sequence with compensatory 3' base pairing (usually more than 4-5 base pairs), are classified as insufficient target regulation (Carroll *et. al.*, 2014).

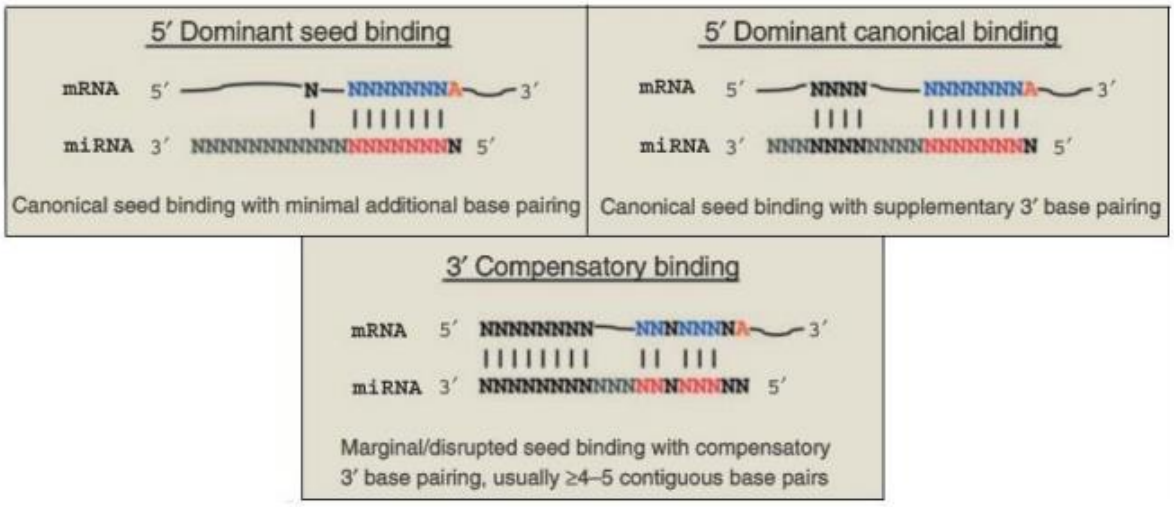

Figure 1.6. Three types of miRNA binding sites (Carroll *et. al.*, 2014). Minimal additional base pair with seed sequence in 5'- dominant seed binding sites. In 5'-dominant canonical binding site, the binding effectiveness increases due to the supplementary 3' base pairing. The 3'-compensatory binding sites consist of disrupted seed binding leading to insufficient target regulation.

A number of bioinformatic algorithms to predict miRNA-mRNA binding have been developed, which have been very useful in determining potential functions of different miRNAs by looking at the identities of their target mRNAs. The algorithms for predicting miRNA target sites incorporate various parameters, such as base-pairing complementarity, binding site accessibility and thermodynamic stability of the predicted interaction (Table 1.1). The most commonly used prediction algorithms (freely available online) are microRNA.org, TargetScan, RegRNA, DIANA microT and PicTar. TargetScan predicts the miRNA binding sites by searching 8mer (the seed and position 8 which followed by an A) and 7mer (the seed and position 8; and seed followed by an A) sites which exactly match the seed region of each miRNAs (Lewis *et. al.*, 2005). Apart from the seed region, microRNA.org includes experimentally validated targets for those miRNAs that do not contain perfect seed matches; and includes other approaches introduced 3'-compensatory matches or the seed and 3' match rules (Betel *et. al.*, 2008). RegRNA collects data from miRBase and integrates it with the miRanda algorithm to detect miRNA binding sites in the target sequence (Chang *et. al.*, 2013). miRanda is one of the prediction tools used in microRNA.org, it enhances sequence complementarity by using multiple position-specific rules from different experiments and evolutionary conservation (John *et. al.*, 2004).

Table 1.1. The features of different available prediction algorithms (Liu *et. al.*, 2014). Letters in species indicate prediction for human (H), mouse (M), rat (R), fly (F), worm (W), dog (D), chicken (C), and any species (A).

Algorithm	Region Scanned	Species Conservation	Species	Brief Description of the Prediction Method	Download/ Web server
miRanda	3'UTR	Yes	H, M, R, F, W	Predict targets based on rules: (i) sequence complementarity; (ii) binding energy; and (iii) evolutionary conservation.	http://www.microrna.org
mirSVR	No restriction	Yes	H, M, R, F, W	To score and rank miRanda-predicted miRNA target sites with a supervised vector regression model (SVR) for features including secondary structure accessibility of the site and conservation.	http://www.microrna.org
PicTar	3'UTR	Yes	H, M, R, F, W	Filter alignments according to the thermodynamic stability, then score and rank the predicted target by Hidden Markov Model (HMM) maximum-likelihood fit approach.	http://pictar.mdc-berlin.de/
TargetScan	7mer and 8mer sites, and ORF	Yes	H, M, R, D, C	Predict targets by searching for the presence of conserved 8mer and 7mer sites that match the seed region. Predictions are ranked by a combinatorial score based on site number, site type, and site context.	http://www.targetscan.org/
TargetScanS	3'UTR	Yes	H, M, R, D, C	Predict targets that have a conserved 6-nt seed match flanked by either a m8 match or a t1A anchor.	http://genes.mit.edu/tscan/targetscanS2005.html
RNA22	No restriction	No	A	Use the patterns discovered from the known mature miRNAs for predicting candidate miRNA target sites in a sequence.	http://cm.jefferson.edu/rna22v1.0/
EIMMo	8mer sites	Yes	A	A Bayesian method infers miRNA target sites by explicitly model the evolution of orthologous target sites in a set of related species.	http://www.mirz.unibas.ch/EIMMo2/
PITA	3'UTR	Yes	H, M, W, F	Predict miRNA targets using a nonparameter model that computes the difference between the free energy gained from the formation of the miRNA-target duplex and the energetic cost of unpairing the target to make it accessible to the miRNA.	http://genie.weizmann.ac.il/pubs/mir07/
RNAhybird	3'UTR and coding sequence	No	A	A tool to identify mRNA secondary structure and energetically favourable hybridization between miRNA and target mRNA.	http://bibiserv.techfak.unibielefeld.de/rnahybrid/submission.html
DIANA microT	3'UTR and coding DNA sequence (CDS)	No	H, M	The fifth version of microT algorithm which is specifically trained on a positive and negative set of miRNA recognition elements located in both the 3'-UTR and Coding DNA Sequence (CDS) region. The conserved and nonconserved miRNA recognition elements are combined into a final prediction score.	http://diana.cslab.ece.ntua.gr/microT/
miRmap	3'UTR	Yes	A	Predicting targets by taking into account of probabilities, base pairing, target accessibility, and evolutionary conservation using 11 predictor features.	http://mirmap.ezlab.org/

1.4.3 miRNA regulates gene expression via an indirect mechanism

Evidence suggests that the regulation of miRNAs is not restricted to downregulating gene expression but also mediate upregulation of gene expression. miRNAs mediate upregulation of gene expression through targeting transcription factors, such as STAT5B and XBPI. A report by Williams *et al*. (2012) demonstrated that miR-200a in human myometrial cells directly downregulates signal transducer and activator of transcription (STAT) 5B, which is a transcriptional repressor of 20α-hydroxsteroid dehydrogenase (20α-HSD). These results suggest that miR-200a indirectly enhances 20α-HSD expression through directly supressing STAT5B expression. Duan *et al.* (2015b) reported that a significant increase of miR-214 was identified in heart failure patients. miR-214 overexpression reduces the XBPI expression, a key transcription factor of unfolded protein response, by binding to its 3'UTR sequence. The XBPI downregulation causes regulation of other gene expression, leading to decreased cell migration and angiogenesis. In contrast, miRNAs indirectly downregulates gene expression by targeting transcriptional activator of a gene. Garzon *et al.* (2009) reported that miR-29b regulates the expression of DNA (cytosine-5)-methyltransferase 1 (*DNMT1*) without miR-29b binding sites in the 3'UTR sequence of *DNMT1*, however, miR-29b directly downregulates a transcriptional activator of *DNMT1* - specificity protein 1 (SP1) - to indirectly repress *DNMT1* expression. These studies showed that miRNAs can indirectly up- or downregulate gene expression by targeting transcriptional activators or repressors.

1.4.4 Functional roles of miRNAs

Krek *et al.* (2005) estimated that approximately 30% of protein coding genes are regulated by miRNAs. According to the latest edition of miRbase (released on 21 June 2014), more than 2,500 mature miRNAs in humans have been discovered (Manchester, 2015). Many miRNAs have been demonstrated to play important roles in the regulation of key cellular processes, such as apoptosis and cell proliferation. Furthermore, miRNAs have also been implicated in

the pathophysiology of various cancers. In contrast, miRNA's role in coagulation and haemostasis is still poorly characterised.

1.4.4.1 miRNAs in haemostasis and coagulation

Recent studies have identified several miRNAs that directly target important genes in coagulation and haemostasis (Figure 1.7). Multiple miRNAs have been ascribed roles in regulating the coagulation cascade by targeting the major procoagulants, fibrinogen and tissue factor, as well as Factor XI (FXI). Recent studies showed that the miR-17-92 cluster and miR-223 downregulates the expression of TF and regulates the coagulation cascade (Li *et. al.*, 2014b; Li *et. al.*, 2014c). The expression of TF, encoded by the *F3* gene, is a critical regulatory point of the coagulation cascade. Moreover, miR-223 directly downregulates TF expression (Li *et. al.*, 2014b). Overexpression of miR-223 partially reduces the effects of increased TF procoagulant activity induced by tumour necrosis factor α (TNF-α) (Li *et. al.*, 2014b). The miR-17-92 cluster, miR-19a, miR-19b and miR-20a, involve in regulating TF expression. Increased miR-19b expression in the plasma of unstable angina patients directly suppresses the expression of TF (Li *et. al.*, 2014c). Furthermore, miR-106b and miR-20a share the same binding sites in the 3'UTR sequences of TF, where miR-19b is binding to a different site. These miRNAs downregulate mRNA and protein expression of TF in both breast cancer and monocytic leukaemia cells (Teruel *et. al.*, 2011). In addition, miR-19 and miR-19a directly target TF and cause cell migration and carcinogenesis in the breast cancer cell line (MCF-7) and colon cancer cells respectively (Zhang *et. al.*, 2011; Yu *et. al.*, 2013a). An additional study reported that TF expression can be regulated by both miR-20b and Erk1/2 pathway independently (Yu *et. al.*, 2013b). Although these three studies did not discuss the impacts of TF expression in haemostasis, these miRNAs may still have an important role in inhibiting thrombogenesis by targeting TF.

Fibrinogen and Factor XI (FXI) are also one of the coagulation factors which are targeted by miRNAs. miR-409-3p directly targets *FGB* mRNA, which is β-polypeptide chain of fibrinogen; and miR-29c specifically downregulates one of the five fibrinogen transcripts (FGA-αE) (Fort *et. al.*, 2010). miR-29 family members (a, b or c) were able to significantly downregulate the expression of all five transcripts of fibrinogen (*FGA, FGA-αE, FGB, FGG and FGG'*) in HuH-7 cells, which was postulated to occur via direct 3'UTR binding of miR-29 or indirectly through miR-29 targeting of other undetermined regulators (Fort *et. al.*, 2010). Hatziapostolou *et al*. (2011) identified that the transcription factor hepatocyte nuclear factor 4α (HNFα) contains functional binding sites for miR-29a and miR-29b, which can explain the indirect mechanism of fibrinogen gene regulation by miR-29a and miR-29b. miR-181a-5p expression was shown to be inversely correlated with FXI levels in human livers. In addition, FXI-3'UTR was found to contain functional miR-181a-5p binding sites where miR-181a-5p was able to downregulate FXI-3'UTR-dependent luciferase activity in HepG2 liver cells (Salloum-Asfar *et. al.*, 2014).

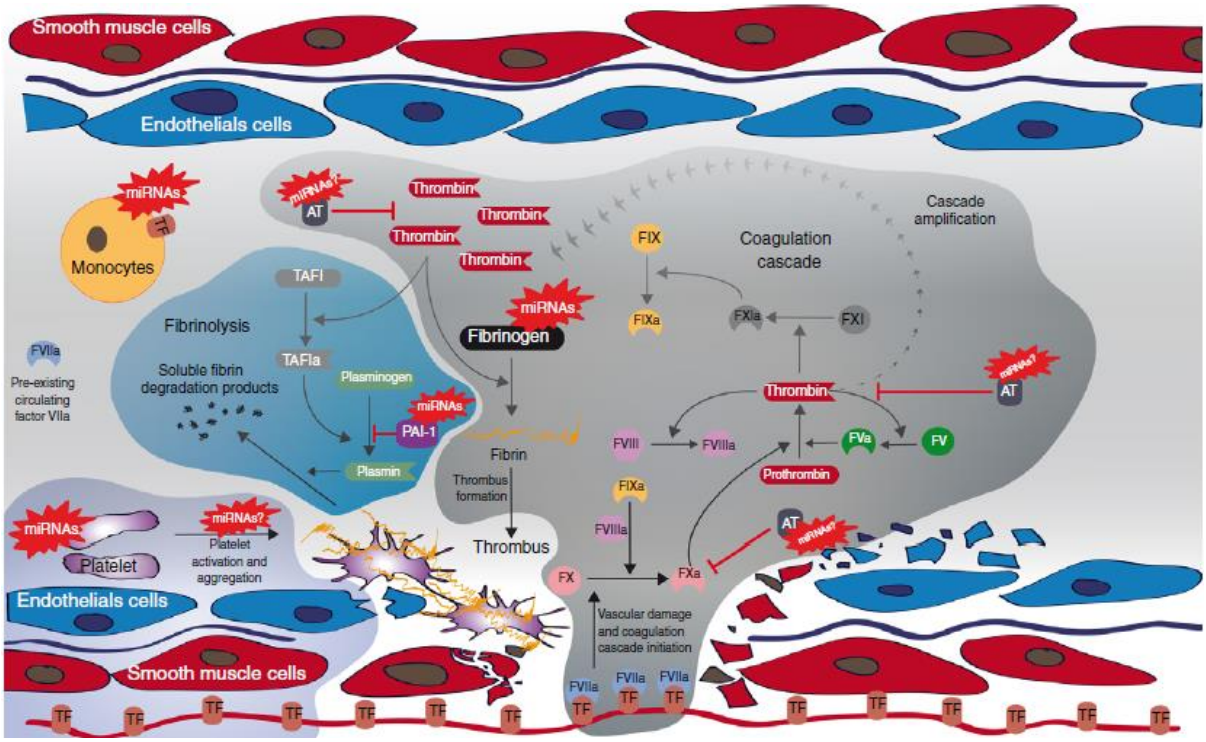

Figure 1.7. The regulation of haemostasis and coagulation by miRNAs (Teruel-Montoya *et. al.*, 2015). Multiple miRNAs have been reported to have important functions in megakaryocytopoiesis and platelet aggregation.

1.5 Micro-ribonucleic acid 494:

The miRNA, miR-494 (hsa-miR-494-3p), is located on chromosome 14 (14q32.31) and related to the miR-154 family that consists of 18 members. Members of the miR-154 family, including miR-494, have been identified to be deregulated in cystic fibrosis (Megiorni *et. al.*, 2011). Studies have shown that miR-494 expression is reduced in different carcinoma cells, such as oral cancer and esophageal squamous cell carcinoma, as well as in skeletal muscle cells during endurance exercise (Yamamoto *et. al.*, 2012; Yamanaka *et. al.*, 2012; Liu *et. al.*, 2012). In addition, miR-494 expression has been reported to be increased in chronic heart failure, hepatocellular carcinoma, breast cancer and glioblastoma cells (Mohnle *et. al.*, 2014; Sun *et. al.*, 2014; Chuang *et. al.*, 2015; Li *et. al.*, 2015). Taken together, these studies demonstrate multiple roles for miR-494 in promoting carcinogenesis and other diseases.

1.5.1 Known functions of miR-494

Many studies investigating the function of miR-494 in various cell types have identified several gene targets directly inhibited by miR-494 to regulate numerous cellular processes. These include processes, such as apoptosis, cell cycle progression and kinase signalling, as well as progression of various cancers (Table 1.3).

Table 1.2. Published studies of the miR-494 functions.

Literatures summary of miR-494 functions					
miR-494 functions	Target genes	Gene symbol	Cell types used	Characterised miR-494 function	References
Cause cancer	Ten methylcytosine dioxygenase	*TET1*	Human hepatocellular carcinoma cells	miR-494 suppresses TET1 gene expression to inactivate gene transcription of several invasion-suppressor miRNAs leading to tumour vascular invasion.	(Chuang *et. al.*, 2015)
	p190B RhoGAP	*p190B*	Human glioma cells	miR-494 directly downregulates RhoA regulator p190B to increase the expression of EGFR and MMP-2, and promotes invasion.	(Kwak *et. al.*, 2014)
	Phosphatase and tensin homolog	*PTEN*	Human bronchial epithelial cells	In anti-BPDE-induced transformed cells, overexpressed miR-494 negatively regulates PTEN expression so miR-494 acts as a micro-oncogene in carcinogenesis.	(Liu *et. al.*, 2010)
			Murine breast cancer cells	miR-494 activates Akt, mTOR and NF-$_K$B and inhibits MMP expression by targeting PTEN. Active PTEN/AKT pathway enhances tumour growth and metastasis.	(Liu *et. al.*, 2012)
			Human colorectal carcinoma cells	Increased expression of miR-494 in human colorectal carcinoma cells leads to direct reduction of PTEN expression and promotes cell migration and invasion.	(Sun *et. al.*, 2014)
			EBV-infected lymphoma of nasal natural killer cells	miR-494 directly inhibits PTEN to activate AKT pathway. miR-494/PTEN/AKT pathway is critical in the pathogenesis of nasal natural killer cell lymphoma.	(Chen *et. al.*, 2015b)
			Human glioblastoma cells	miR-494 promotes invasion, proliferation, migration and prevents apoptosis by downregulating PTEN expression through PTEN/AKT pathway.	(Li *et. al.*, 2015)
			Human NSCLC tissue	Overexpressed miR-494 directly downregulates PTEN expression and causes non-small cell lung cancer (NSCLC).	(Wang *et. al.*, 2015a)
Inhibits tumourigenesis	Polypeptide N-acetylgalactosaminyl-transferase 7	*GALNT7*	Human nasopharyngeal epithelial and carcinoma cells	miR-494 directly downregulates GALNT7 and CDK16 to inhibit the nasopharyngeal carcinoma tumourigenesis.	(Duan *et. al.*, 2015a)
	Cyclin-dependent kinase 16	*CDK16*			
	Pituitary tumour-transforming gene 1	*PTTG1*	Human Cervical carcinoma cells	miR-494 inhibits the tumour metastasis of cervical cancer by directly downregulating PTTG1.	(Chen *et. al.*, 2015a)
	Vascular endothelial growth factor	*VEGF*	Human mesenchymal stem cells	Overexpression of miR-494 directly suppresses the VEGF expression and inhibits angiogenesis.	(Chen *et. al.*, 2015c)
	Phosphorprotein enriched in diabetes	*PEA15*	Human epithelial cells	Downregulation of miR-494 mediated by AP1 increases BIM and PED expression. This causes inhibition of proliferation.	(Romano *et. al.*, 2012)
	c-myc	*MYC*	Human gastric epithelial mucosa cells	Decreased expression of miR-494 in gastric carcinoma cells results in increased expression of c-myc. miR-494 acts as an anti-oncogene in gastric carcinoma cells.	(He *et. al.*, 2014)
			Human pancreatic carcinoma	miR-494 inhibits proliferation and invasion of pancreatic cancer by inhibiting the c-myc/SIRT1 positive feedback loop .	(Liu *et. al.*, 2015)
	Sirtuin 1	*SIRT1*			
	Sybdecan 1	*SDC1*	Human medulloblastoma	miR-494 regulates the MMP-9/SDC1 negative feedback loop by downregulating MMP-9 and SDC1. This regulatory loop has a significant impact on the tumour growth and angiogenesis.	(Asuthkar *et. al.*, 2014)
	Matrix metallopeptidase 9	*MMP9*			

miR-494 functions	Target genes	Gene symbol	Cell types used	Characterised miR-494 function	References
Inhibits tumourigenesis	Homeobox A10	*HOXA10*	Human tongue squamous cells	miR-494 directly downregulates HOXA10 expression and prevents cell proliferation in oral cancer, thus, miR-494 acts as a tumour suppressor miRNA.	(Liborio-Kimura *et. al.*, 2015)
	Forkhead box M1	*FOXM1*	Human pancreatic ductal adenocarcinoma cells	miR-494 acts as a negative regulator of FOXM1 in pancreatic cells and causes inhibition of FOXM1/β-catenin signalling. This protects pancreatic tumourigenesis from inhibiting the promotors of proto-oncogenes.	(Li *et. al.*, 2014a)
	Dihydropyrimidine dehydrogenase	*DPYD*	Human colorectal carcinoma cells	miR-494 acts as a tumour suppressor in colon cancer and increased the sensitivity of 5-Fu by downregulating DPYD expression.	(Chai *et. al.*, 2015)
	Insulin-like growth factor 2 mRNA-binding protein 1	*IGF2BP1*	Human lung cancer cells	miR-494 downregulates the mRNA expression of *IGF2BP1.* IGF2BP1 suppress IGF2 expression and inhibit cell proliferation.	(Ohdaira *et. al.*, 2012)
	Chemokine Receptor 4	*CXCR4*	Human prostate epithelial cell line	miR-494 suppresses proliferation, invasion and migration of prostate cancer via targeting CXCR4.	(Shen *et. al.*, 2014)
Promotes or prevents apoptosis	Phosphatase and tensin homolog	*PTEN*	Hearts of transgenic mice and human embryonic kidney cells	miR-494 directly downregulates proapoptotic proteins (PTEN, ROCK1, CaMII*δ)* and antiapoptotic proteins (FGFR2, LIF) and causes activation of Akt pathway to trigger cell apoptosis.	(Wang *et. al.*, 2010)
	Leukemia inhibitory factor	*LIF*			
	Calcium/calmodulin-dependent protein kinase II delta	*CaMK2D*			
	Hypoxia-inducible factor-1α	*HIF1A*	Human hepatic cells	miR-494 causes increased HIF-1α and *HO-1* expression via PI3K/Akt pathway to protect L02 cells against hypoxia-induced apoptosis.	(Sun *et. al.*, 2013)
	JunD proto-oncogene	*JunD*	Human nucleus pulposus cells	Downregulation of miR-494 causes upregulation of JunD and prevent nucleus pulposus cells from apoptosis.	(Wang *et. al.*, 2015b)
Promotes apoptosis and Inhibits tumourigenesis	BCL2-associated athanogene	*BAG-1*	Huamn gastric cancer cells	miR-494 directly suppresses BAG-1 expression to promote apoptosis and inhibit proliferation in BGC-823 cells.	(Zhou *et. al.*, 2014)
	cleft lip and palate transmembrane 1-like	*CLPTM1L*	Human esophageal squamous cell carcinoma	miR-494 suppresses CLPTM1L expression by directly binding to its 3'UTR sequence. This causes apoptosis and inhibition of proliferation.	(Zhang *et. al.*, 2015)
	Tyrosine-protein kinase Kit	*KIT*	Human gastrointestinal stromal tumours cells	In gastrointestinal stromal tumours cells, miR-494 acts as a negative regulator of KIT. This promotes apoptosis and inhibits cell growth and proliferation.	(Kim *et. al.*, 2011)
	Rho-associated, coiled-coil containing protein kinase	*ROCK1*	Mouse osteoblast cells	miR-494 reduces the expression of ROCK1 to inhibit cell proliferation.	(Wang *et. al.*, 2010; Iwawaki *et. al.*, 2015)
			Hearts of transgenic mice and human embryonic kidney cells	miR-494 directly downregulates proapoptotic proteins (PTEN, ROCK1, CaMII*δ)* and antiapoptotic proteins (FGFR2, LIF) and causes activation of Akt pathway to trigger cell apoptosis.	
	Fibroblast growth factor receptor2	*FGFR2*	Mouse osteoblast cells	miR-494 reduces the expression of FGFR2 to inhibit cell proliferation.	(Wang *et. al.*, 2010; Iwawaki *et. al.*, 2015)
			Hearts of transgenic mice and human embryonic kidney cells	miR-494 directly downregulates proapoptotic proteins (PTEN, ROCK1, CaMII*δ)* and antiapoptotic proteins (FGFR2, LIF) and causes activation of Akt pathway to trigger cell apoptosis.	
	Nucleolin	*NCL*	Human immoral cells	miR-494 promotes apoptosis and inhibits cell proliferation by directly repressing the expression of NCL.	(Tominaga *et. al.*, 2011)
	Secretagogin	*SCGN*	Human SCLC cell line	miR-494 directly represses the expression of SCGN to promote apoptosis and prevent small cell lung cancer.	(Bai *et. al.*, 2014)

miR-494 functions	Target genes	Gene symbol	Cell types used	Characterised miR-494 function	References
Regulating cell cycle	Cyclin-dependent kinase 6	*CDK6*	Rat liver homogenates	miR-494 regulates B[a]P-exposed cell cycle progression and G_1/S transition by reducing the expression of CDK6 in primary murine bronchial epithelial.	(Duan *et. al.*, 2010)
			mesenchymal stem cells	Overexpressed miR-494 downregulates CDK6 and CCND1 to arrest cell cycle at G_1/S transition.	(Olaru *et. al.*, 2011; Chen *et. al.*, 2015c)
	Cyclin D1	*CCND1*	mesenchymal stem cells	Overexpressed miR-494 downregulates CDK6 and CCND1 to arrest cell cycle at G_1/S transition.	
	Cyclin-dependent kinase 4	*CDK4*	Human cholangiocarcinoma cells	miR-494 represses the expression CDK4, CDK6, CCND1, CCNE2 and HDAC1, resulting in inhibiting cell cycle at G_1/S transition.	(Olaru *et. al.*, 2011)
	Cyclin E2	*CCNE2*			
	Histone deacetylase 1	*HDAC1*			
	Pituitary tumour-transforming gene 1	*PTTG1*	Human cholangiocarcinoma cells	miR-494 directly downregulates PLK1, CCNB1, CDC20, CDC2 PTTG1 and TOP2A expression and regulates the cell cycle at G_2/M transition.	(Yamanaka *et. al.*, 2012)
	Topoisomerase II α	*TOP2A*			
	Polo-like kinase 1	*PLK1*			
	Cyclin B1	*CCNB1*			
	Cell-division cycle 20	*CDC20*			
	Cell-division cycle 2	*CDC2*			
	Mutated in Colorectal cancer	*MCC*	Mouse normal liver and tumour tissue	miR-494 directly inhibits MCC expression, leading to downregulating two important regulators of G_1/S transition, p27 and p21. This causes transformation in human liver cells.	(Lim *et. al.*, 2014)
Coagulation	Protein S	*PROS1*	Human liver carcinoma cells	Increased circulating oestrogen levels results in upregulation of miR-494, and miR-494 directly downregulate Protein S and causes Protein S deficiency.	(Tay *et. al.*, 2013)
Other	Phosphatase and tensin homolog	*PTEN*	Human proximal tubular epithelial cells	Increased expression of miR-494 in cells with cyclosporine A treatment lead to PTEN downregulation and causes tubular epithelial cell epithelial-mesenchymal transition.	(Yuan *et. al.*, 2015)
	Mitochondrial transcription factor A	*TFAM*	Mouse myoblast cells	Decreased expression of miR-494 during exercise or cell differentiation causes downregulation of TFAM and FOXJ3, leading to mitochondrial biogenesis.	(Yamamoto *et. al.*, 2012)
	Forkhead box j3	*FOXJ3*			
	Protein deglycase DJ-1	*PARK7*	Mouse neuroblastoma cell and fibroblast	DJ-1 protein expression is negatively regulated by miR-494 and causes oxidative stress and loss of dopaminergic neurons.	(Xiong *et. al.*, 2014)
	Cystic fibrosis transmembrane conductance regulator	*CFTR*	Human airway epithelium	TNF-α and IL-1β upregulates the miR-494 expression via transcriptional activator NF-$_K$B. miR-494 represses the mRNA expression of *CFTR*, therefore, miR-494 is an important regulator of homeostatic in respiratory tract.	(Ramachandran *et. al.*, 2013)
			Human bronchial epithelial	Increased expression miR-494 represses CFTR expression to increase expression of ΔF508 CFTR, which is the common CFTR mutants.	(Oglesby *et. al.*, 2013)
			CF airway epithelium	miR-494 and miR-101 downregulate CFTR expression and might explain the mutation of CFTR in CF patients.	(Megiorni *et. al.*, 2011)
	Solute carrier family 26, member 3	*SLC26A3*	Human intestinal epithelial cells	Downregulated in adenoma (DRA) protein is directly downregulated by miR-494 and causes inflammatory diarrheal diseases.	(Anbazhagan *et. al.*, 2014)
	Canabinoid receptors (CB1)	*CNR1*	Human cardiomyocytes	miR-494 in cardiomyocytes directly downregulates CB1 receptor expression and acts as a biomarker of chronic heart failure.	(Mohnle *et. al.*, 2014)
	Activating transcription factor 3	*ATF3*	Mouse kidney tissue	miR-494 is upregulated in I/R-induced kidney injury and directly downregulates ATF3 to cause severe kidney injury.	(Lan *et. al.*, 2012)

1.5.1.1 miR-494 regulates different coagulation factors

Recently, Tay *et al.* (2013) reported that functional miR-494 binding sites are present in the *PROS1* mRNA-3' UTR sequence. miR-494 downregulates the mRNA expression of *PROS1* by directly binding to these specific binding sites. The authors also demonstrated that oestrogen treatment of HuH-7 liver cells results in elevated miR-494 levels and is associated with decreased PS expression. The study showed a miRNA-mediated mechanism leading to PS deficiency under conditions of high circulating oestrogen levels. Further studies on the potential role for miR-494 in haemostasis was investigated by performing computational analyses of 40 coagulation genes using a number of miRNA binding site prediction tools – TargetScan, MicroRNA.org and RegRNA (Dr. Jasmine Tay, personal communication). These results showed that putative miR-494 binding sites are found in the 3' UTR sequence of multiple coagulation factors, including thrombin (*F2*), PAI-1, PS (*PROS1*), thrombomodulin (*TM*), thrombospondin 1 (*THBS1*), Factor V (*F5*), FVIII (*F8*), FIX (*F9*), TFPI and Urokinase (*PLAU*) (Dr. Jasmine Tay, personal communication). Interestingly, research in the laboratory demonstrated that, with transfected miR-494 in HuH-7 cells, some coagulation factors without miR-494 binding sites in their 3'UTR sequences showed significant changes in their mRNA expression, including plasminogen (*PLG*), TF (*F3*) and C4BPα (*C4BPA*) (Figure 1.8). These results suggested that miR-494 is able to regulate the expression of different coagulation factors with or without miR-494 binding sites. It is possible that miR-494 directly targets transcriptional activators or repressors to indirectly regulate the expression of those coagulation factors without miR-494 binding sites.

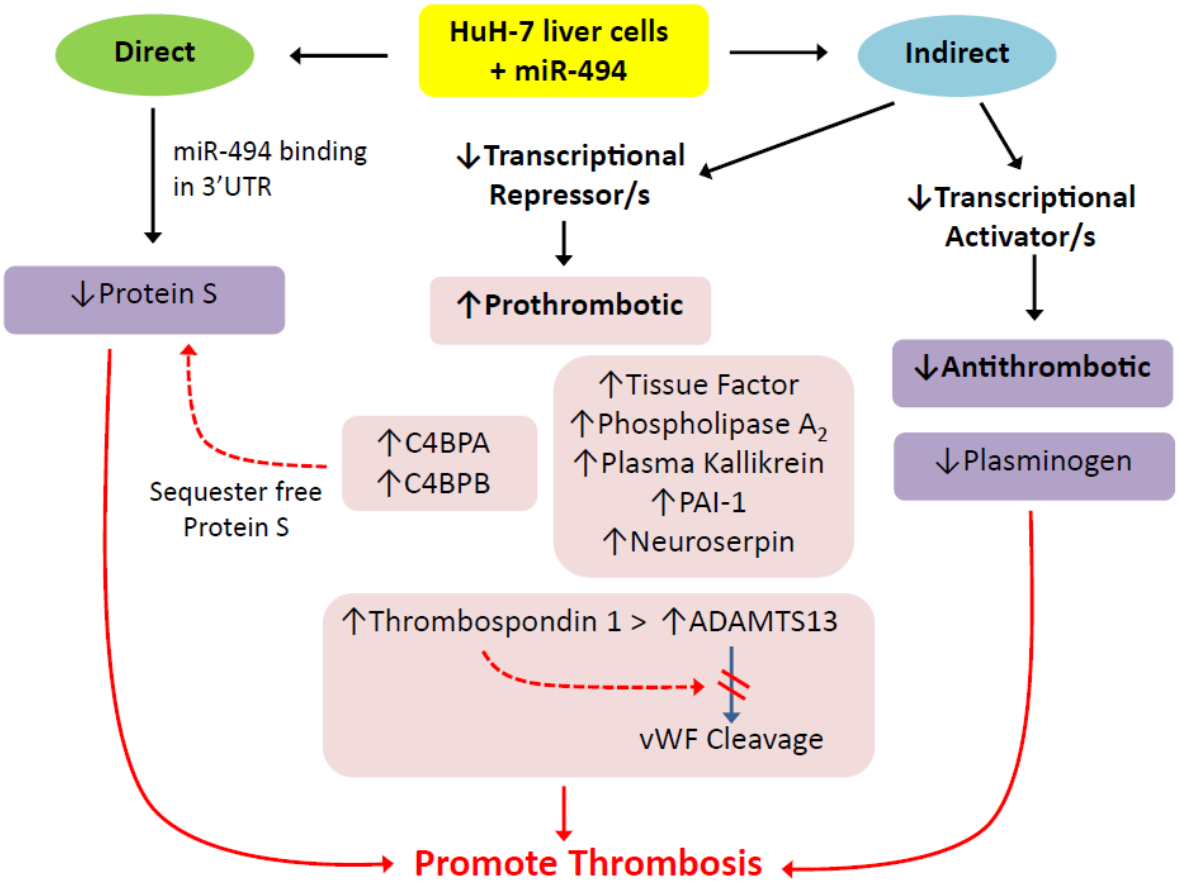

Figure 1.8. The regulation of different coagulation factors by miR-494 (Tay *et al.* personal communication). miR-494 downregulates Protein S expression through a direct interaction between miR-494 and the 3'UTR sequence of Protein S. Moreover, miR-494 may indirectly regulates multiple coagulation factors through transcriptional activator or repressors.

1.5.3 miR-494 and transcription factors

Internal laboratory computational analyses of miR-494 binding sites have identified more than 9000 putative targets of miR-494 (unpublished results). Moreover, more than 100 transcription factor 3'UTRs contain one or multiple miR-494 binding sites, and key transcription factors AP1, Sp1 and STAT5B were selected for further investigation in this project.

Activator protein 1 (AP1) is an important tumorigenic transcription factor through regulating differential gene expression. Multiple AP1 family members, including c-Jun and junB, are involved in regulating cell apoptosis and proliferation. The activation of c-Jun and Jun NH_2-terminal kinase (JNK) prevents cell apoptosis and promotes proliferation, however, downregulation of JNK represses antiapoptotic genes and induces apoptosis through upregulation of junB (Jacobs-Helber *et. al.*, 1998). Oeth *et al.* (1997) suggested that a distal and proximal AP1 binding sites were identified in the promoter region of tissue factor. On the other hand, evidence suggested that high circulating oestrogen levels results in downregulation of *PROS1* gene expression. Suzuki *et al.* (2010) reported that high oestrogen levels in $HepG_2$ cells results in downregulation of *PROS1* through the Sp1-ERα interaction in the *PROS1* promoter region. Moreover, Sp1 acts as a transcriptional activator of PS and plasminogen, with several functional Sp1 binding sites identified in the *PROS1* and *PLG* promoter regions (de Wolf *et. al.*, 2006; Gutierrez-Fernandez *et. al.*, 2007). In addition, STAT5B is another important transcription factor involved in the JAK-STAT5 signalling pathway (Dalgic *et. al.*, 2015). Interestingly, a recent report suggested that a STAT5-deificent mouse model increases thrombosis susceptibility through accelerating fibrin formation (Nordstrom *et. al.*, 2010). These studies showed that AP1 and Sp1 regulate several important coagulation factors and the absence of STAT5B is prothrombotic.

1.6 Statement of Aims:

Non-coding miRNAs are involved in regulating important physiological processes, and in the pathogenesis of various diseases. Recently, a role for miR-494 in the regulation of the coagulation pathway has been reported; where miR-494 was found to downregulate the expression of the anticoagulant factor, PS, through direct binding within the 3'UTR sequence of *PROS1* mRNA transcript. Further studies also demonstrated that miR-494 was able to regulate the expression of multiple coagulation factors at the mRNA levels, including those without predicted miR-494 binding sites within their 3'UTR sequences. Therefore, it is hypothesised that miR-494 has an important role in the regulation of haemostasis and coagulation pathways by targeting multiple coagulation factor genes via both direct and indirect mechanisms.

Hence, the aims of this study are to further characterise miR-494 function by:

1. Determining the effects of miR-494 on regulating coagulation factors' (PS, PLG, C4BPA and TF) protein levels.
2. Characterising the miR-494 direct regulation of transcription factors AP1, Sp1, and STAT5B.

Chapter 2: Materials

2.1 Chemical Reagents

2.1.1 Cell Culture

Item	Company	Catalog No.
0.25% Trysin-EDTA	Gibco Life Technologies, USA	25200-056
DMEM	Gibco Life Technologies, USA	21063-029
Fetal Bovine serum Charcoal Stripped	PA`A Laboratories GmbH, Germany	A11-519
Metafectene® Pro	Biontex Laboratories GmbH, Germany	T040-5.0
Penicillin Streptomycin	Gibco Life Technologies, USA	15140-122
RPMI-1640 Medium	Gibco Life Technologies, USA	11835-030
Sodium pyruvate (100mM)	Gibco Life Technologies, USA	11360-070
Non-essential amino acids	Gibco Life Technologies, USA	11140-050
HuH-7 cell line	Given by Mark Watson (IIID, Murdoch)	
MCF-7 cell line	Given by Jacky Bentel (Royal Perth Hospital)	

2.1.2 Total RNA extraction

Item	Company	Catalog No.
RNA*later*® Stabilization Solution	Ambion™ Life Technologies, USA	AM7021
RNase*Zap*® RNase Decontamination Solution	Ambion™ Life Technologies, USA	AM9780
Ethanol	Ajax Finechem Pty. Ltd, USA	5077-20L
*mir*Vana™ PARIS™ Kit	Ambion™ Life Technologies, USA	AM1556
• Cell disruption buffer • 2x denaturing solution • Acid-phenol:choloroform	• miRNA Wash solution 1 • Wash solution 2/3 • Elution solution	
TURBO DNA-*free*™ Kit	Invitrogen™ Life Technologies, USA	AM1907
• 10x TURBO DNase buffer • TURBO DNase	• DNase Inactivation Reagent	

2.1.3 Reverse Transcription Polymerase Chain Reaction (RT-PCR)

Item	Company	Catalog No.
SuperScript™ III Reverse Transcriptase	Invitrogen™ Life Technologies, USA	18080-044
Random Hexamers (50µM)	Invitrogen™ Life Technologies, USA	N8080127
RNaseOUT™ Recombinant RNase Inhibitor	Invitrogen™ Life Technologies, USA	10777-019

0.1M DTT	Invitrogen™ Life Technologies, USA	18080-044
5x First Strand Buffer	Invitrogen™ Life Technologies, USA	18080-044
10mM dNTPs	Invitrogen™ Life Technologies, USA	18427-013

2.1.4 Real-time Polymerase Chain Reaction (qPCR)

TaqMan® assay from Applied Biosystems™ Life Technologies, USA

Item	**Catalog No.**	**Assay ID**
TaqMan® Universal Master Mix II, no UNG	4440040	
TaqMan® Gene Expression Assay, PROS1 (human)	4331182	Hs00165590_m1
TaqMan® Gene Expression Assay, PLG (human)	4331182	Hs00264877_m1
TaqMan® Gene Expression Assay, C4BPA (human)	4331182	Hs00426339_m1
TaqMan® Gene Expression Assay, F3 (human)	4331182	Hs01076029_m1
TaqMan® Gene Expression Assay, JUN (human)	4331182	Hs01103582_s1
TaqMan® Gene Expression Assay, SP1 (human)	4331182	Hs00916521_m1
TaqMan® Gene Expression Assay, STAT5B (human)	4331182	Hs00273500_m1
TaqMan® Gene Expression Assay, 18S (human)	4331182	Hs99999901_s1
TaqMan® Gene Expression Assay, ACTB (human)	4331182	Hs99999903_m1
TaqMan® Gene Expression Assay, GAPDH (human)	4331182	Hs02758991_g1

2.1.5 Western Blot

Item	**Company**	**Catalog No.**
β-mercaptoethanol	Gibco Life Technologies, USA	21985-023
Glycine	Sigma-Aldrich Co., USA	G8898
Methanol (AnalaR NORMAPUR)	VMR International Pty Ltd., Australia	20847.307
Precision Plus Protein ™ Dual Strandard	Bio-Rad Laboratories Inc., USA	161-0374
Precision Plus Protein ™ WesternC Standard	Bio-Rad Laboratories Inc., USA	161-0376
Sodium Chloride	Amresco Inc., USA	X190-1kg
Sodium dodecyl sulfate	Amresco Inc., USA	0227
Sucrose	AnalaR	10274
Trizma® Base	Sigma-Aldrich Co., USA	T6066
Tween 20	British Drug Houses, London	663684B
Clarity™ Western ECL substrate	Bio-Rad Laboratories Inc., USA	170-5061
0.1% Ponceau S with 5% acetic acid	Sigma-Aldrich Co., USA	P-7170

Hydrochloric acid	Amresco® LLC, USA	A1367-2.5L
Skim milk powder	Fonterra Foodservices, Australia	-

2.1.6 Bacterial Culture and Plasmid Extractions

Item	Company	Catalog No.
Ampicillin sodium salt	Sigma-Aldrich Co., USA	A9518
Yeast extract, bacteriological	Amresco® LLC, USA	J850-500G
Tryptone (bacteriological grade)	Amresco® LLC, USA	J859-500G
Sodium chloride	Amresco® LLC, USA	X190-1kg
Riedel-de Haën® Sodium hydroxide	Sigma-Aldrich Co., USA	06203
NucleoBond® Xtra Midi Endotoxin-free plasmid DNA	MACHEREY-NAGEL GmbH & Co. KG, Germany	740420.10

2.1.7 Luciferase Reporter Assay

Item	Company	Catalog No.
Firefly substrate (10x)	Gene Stream Pty. Ltd, Australia	-
5x lysis Buffer	Gene Stream Pty. Ltd, Australia	-
Firefly enhancer (10x)	Gene Stream Pty. Ltd, Australia	-
Flash and grow (200x)	Gene Stream Pty. Ltd, Australia	-

2.2 Laboratory Equipment

2.2.1 General

Item	Company	Catalog No.
Weigh Tray (72x72mm)	Sarstedt Australia Pty Ltd, Australia	71.9923.212
Weigh Tray (128x128mm)	Sarstedt Australia Pty Ltd, Australia	71.9923.210
2mL tube	Axygen® Corning Inc, USA	MCT-200-C
5mL tube	Sarstedt Australia Pty Ltd, Australia	63.9921.522
Falcon™ 15mL tube	Thermo Fisher Scientific, USA	05-527-90
Falcon™ 50mL tube	Thermo Fisher Scientific, USA	14-432-22
0.2mL thin wall PCR tubes	Axygen® Corning Inc, USA	AXYPCR02LC
Parafilm M®	Bemis Company, Inc., USA	PM996
ND 1000 spectrophotometer	Nanodrop® Thermo Scientifi, USA	-

2.2.2 Cell culture and Total RNA extraction

Item	Company	Catalog No.
Falcon™ Tissue Culture Flask, 75cm^2	Thermo Fisher Scientific, USA	353136
Cellcoat® Petri Dishes 100x20mm	Greiner Bio-One, Australia	664160
Countess automated cell counter	Invitrogen™ Life Technologies, USA	-
Allegra® X15R Centrifuge	Beckman Coulter Inc., USA	-
Allegra™ 25R Centrifuge	Beckman Coulter Inc., USA	-

2.2.3 RT-PCR and qPCR

Item	Company
Microfuge® 16 Centrifuge	Beckman Coulter Inc., USA
C100™ Thermal Cycler	Bio-Rad Laboratories Inc., USA
CFX96™ Real-Time PCR Detection System	Bio-Rad Laboratories Inc., USA
CFX384™ Real-Time PCR Detection System	Bio-Rad Laboratories Inc., USA

2.2.4 Western Blot

Item	Company	Catalog No.
Mini-protean® TGX™ Gel 4-15% 10 well comb	Bio-Rad Laboratories Inc., USA	456-1083
Mini-protean® Tetra cell 4 Gel system	Bio-Rad Laboratories Inc., USA	165-8004
Amersahm ™ Protran ™ 0.45µm NC	GE Healthcare Life Sciences, Germany	10600016
Medium Reciprocating Shaker	Ratek Laboratory Equipment, Australia	RM2
Power PAC 3000	Bio-Rad Laboratories Inc., USA	-
Fusion-FX	Vilber Lourmat, Germany	-
Transfer tank	Bio-Rad Laboratories Inc., USA	-

2.2.5 Luciferase Reporter Assay

Item	Company	Catalog No.
24 well plate		
Micro-Assay 96 wells plate	Greiner bio-one International GmbH, Germany	655098
Victor™ Light Luminescence Counter	Perkin Elmer Inc., USA	-

2.3 Antibodies

Antibody	Company	Catalog No.
Rabbit anti-human C4BPA antibody	Pierce™ Thermo Fisher Scientific, USA	PA5-25861
Rabbit anti-human TF antibody	Pierce™ Thermo Fisher Scientific, USA	PA5-27278
Rabbit anti-human PROS1 antibody	Sigma-Aldrich Co., USA	SAB2107166
Rabbit anti-human TFPI antibody	Sigma-Aldrich Co., USA	SAB1408636
Rabbit anti-human PLG antibody	Santa Cruz Biotechnology Inc., USA	SC-25546
Mouse anti-human THBS1 antibody	Santa Cruz Biotechnology Inc., USA	SC-393504
Rabbit anti-human ADAMTS13 antibody	Santa Cruz Biotechnology Inc., USA	SC-25584
Goat anti-human Actin antibody	Santa Cruz Biotechnology Inc., USA	SC-1616
Goat anti-rabbit IgG-HRP	Santa Cruz Biotechnology Inc., USA	SC-2004
Donkey anti-goat IgG-HRP	Santa Cruz Biotechnology Inc., USA	SC-2020
Goat anti-mouse IgG-HRP	Santa Cruz Biotechnology Inc., USA	SC-2005

2.4 Computer Programmes

Programme	Company
Microsoft Excel	Microsoft® Corporation, USA
Bio-Rad CFX Manager	Bio-Rad Laboratories Inc., USA
BioProfil® Bio1D	Bio-Profil Polska, Poland
Endnote x7	ISI ResearchSoft, USA

Chapter 3: Methods

3.1 Computational analyses

3.1.1 Identifying putative miR-494 binding sites in the 3'UTR sequences of transcription factor genes

Online miRNA binding site prediction tools, MicroRNA.org (http://www.microrna.org/), RegRNA 1.0 (http://regrna.mbc.nctu.edu.tw/index1.php) and, TargetScan 7.0 (http://www.targetscan.org/) were used to identify putative binding sites for hsa-miR-494 (MI0003134) in the 3'UTR sequences of *JUN, SP1, STAT5B*. The 3'UTR sequences of *JUN*, *SP1* and *STAT5B* were obtained from Ensembl data base (Table 3.1).

Table 3.1. Ensermbl genome ID and numbers of base pairs of the 3'UTR sequences of the target gene.

3'UTR Sequences	Ensembl Genome ID	Sequence Length (bp)
JUN	ENST00000371222	1287
SP1	ENST00000426431	5206
STAT5B	ENST00000293328	2570

3.1.2 Identification of transcription factor binding sites in the promoter region of coagulation factor genes.

PROSCAN 1.7 (http://www-bimas.cit.nih.gov/molbio/proscan/) and PROMO analysis 3.0.2 (http://alggen.lsi.upc.es/cgi-bin/promo_v3/promo/promoinit.cgi?dirDB=TF_8.3) were prediction tools for predicting transcription factor binding sites in a gene sequence. The 20,000 bases upstream of the transcription start site of *PLG*, *C4BPA* and *F3* were obtained from the Ensembl data-base (Table 3.2.), and analysed by PROMO to identify putative binding sites for transcription factors with a 15% maximum matrix dissimilarity rate.

Table 3.2. Ensermbl genome ID for the promoter regions of coagulation factor.

Promoter sequences	Ensembl Genome ID
PLG	ENST00000308192
C4BPA	ENSG00000123838
F3	ENSG00000091513

3.2 Cell Culture

3.2.1 Maintenance of HuH-7 and MCF-7 cell lines

The human liver carcinoma cell line, HuH-7, was cultured in phenol red-free Dulbecco's Modified Eagle Medium (DMEM) medium[1], supplemented with 10% (v/v) fetal calf serum (FCS), 10mM sodium pyruvate (NaPyr/$C_3H_3NaO_3$), 100 IU/mL penicillin, 100 IU/mL streptomycin and 10mM non-essential amino acids solution (NEAA). Human breast cancer cell line, MCF-7, was maintained in phenol red-free RPMI-1640 medium[2], containing 10% (v/v) FCS, 10mM NaPyr, 100 IU/mL penicillin and 100 IU/mL streptomycin.

Both HuH-7 and MCF-7 cells were grown at 37°C/5% CO_2 and observed every 2-3 days using the Nikon Eclipse TS100 light microscope to monitor cell confluency. The culture medium was replaced every 2-3 days and cells were passaged when they were above 80% confluence. To passage the cells, medium was removed from the flask and washed with 4-5mL of Phosphate Buffered Saline (PBS)[3] to remove any remaining culture medium, after which 2mL of 0.25% trysin-EDTA was added into the flask and incubated at 37°C/5% CO_2 for approximately 2min until the cells have started to detach from the plastic culture surface. The trysin-EDTA was inactivated by adding an equal or greater volume of fresh culture medium. HuH-7 and MCF-7 cells were passaged at 1:15 and 1:10 dilutions respectively at which the cells will reach confluency and be passaged once a week.

3.2.2 miR-494 transfection in HuH-7

To determine miR-494 effects on the mRNA and protein expression of target genes, HuH-7 cells were transfected with 50nM negative control miRNA (miR-NC) or 50nM miR-494 precursors. HuH-7 cells were trypsinised (section 3.2.1) and the concentration and viability of the cell suspension were determined using the Countess Automated Cell Counter (Invitrogen™ Life Technologies). A total of 1.5 x 10^6 or 2.0 x 10^6 cells were seeded in each

10cm Petri dish with 10mL of stock culture medium and incubated overnight at 37°C/5% CO_2. The next day, the cells were transfected with 50nM miR-NC or miR-494 using Metafectene® Pro transfection reagent according to the manufacturer's instructions. For transfections in a 10cm Petri dish, 700µL of DMEM media alone (without antibiotics and other supplements) and 10µL of 50µM pre-miR-NC or pre-miR-494 (Solution A) was added into 700µL of DMEM media and 42µL of Metafectene® Pro (Solution B), pipetted once to mix and incubated for 15min at room temperature. The medium in the petri dishes was replaced with 8.6mL of fresh culture medium just before the addition of the transfection mix to ensure a total final volume of 10mL. The transfection mix was added to the cells dropwise and the HuH-7 cells in Petri dishes were incubated at 37°C/5 % CO_2 and harvested at 48h or 72h post transfection before they were harvested by trysinisation (section 3.2.1) for total RNA extraction (section 3.3.1) or for the preparation of whole cell lysates for western blotting (section 3.5.1)

To harvest the cells, all medium was removed from the petri dishes and washed with 4-5mL of PBS[3], after which 2mL of trysin-EDTA was added and incubated at 37°C for 1-2min to dislodge the cells from the plastic culture surface. Countess automated cell counter and the EVE™ cell counting slide were used again for counting cell numbers and determining cell viability. A total of 2.0 x 10^6 of cells were transferred into a clean tube for total RNA extraction (section 3.3.1) and the remaining cells were lysed with whole cell lysis buffer[16] for use in western blotting (section. 3.5.2).

3.3 Total RNA extraction

3.3.1 Total RNA Extraction

*mir*Vana™ PARIS™ Kit from Ambion life technologies was used for total RNA extraction. The trypsinised transfected cells were centrifuged using the Beckman Coulter Allegra® X-15R centrifuge at 359x*g* at room temperature for 5min. The culture supernatant was removed and 1mL of RNA*later*® solution was added and the cell pellets were resuspended by pipetting up and down. The cell suspension was stored at 4°C for at least 24h up to a week before RNA extraction. An equal volume of PBS[3] (1mL) added into the cell suspension in RNA*later*® solution and centrifuged at 3157x*g* for 10min at room temperature and the RNA*later*® solution was removed. For RNA extraction, 500µL of ice-cold cell disruption buffer was added and the cell pellet resuspended by vortexing. An equal amount of 2x denaturing solution (500µL) warmed to 37°C was then added and incubated in ice for 10min. After the incubation, 1mL of acid-phenol:chloroform was added into the mixture, and vortexed vigorously to mix for 30s to obtain an emulsion. The mixture was then centrifuged using Beckman Coulter Allegra™ 25R centrifuge for 5min at 10,000x*g* at room temperature to separate the aqueous and organic phases. Checking that the interphase is compact after centrifugation, 800µL of the aqueous (top) phase were carefully removed and transferred into a fresh 2mL tube for RNA isolation.

To isolate the total RNA, 1.25 volume of room temperature 100% ethanol (v/v) (1mL) was added into the lysate and mixed it using a pipette. Each sample was transferred into the collection tubes with a filter cartridge and centrifuged at 10,000x*g* for 1min at room temperature allowing the mixture to pass through the filter. After all the lysate/ethanol had passed through the filter, the filter was washed with 700µL of miRNA wash solution 1, followed by two washed with 500µL of wash solution 2/3, with centrifugation at 10,000x*g* between washes. After the third wash, the filter was centrifuged in the collection tube to remove any residual wash buffer and transferred into a fresh collection tube. To elute the total RNA, 100µL

of preheated elution buffer (95°C) was applied into the filter cartridge and centrifuged at 10,000x*g* for 1min at room temperature.

3.3.2 DNase Treatment

Turbo DNA-free™ kit was used for digesting the DNA to eliminate genomic DNA contamination from the eluted RNA according to the manufacturer's protocol. Briefly, 10µL of 10x Turbo DNase buffer and 1µL of Turbo DNase were added into the extracted RNA, and incubated at 37°C for 30min. To inactive the DNase activity, 10µL of the DNase inactivation reagent were added and incubated at room temperature for 5min with constant mixing. The mixture was centrifuged at 10,000x*g* for 1.5min at room temperature by using Beckman Coulter Microfuge® 16 centrifuge to pellet the DNase inactivation reagent. The clear aqueous top layer containing the total RNA was transferred into a clean tube, the concentration and quality of the extracted RNA were determined by using ND 1000 spectrophotometer, and the total RNA was aliquoted in multiple 20µL volumes into RNase-free tubes and stored at -80°C.

3.4 Real-time Quantitative Polymerase Chain Reaction (RT-qPCR)

3.4.1 Reverse Transcription

Total RNA was converted to cDNA using Superscript III reverse transcriptase (Invitrogen™ Life Technologies) before performing qPCR. For first strand synthesis, 1µL of 50µM random hexamers, 1µL of 10mM dNTP mix[19], 1µg of total extracted RNA (section 3.3.5) and 6µL of distilled water were added into a fresh nuclease-free microcentrifuge tube. The mixture was heated to 65°C for 5min and incubated in ice for 2min. For cDNA conversion, a master mix containing 4µL of 5x first-strand buffer, 1µL of 0.1M DTT, 1µL of 40U/µL RNaseOUT™ recombinant RNase inhibitor and 1 µL of 200U/µL SuperScript™ III Reverse Transcriptase was added into the mixture. The mixture was mixed and incubated at 25°C for 5 min, followed

by 55°C for 60min and the reaction was inactivated by heating at 70°C for 15min. The cDNA was used immediately for qPCR or stored at -20°C until required.

3.4.2 Quantitative PCR (qPCR)

Levels of *PROS1*, *PLG*, *C4BPA*, *TF*, *JUN*, *SP1* and *STAT5B* mRNA were determined by using TaqMan Gene Expression Assay and normalised to mRNA levels of housekeeping genes *18S*, β-Actin (*ACTB*) and glyceraldehyde 3-phosphate dehydrogenase (*GAPDH*), which were the endogenous controls in this experiment. The master mixes were prepared with 0.5µL of 20x TaqMan Gene Expression Assays and 5µL of 2x master mix reagents per well, and vortex the master mix. The master mixes (5.5µL) were loaded into each well of a 96-well PCR reaction plate. The cDNA was diluted 1:7 with RNase-free water and 4.5µL of the diluted cDNA were loaded into the 96-wells reaction plate in triplicates. The plate was placed in the BioRad Real-Time PCR Detection System and cycled under the following conditions: 95°C for 10min, followed by 40 cycles of 95°C for 15s and 60°C for 1min. The relative fold changes to mRNA levels were calculated by the $2^{-\Delta\Delta CT}$ method.

3.5 Western Blotting

3.5.1 Harvesting cells for western blot

To prepare cell lysates for western blotting, total cell numbers in the trypsinised cell suspensions were determined on the countess automated cell counter and the EVE™ cell counting slide. The cells were pelleted by centrifugation at 359x*g* at room temperature for 5min. All the supernatants were removed and the cells were lysed with whole cell lysis buffer[16] (250mL lysis buffer for every 2.0 x 10^6 cells). The lysates were drawn repeatedly through a 23G needle into a 1mL syringe unit until the viscous lysates reached a water-like consistency due the shearing of genomic DNA, and the lysates were stored at -20°C.

3.5.2 Sodium dodecyl sulphate polyacrylamide gel electrophoresis (SDS-PAGE)

Denaturing SDS-PAGE was performed to separate the proteins according to their molecular weight. To prepare whole cell lysates for SDS-PAGE, 18µL of each sample was transferred into 0.2mL PCR tubes with 2µL of western 10x loading dye[15]. All the samples were heated at 95°C for 8min to denature the proteins, after which the samples were loaded into 4-15% TGX precast gradient gel (Bio-Rad Laboratories Inc.). The gel was electrophoresed at constant voltage of 200V for 30-35min or until the loading dye reached to the bottom of the gel.

3.5.3 Western Transfer

After gel electrophoresis, the gel was removed from the casting plates and placed in cold western transfer buffer[12] to be assembled into the transfer cassette. The transfer cassettes were prepared in the following order; from the black side: a sponge, three pieces of filter paper, the gel, a piece of prewetted 0.45µm nitrocellulose or 0.45µm PVDF transfer membrane, three pieces of filter paper and a sponge. The 0.45µm nitrocellulose membrane wetted in the cold transfer buffer but the PVDF membrane can only be wetted in methanol. All the transfer membranes, filter paper and sponge were wetted before preparing the transfer cassettes and air bubbles between each layer were ejected. The transfer cassettes were inserted into the transfer tank with cold transfer buffer[12] and were transferred at constant voltage 30V for overnight at 4°C.

3.5.4 Immunoblotting

The 0.45µm nitrocellulose or PVDF transfer membranes were removed from the transfer cassettes after overnight transfer. A reversible protein stain, Ponceau Red, was used to stain the membrane to check the overnight transfer was successful and complete. Deionised water was used to wash off excess ponceau red before immunoblotting. The membranes were

incubated in 3% (w/v) skim milk/TBST blotto blocking solution[14] for 90min on a rotary shaker and then incubated with primary antibody diluted in 3% (w/v) skim milk/TBST blotto blocking solution[14] for 90min. Primary antibody solution was removed and the membranes were washed with tris buffered saline with Tween 20 (TBST)[13] for 3 x 5min. After the wash, the membranes were incubated in secondary antibody diluted in 3% (w/v) skim milk/TBST blotto blocking solution[14] for another 90min, and washed 3 x 5min with TBST. The dilutions used for HRP-conjugated secondary antibodies are listed in Table. 3.3.

Table 3.3. Dilution of HRP-conjugated secondary antibodies used for immunoblotting.

Secondary antibody	**Dilution**
Goat anti-rabbit IgG-HRP	1:2000
Donkey anti-goat IgG-HRP	1:2000
Goat anti-mouse IgG-HRP	1:2000

Clarity™ western enhanced chemiluminescence (ECL) substrate ((Bio-Rad Laboratories In.) was used for detecting immunoreactivity. Excess TBST on the membranes was removed by draining the liquid off onto a clean paper towel, after which the ECL substrate was added dropwise on to the membranes, ensuring that the entire membrane was covered. The membranes were incubated with ECL for 5min at room temperature, the excess liquid drained off onto a clean paper towel and the immunoreactivity detected by exposing the membranes in the Fusion-FX imager between 10sec up to 10min. The optical density of the protein bands were analysed and quantitated using the Bio1D software (Bio-Profil Polska).

3.6 Plasmid DNA Extraction and Purification

DH5α *E. coli* glycerol stocks containing pMIR-REPORT luciferase construct (see Appendix II) or pRL-SV40 Renilla luciferase vectors (see Appendix II) were inoculated into 5mL of lysogeny broth (LB) medium[14] with ampicillin (1μg/mL) overnight at 37°C with sharking and allowed to grow overnight. The next day, the overnight cultures were transferred into 100mL of fresh LB medium supplemented with 100μg/mL ampicillin and incubated with sharking overnight at 37°C, and harvested for plasmid extraction the next day.

Plasmid constructs required for transient transfection (section 3.7) were extracted from 100mL of overnight DH5α *E.*coli culture using the NucleoBond® Xtra Midi Endotoxin Free kit (Macherey-Nagel GmbH & Co.) according to the supplied protocol. To harvest the bacterial cells, the overnight bacterial culture was centrifuged at 4064x*g* and 4°C for 20min. The supernatant was poured off and the cell pellet was resuspended with 8mL of resuspension buffer containing RNase A by vortexing. The cells were then lysed with 8mL of lysis buffer, mixed by gentle inversion 5 times and incubated at room temperature for 5min. During this time, 15mL of equilibration buffer was applied on the column filter to equilibrate the NucleoBond® Xtra column by gravity flow. Following incubation, the lysis buffer was neutralised with 8mL of neutralisation buffer and mixed completely by inversion. The neutralised bacterial cell lysate was slowly loaded into the column filter and allowed to pass through the filter by gravity flow. The filter was washed with 5mL of filter wash buffer and the filter was discard after all the solution follow through the filter. The NucleoBond® Xtra column was then washed with 35mL of ENDO-EF wash buffer followed by 15mL of WASH-EF wash buffer. To elute the plasmid DNA from the column, 5mL of elution buffer was added into the column and the flowthrough elute containing the plasmid DNA collected in a clean 15mL tube. To precipitate the plasmid DNA, 3.5mL of isopropanol was added to the eluted DNA mixed well by inversion, and centrifuged at 4064g for 60min at 4°C. After centrifugation, the

supernatant was removed using a pasteur pipette, with special care taken to not disturb the plasmid pellet. The plasmid DNA pellet was washed with 2mL of 70% ethanol and centrifuged again at 4064g for 20min at room temperature (22°C). The supernatant was removed using a pasteur pipette, again taking care not to disturb the plasmid pellet and the pellet was air dried at room temperature approximately 30 - 60min, to evaporate off the mixture. The dried plasmid DNA pellet was dissolved in 200µL of endotoxin free water (H_2O-EF). The concentration and quality of the extracted plasmid were determined by using ND 1000 spectrophotometer. The extracted plasmid DNA was aliquoted into 10µL aliquots into nuclease-free tubes and stored at -80°C.

3.7 Transfection of luciferase reporter vectors and pre-miRNA precursors

HuH-7 cells in T75 flasks were trypsinised (section 3.1.1) and seeded into 24-well cell culture plates at a density of 2.5 x 10^5 cells per well. The seeded plate was incubated at 37°C/5% CO_2 overnight to allow the cells to adhere before transfection. In each well, HuH-7 cells were co-transfected with 50nM of pre-miR-NC or pre-miR-494, 100ng of pRL-SV40 Renilla luciferase vector and 400ng of the pMIR-REPORT Firefly luciferase vector containing the full *PROS1*, *JUN*, *SP1* or *STAT5B*-3'UTR insert. To prepare the transfection reaction mix, 50µL of the DMEM medium alone (without antibiotics or additives) with luciferase vectors and pre-miRNAs were added 50µL of the DMEM medium alone with Metafectene® Pro, and incubated at room temperature for 15min. The transfection mixture was added dropwise into the 24-well cell culture plate and incubated at 37°C for 6h. After this time, the transfected cells were trysinised (section 3.2.1) and reseeded into a white 96-well cell culture plate, and incubated at 37°C/5% CO_2 for 18h.

3.8 Dual Luciferase Reporter Assay

After 24h post-transfection, the cells were lysed with 20µL of Firefly Lysis buffer per well and incubated at room temperature for 30min. To assay for luciferase activities, RapidReporter® Firefly glow assay kit and RapidReporter® flash and glow assay kit from GeneStream Laboratory were used. For the detection of Firefly luciferase activity, 60µL of Firefly glow assay buffer containing the luciferin substrate diluted in Firefly luciferase buffer was added into each well. Renilla luciferase activity was detected with 60µL of Flash and Glow assay buffer containing coelantrazine substrate. The plate was incubated at room temperature for 10 to 30min to allow the light signals to reach a steady glow phase before being measured on the Victor™ light luminescence counter. The relative luciferase activity was determined by the ratio of Firefly and Renilla counts and the miR-494 effects on these 3'UTR constructs (*PROS1, JUN, SP1* and *STAT5B*) were determined by normalising the relative luciferase activity of miR-494 transfected samples to the relative luciferase activity of miR-NC transfected samples.

3.9 Statistical analysis

Two-tailed Student's t-test with unequal variance was performed for the statistical analyses in luciferase reporter assays, RT-qPCR and western blot. A value of $p<0.05$ was set as statistically significant.

Chapter 4: Results

4.1 Optimising Immunoblotting primary antibodies

To analyse protein expression, both qualitative and quantitative, the primary antibodies required optimisation under western blotting conditions. Anti-human C4b binding protein α (C4BPA), plasminogen (PLG), Protein S (PS) and tissue factor (TF) antibodies were optimised for immunoblotting before quantitating the protein levels in HuH-7 following miR-494 transfection. The best primary antibody dilutions to use and expected sizes of C4BPA, PLG, PS and TF in western blots were listed in Table 4.1 and Table 4.2 respectively. Rabbit anti-human C4BPA, PLG and PS antibodies were blotted on a 0.45 µM nitrocellulose membrane with 3% (w/v) skim milk/TBST blotto blocking solution[14]. However, rabbit anti-human TF antibody did not show a clear band on the nitrocellulose membrane. Therefore, TF antibody was blotted on a 0.45 µM PVDF membrane with 5% (w/v) skim milk/TBST blotto blocking solution[18] because a high background was observed with 3% (w/v) skim milk/TBST blotto blocking solution[14]. Unfortunately, rabbit anti-human tissue factor pathway inhibitor (TFPI) and ADAMTS13, and mouse anti-human thrombospondin 1 (THBS1) could not be optimised because non-reactive antibody or multiple non-specific bands were found in the optimisation blot (Figure 4.1 E-G). No band was found at the expected size of THBS1 and TFPI primary antibodies in the optimisation blots, and multiple non-specific bands were found in the ADAMTS13 primary antibody optimisation blot. The use of these primary antibodies required further optimisation. Due to time limitations, the primary antibodies of THBS1, TFPI and ADAMTS13 could not be optimised and the protein levels of these proteins were not determined in this study.

Table 4.1 Dilution optimisation of primary antibodies

Primary antibody	Recommended dilution	Best dilution in optimisation blot
Sigma-Aldrich Rabbit anti-human PS antibody	1:1000	1:1000
Santa Cruz Rabbit anti-human PLG antibody	1:200	1:500
Pierce™ Rabbit anti-human C4BPA antibody	1:1000	1:200
Pierce™ Rabbit anti-human TF antibody	1:1000	1:2000
Santa Cruz Rabbit anti-human ADAMTS13 antibody	1:200	-
Santa Cruz Mouse anti-human THBS1 antibody	1:100	-
Sigma-Aldrich Rabbit anti-human TFPI antibody	1:1000	-

Table 4.2 The expected and actual size of proteins

Primary antibody	Expected size	size showed in optimisation blot
Sigma-Aldrich Rabbit anti-human PS antibody	75 kDa	60–75 kDa
Santa Cruz Rabbit anti-human PLG antibody	90 kDa	90 kDa
Pierce™ Rabbit anti-human C4BPA antibody	70 kDa	~ 110 kDa
Pierce™ Rabbit anti-human TF antibody	47 kDa	~65kDa
Santa Cruz Rabbit anti-human ADAMTS13 antibody	176 kDa	-
Santa Cruz Mouse anti-human THBS1 antibody	165-198 kDa	-
Sigma-Aldrich Rabbit anti-human TFPI antibody	41 kDa	-

A Pierce™ Rabbit anti-human PS antibody

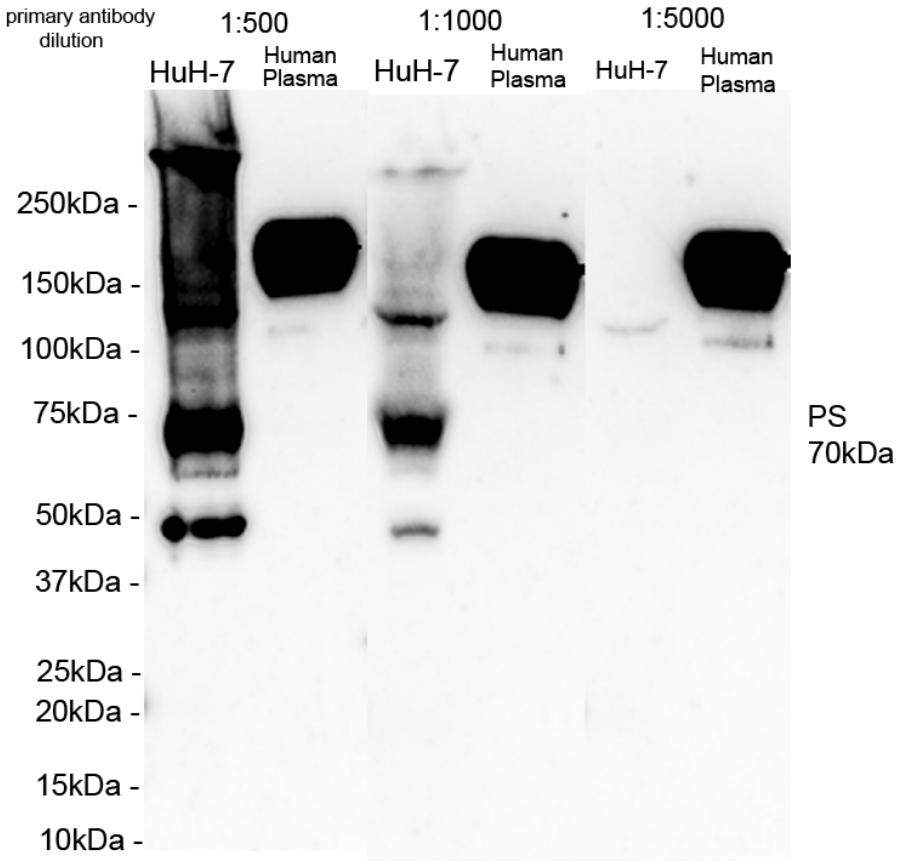

B Santa Cruz Rabbit anti-human PLG antibody

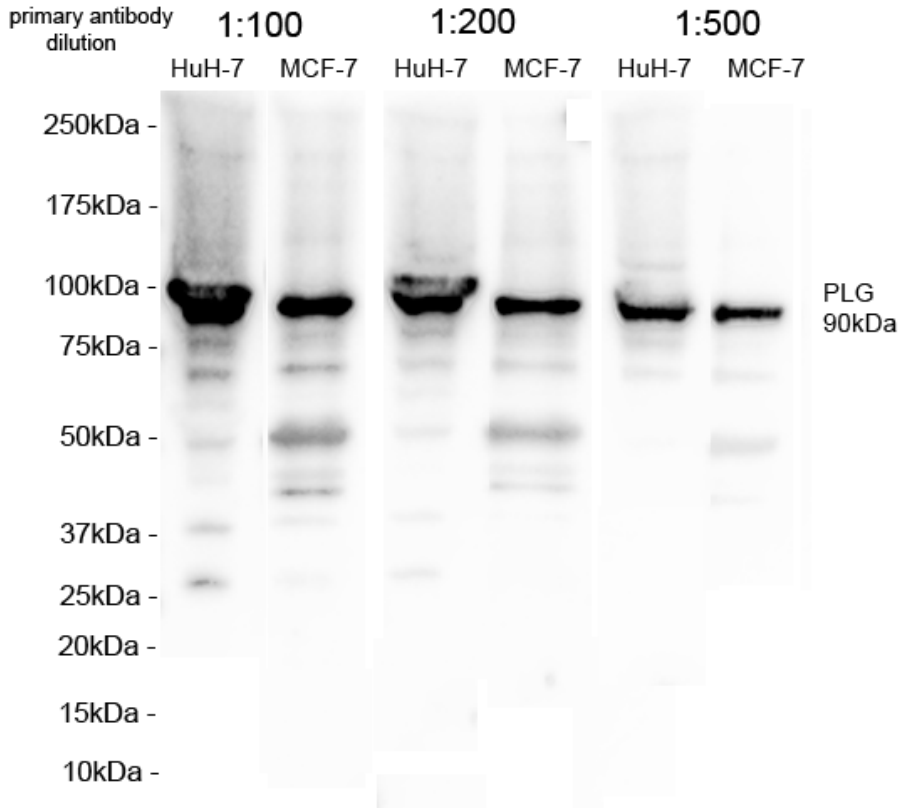

C Pierce™ Rabbit anti-human C4BPA antibody

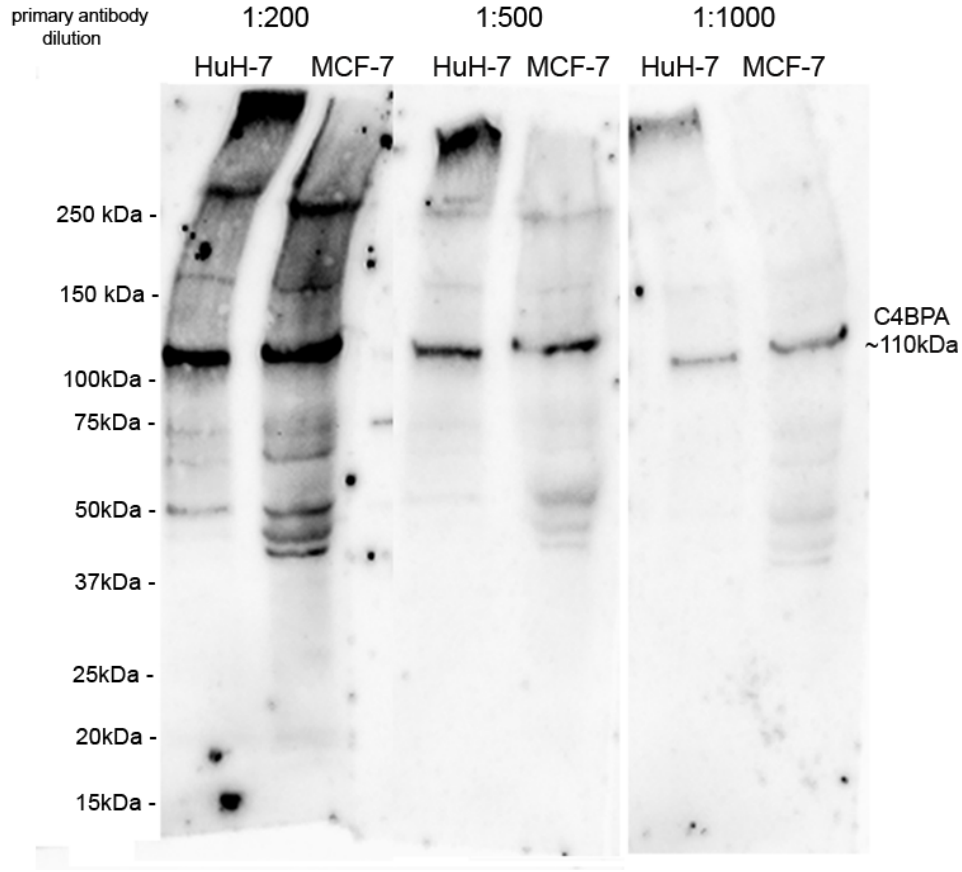

D Pierce™ Rabbit anti-human TF antibody

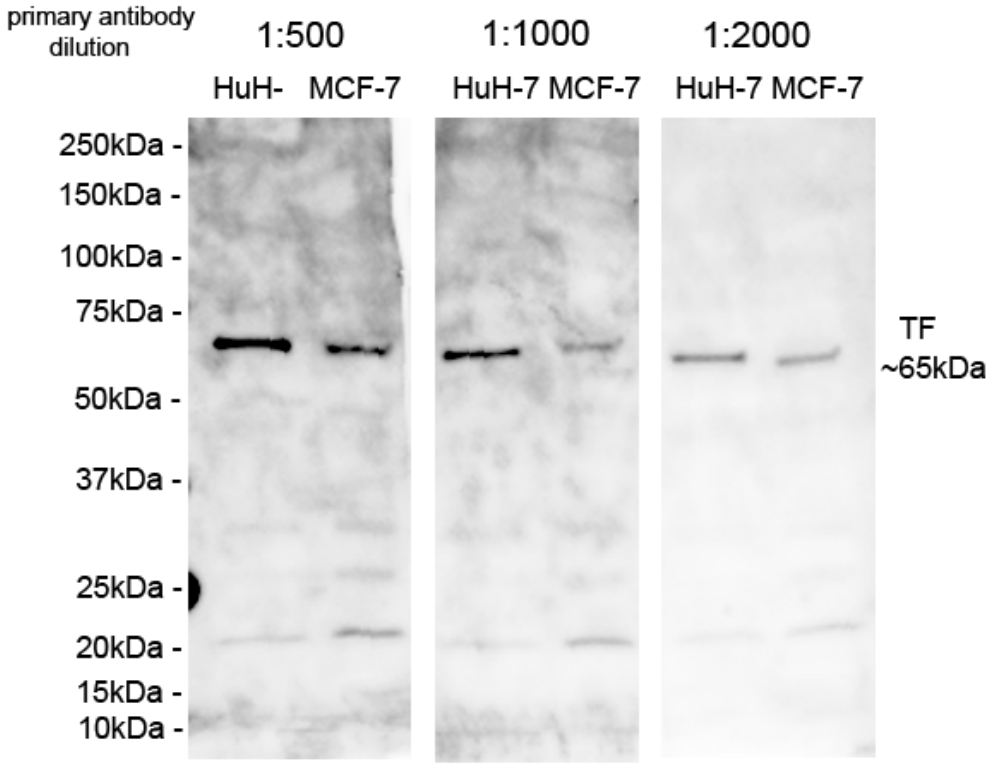

E Santa Cruz Rabbit anti-human ADATMS13 antibody

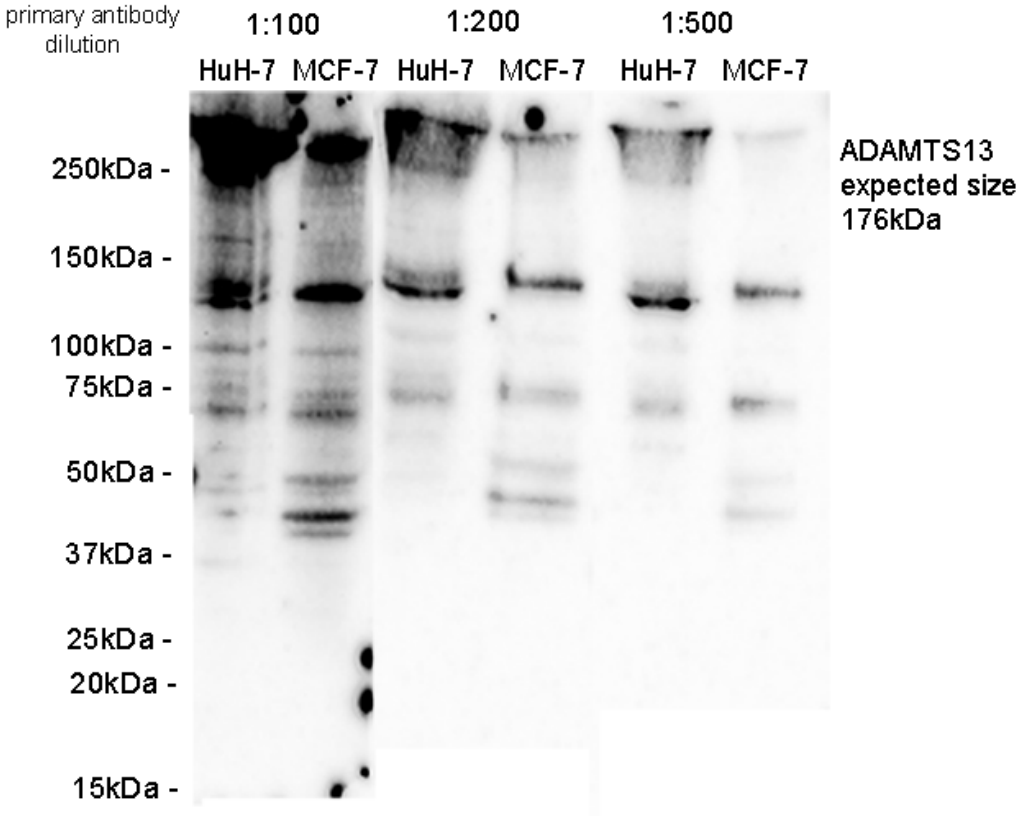

F Santa Cruz Rabbit anti-human THBS1 antibody

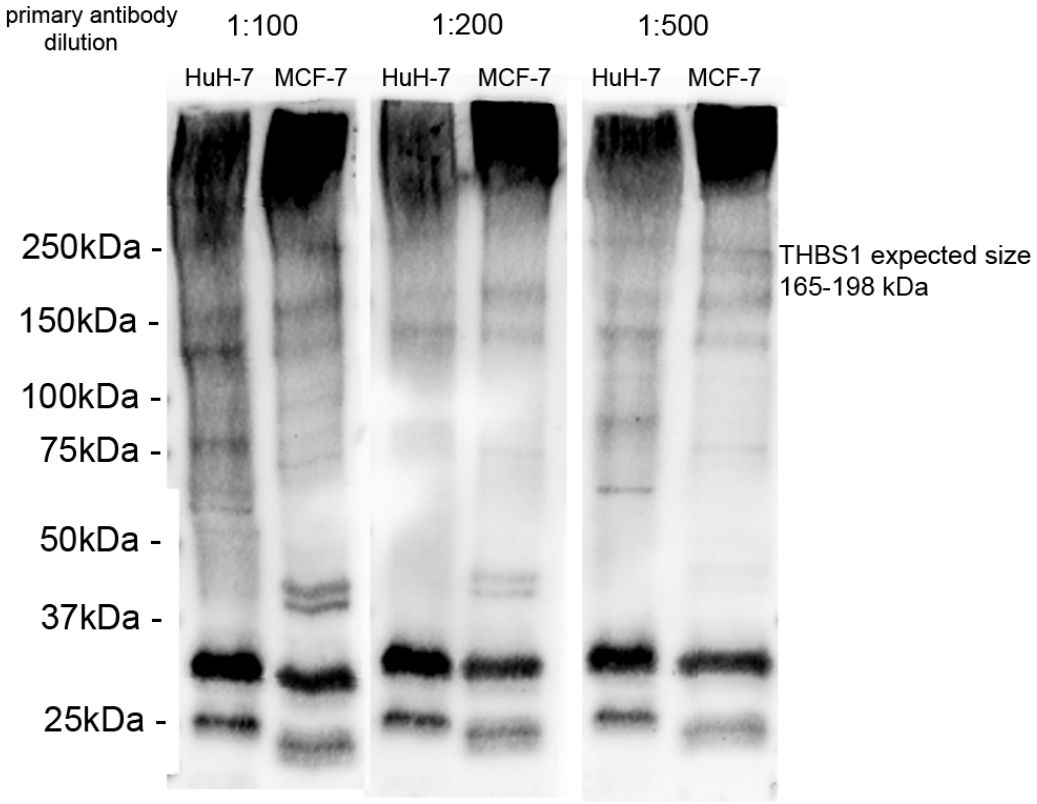

G Sigma-Aldrich Rabbit anti-human TFPI antibody

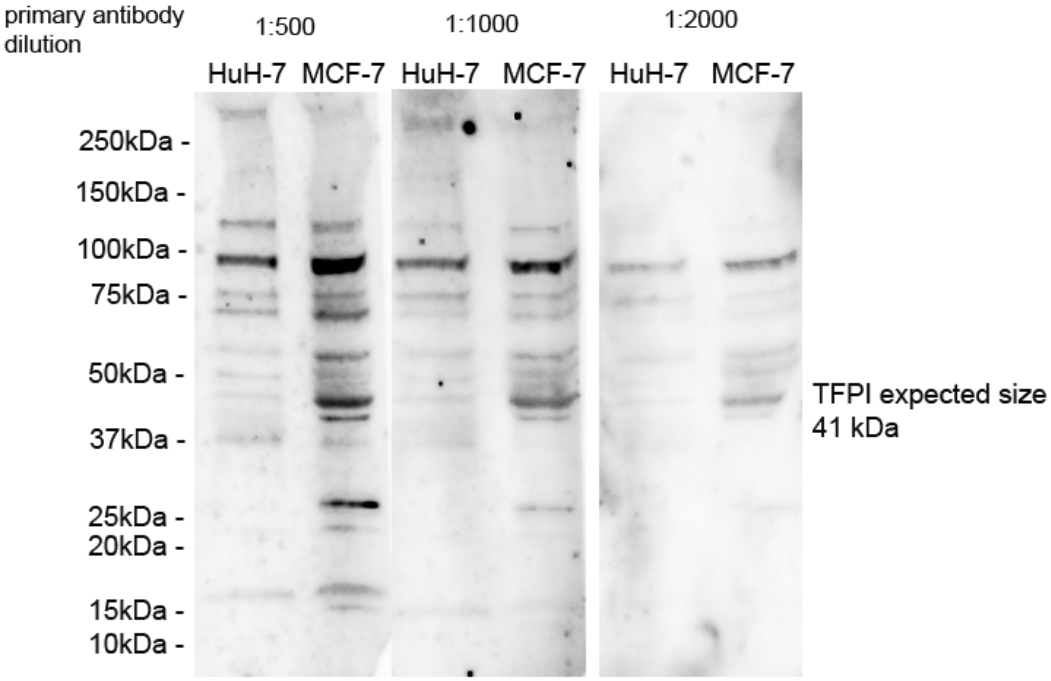

Figure 4.1 Primary antibodies optimised for immunoblot. Antibodies tested including rabbit anti-human PS antibody (A), rabbit anti-human PLG antibody (B), rabbit anti-human C4BPA antibody (C), rabbit anti-human TF antibody (D), rabbit anti-human ADAMTS13 antibody (E), mouse anti-human THBS1 antibody (F) and rabbit anti-human TFPI antibody (G). Optimum immunoblotting conditions for the PS, PLG, C4BPA and TF primary antibodies were determined.

4.2 Effects of miR-494 on different coagulation factors in HuH-7 cells

4.2.1 mRNA expression profile of PLG, C4BPA and TF in miR-494 transfected HuH-7 cells

To determine mRNA levels of *PLG*, *C4BPA* and *F3*, TaqMan® Gene Expression Assay was used in three independent transfections. *PROS1* mRNA was used a positive control. The mRNA levels of these coagulation factors were determined with 5.0nM miR-494 48h and 72h post-transfection. The mRNA levels of *PROS1* and *PLG* were significantly decreased at ~55% and ~38%, respectively ($p < 0.05$). The mRNA expression of *C4BPA* showed an increasing trend, by ~35%, but not statistically significant ($p = 0.06$). *F3* showed no significant changes in mRNA levels with miR-494 48h post-transfection. However, with 72h miR-494 post-transfection, the *F3* mRNA level was significantly increased by ~123% and the mRNA level of *PLG* was again significantly decreased by ~35% ($p < 0.05$). Taken together, RT-qPCR results demonstrated that exogenous miR-494 downregulated *PROS1* and *PLG* mRNA levels, and upregulated *C4BPA* mRNA level (Figure 4.2). However, there was no significant changes in the *F3* mRNA level at 48h post-transfection.

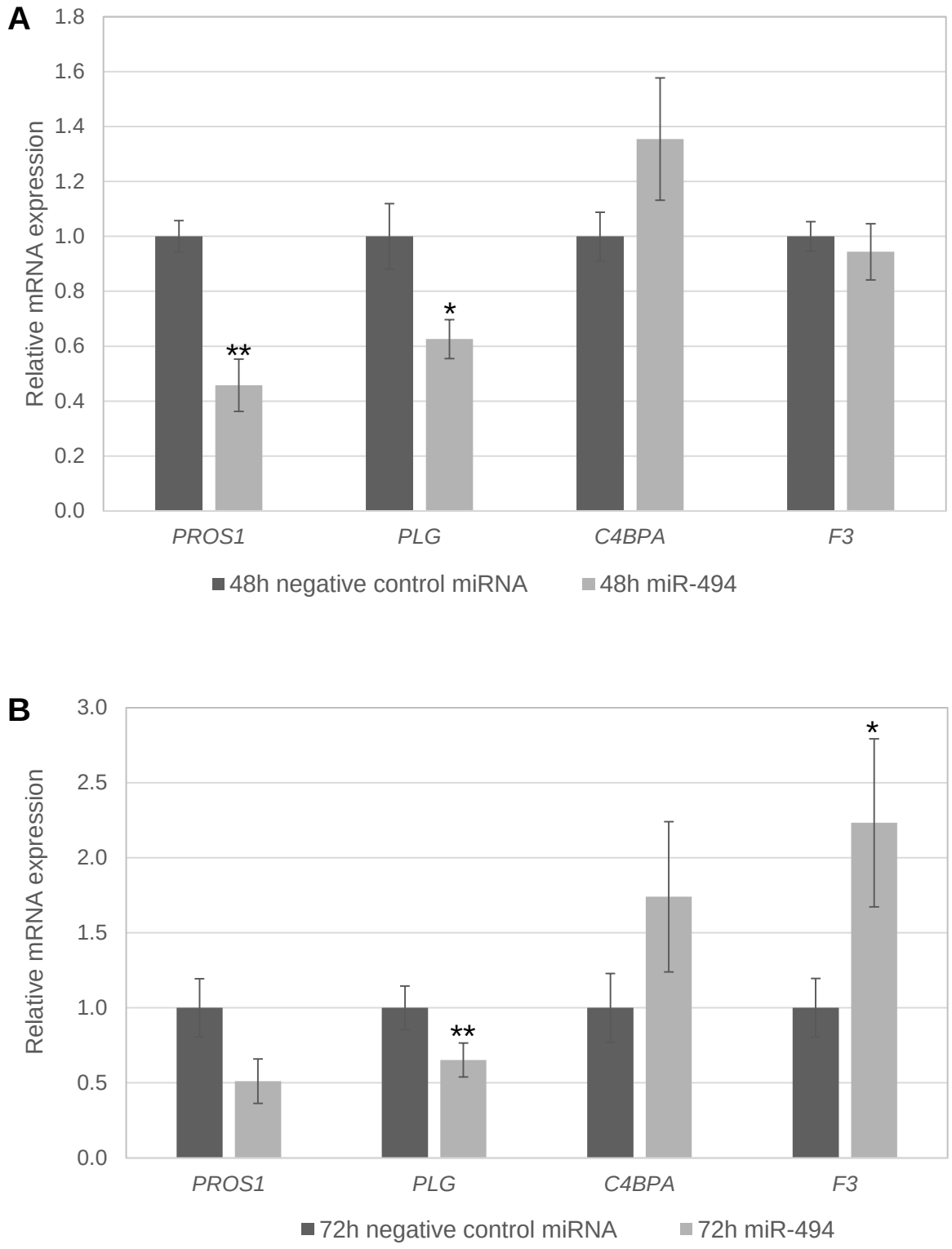

Figure 4.2. Effect of miR-494 in mRNA levels of coagulation factors in HuH-7 cells at 48h (A) and 72h (B) post-transfection. HuH-7 cells were transfected with 50nM negative control miRNA and miR-494, the transfected cells were harvested at 48h and 72h post-transfection. The mRNA levels were determined by RT-qPCR and normalised to three housekeeping genes (*18S*, *ACTB* and *GAPDH*), with the fold changes to mRNA levels calculated with $2^{-\Delta\Delta Ct}$. Results were from three independent transfections (* $p < 0.05$, ** $p < 0.01$).

4.2.2 Protein levels of PS, PLG, TF and C4BPA in miR-494 transfected HuH-7 cells

The protein expression of PS, PLG, TF and C4BPA from three independent miR-494 transfections were determined by western blot. The protein levels were normalised with actin and student's t-test was used in statistical analysis. The protein levels of PS and PLG were significantly decreased, by ~61% and ~69% respectively ($p < 0.05$), with 72h miR-494 post-transfection. At 48h post-transfection, the PS protein level was significantly decreased by ~50% ($p < 0.05$). However, there was no significant changes in the protein levels of C4BPA and TF at both 48h and 72h post-transfection. The protein expression of C4BPA was increased, by ~34% and ~60% respectively, at both 48h and 72h post-transfection. The TF protein level was decreased by ~56% at 72h post-transfection but no changes at 48h post-transfection. Therefore, exogenous miR-494 induced downregulation of PS, PLG and TF protein levels and upregulation of C4PBA protein level.

A

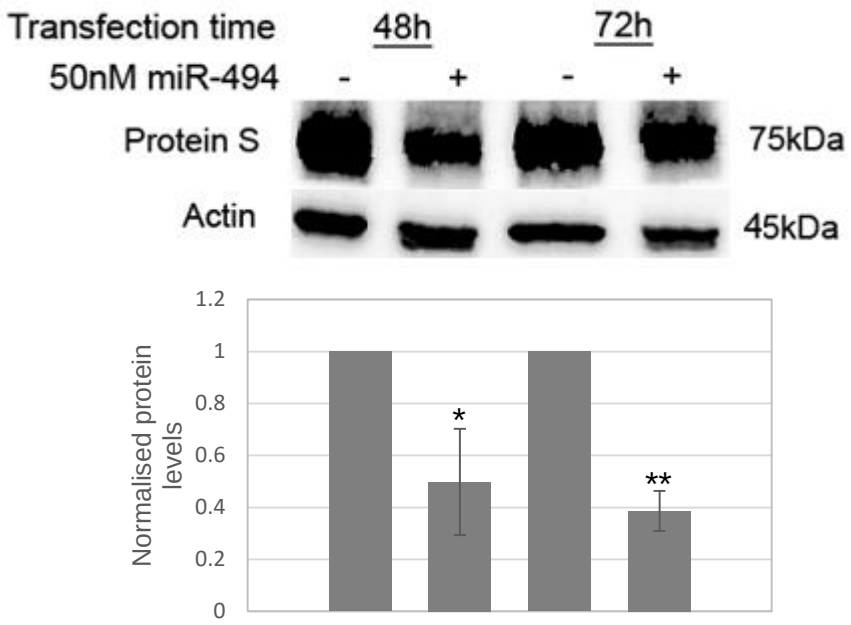
Transfection time
48h
72h
50nM miR-494
-
+
-
+
Protein S
75kDa
Actin
45kDa
Normalised protein levels
1.2
1
0.8
0.6
0.4
0.2
0
*
**

B

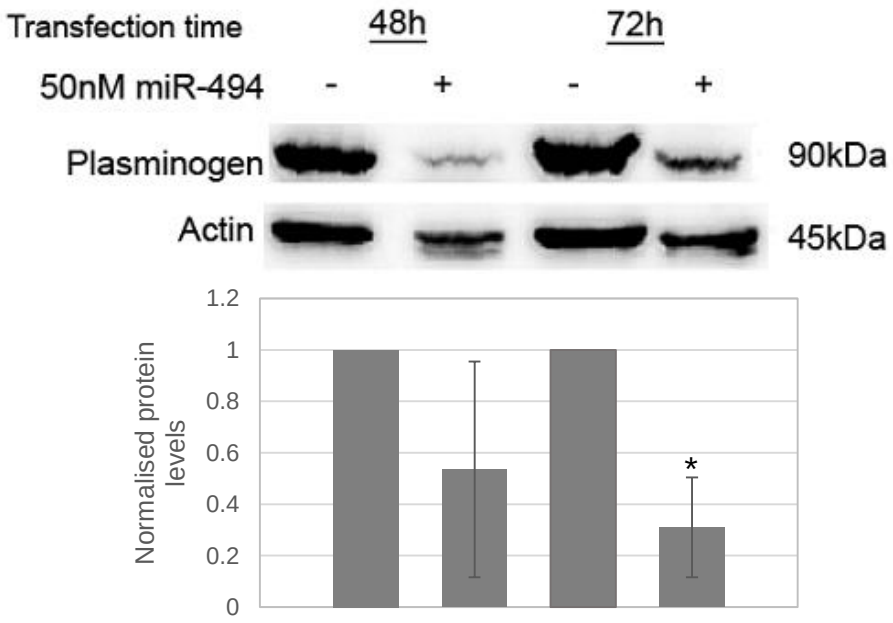
Transfection time
48h
72h
50nM miR-494
-
+
-
+
Plasminogen
90kDa
Actin
45kDa
Normalised protein levels
1.2
1
0.8
0.6
0.4
0.2
0
*

C

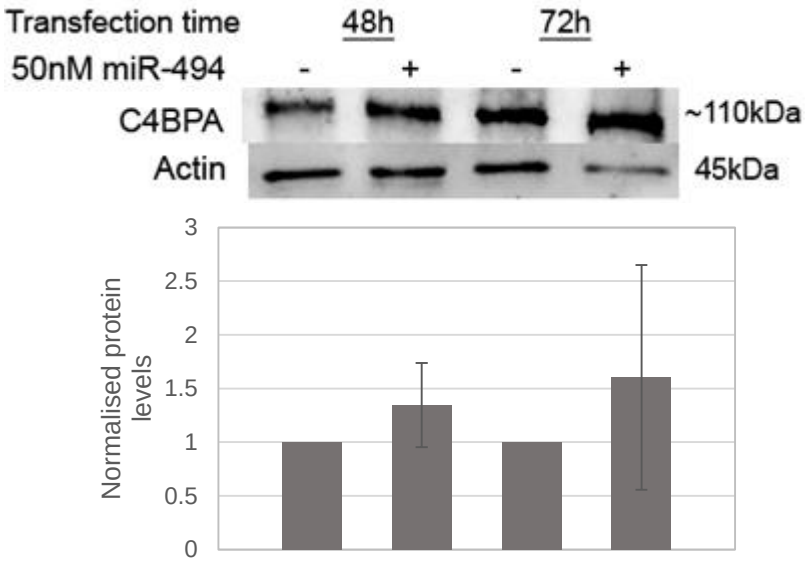

D

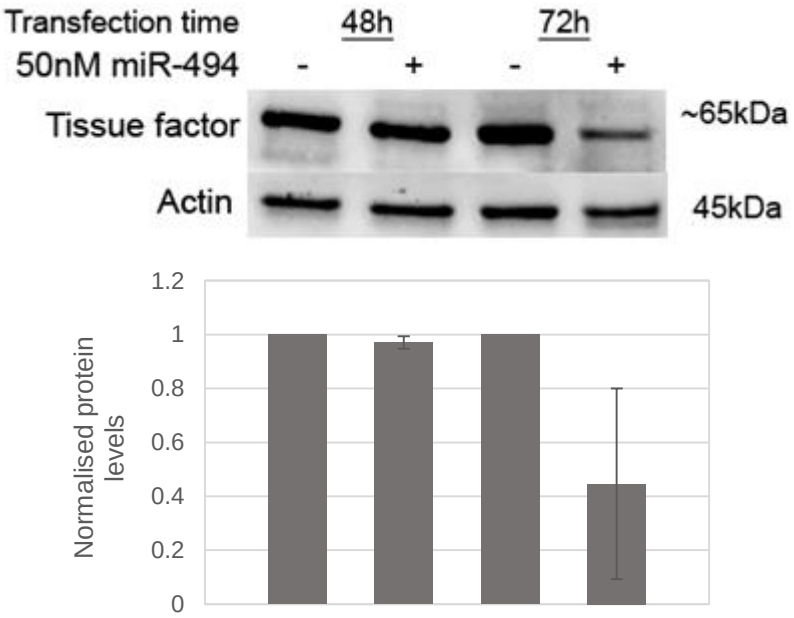

Figure 4.3 Effect of miR-494 in protein expression of Protein S (A), plasminogen (B), C4b binding protein (C) and tissue factor (D) at 48h and 72h post-transfection. The relative protein levels were determined by densitometry scanning of the protein bands and normalised to β-actin. Graphed results were from the combined analysis of three independent transfections (* $p < 0.05$, ** $p < 0.01$). The PS and PLG protein levels were significantly downregulated with miR-494 transfection (A and B). Unfortunately, there was no significant changes in the protein expression of C4BPA and TF with the presence of miR-494 (C and D).

4.3.3 mRNA levels of JUN, SP1 and STAT5B in miR-494 transfected HuH-7 cells

To determine the mRNA expression of the three transcription factors, HuH-7 cells were transfected with miR-494 for 48h and 72h and total RNA extracted for RT-qPCR. TaqMan® Gene Expression Assay was used and three independent transfections were performed to determine the expression of specific mRNA. The mRNA levels of *SP1* and *STAT5B* was significantly decreased, by ~38% and ~52% respectively ($p < 0.05$), at 48h miR-494 post-transfection (Figure 4.4). These results suggested that potential miR-494 binding sites may be present in the *SP1* and *STAT5B* 3'UTRs. Unexpectedly, there was no significant changes in the *JUN* mRNA levels even through a predicted miR-494 binding site was found in the 3'UTR sequence of *JUN*. At 72h miR-494 post-transfection, the mRNA levels of *SP1* and *STAT5B* were decreased and the *JUN* mRNA level was significantly upregulated. Taken together, RT-qPCR results also showed that exogenous miR-494 downregulated *SP1* and *STAT5B* mRNA levels.

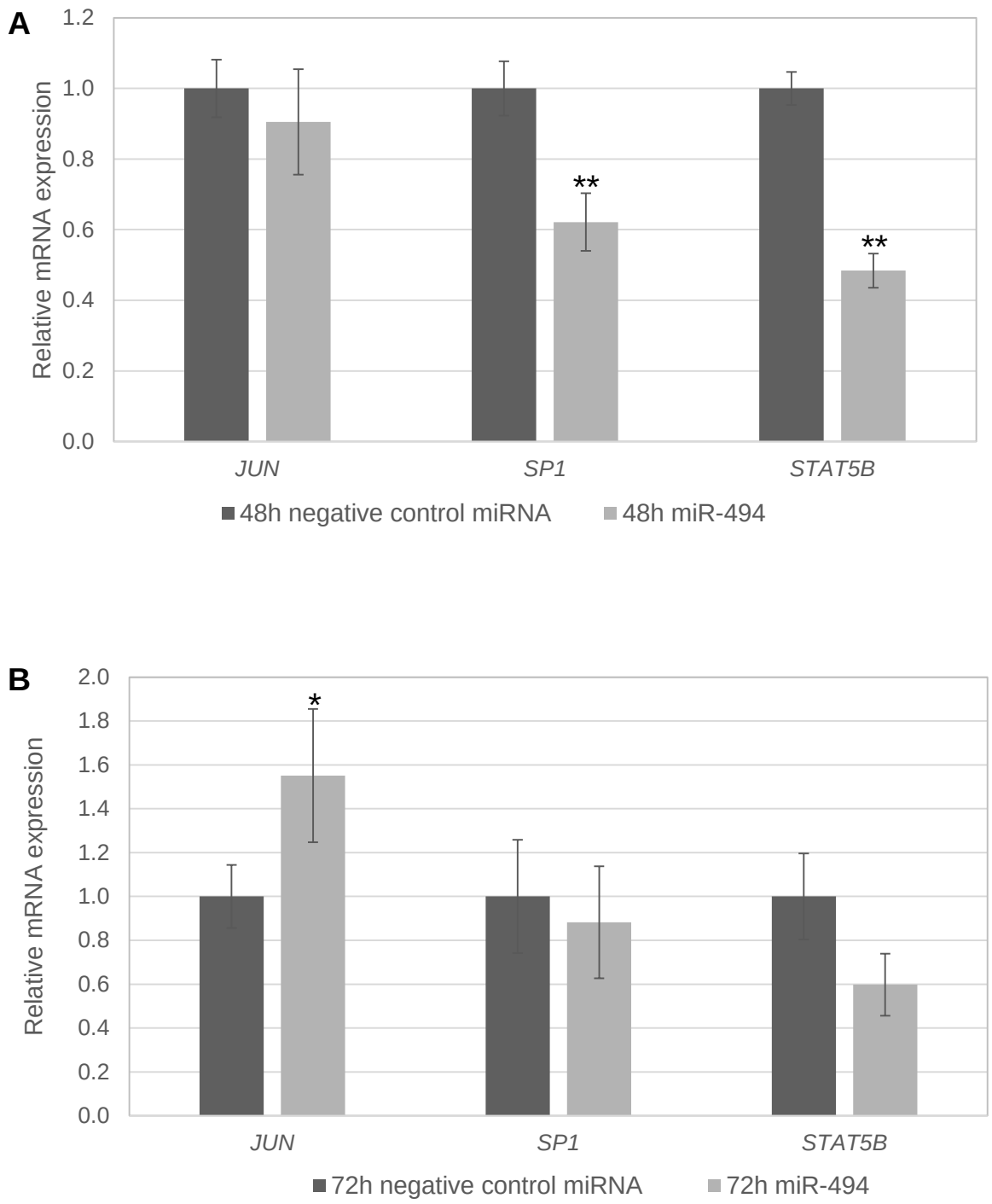

Figure 4.4. Effects of miR-494 in mRNA expression of transfection in HuH-7 cells at 48h (A) and 72h (B) post-transfection. HuH-7 cells were transfected with 50nM negative control miRNA and miR-494, the transfected cells were harvested at 48h and 72h post-transfection. The mRNA levels were determined by RT-qPCR and normalised to three housekeeping genes (*18S*, *ACTB* and *GAPDH*), with the fold changes to mRNA levels calculated with $2^{-\Delta\Delta Ct}$. Results were from three independent transfections (* $p < 0.05$, ** $p < 0.01$).

4.4 Computational analyses

4.4.1 Computational analyses of the JUN, SP1 and STAT5B 3'UTR sequences

Putative miR-494 binding sites were identified in the 3'UTR sequences of *JUN*, *SP1* and *STAT5B*. Using the bioinformatic algorithms (miRanda, TargetScan and RegRNA), a more negative score of predicted miR-494 binding site indicates a stronger binding interaction with miR-494. According to the scores of predicted miR-494 binding sites from RegRNA, the miR-494 binding site in *STAT5B*-3'UTR was stronger, when compared to the 3'UTR sequences of *JUN* and *SP1*, and binding site in the *SP1*-3'UTR was the weakest. A putative miR-494 binding site in the 3'UTR sequence of *JUN* were located near the end of the sequence (973-995). In contrast, the putative miR-494 binding site in the 3'UTR sequence of *SP1* (1337-1375) and *STAT5B* (44-66) were located in the middle or start of the sequence.

Table 4.3. Putative miR-494 binding sites in the 3'UTR sequence of *JUN, SP1* and *STAT5B*

3'UTR sequence	Putative miR-494 binding site	miRanda	TargetScan	RegRNA
JUN	3' cuccaaAGGGCAC-AUACAAAGu 5' JUN ||| ||||||| 973:5'aggataTCTTGTGCGATGTTTTCa 3'miR-494	-0.1095	-	-12.7
SP1	3' cucCAAAGGGCACAUACAAAGu 5' SP1 | |||:: || |||||: 1337:5' agtGGTTCTTATG-ATGTTTTc 3'miR-494	-	-	-9.1
STAT5B	3' cuccaaAGGGCACAUACAAAGu 5' STAT5B ||::||| |||||: 45:5'aatcacTCTTGTGGATGTTTTa 3' miR-494	-	-	-13.9

4.4.2 Computational analyses of PLG, F3 and C4BPA promoter regions

Two online transcription factor binding tools were used to identify the interaction between the three transcription factors (AP1, Sp1 and STAT5B) and the promoter region of *PLG, F3* and *C4BPA* genes. The online transcription factor binding tools, PROMO 3.0.2 and PROSCAN 1.7, showed that one or more AP1, Sp1 or STAT5B binding sites were found in the promoter region (up to 20kb upstream of transcription start site) of *PLG*, *TF* and *C4BPA* (Table 4.4.). The PROMO 3.0.2 results suggested that AP1 appeared to be targeting most of the coagulation factor, with 10, 18 and 19 predicted AP1 binding sites found in the promoter regions of *PLG*, *F3* and *C4BPA,* respectively. The promoter region of *F3* and *PLG* (from PROSCAN 1.7 results) contained a single Sp1 binding site. No Sp1 site was found in the *C4BPA* promoter; and no STAT5B binding site was found in the promoter region of the coagulation factors investigated.

Table 4.4. Predicted AP1, SP1 and STAT5B binding sites and dissimilarity of promoter region of *C4BPA*, *F3* and *PLG*.

20kb 5'flanking sequences	Predicted binding sites and dissimilarity							
	AP1				SP1		STAT5B	
	Sequence	dissimilarity	Sequence	dissimilarity	Sequence	dissimilarity	Sequence	dissimilarity
C4BPA	^{2219}TGACTTCTA^{2227}	13.50%	^{3371}TCAGAGTCA^{3379}	5.50%	--		--	
	^{3656}TGACTCATC^{3664}	0.00%	^{4300}TGACTTTTC^{4308}	13.57%	--		--	
	^{6410}TGACTGCTA^{6418}	13.84%	^{6695}AAGAAGTCA^{6703}	13.42%	--		--	
	^{7645}GATAAGTCA^{7633}	8.51%	^{7737}TGGCAGTCA^{7745}	13.90%	--		--	
	^{8645}AACAAGTCA^{8653}	14.68%	^{8917}CAAGAGTCA^{8925}	5.32%	--		--	
F3	^{544} ATAGAGTCA^{522}	5.46%	^{1236} TGACTACTG ^{1244}	13.67%	^{9795}AGGGCGGGAA^{9804}	2.52%		
	^{1617}GAAGAGTCA^{1625}	5.06%	^{1790}CAGAAGTCA^{1798}	13.33%	--		--	
	^{2536}AGGAAGTCA^{2544}	13.47%	^{3077}TGACTTCAA^{3085}	13.56%	--		--	
	^{3843}AAAAAGTCA^{3851}	13.92%	^{4976}TGACTTTGG^{4984}	13.84%	--		--	
	^{5549}TGACTAAAC^{5457}	8.91%	^{6624}TGACTGATT^{6632}	9.20%	--		--	
	^{7187}TGACTGTAA^{7195}	14.40%	^{7576}TGACTTTGC^{7584}	13.57%	--		--	
	^{7663}CCAAAGTCA^{7671}	13.84%	^{8495}TGACTTTTC^{8503}	13.57%	--		--	
	^{8724}TGACTTCTG^{8732}	13.33%	^{8930}CTGCAGTCA^{8938}	13.72%	--		--	
	^{9217}TGACTGACC^{9225}	8.91%	^{9755}TGACCTGT^{9763}	5.41%	--		--	
PLG	^{300}TGACTGAAC^{308}	8.91%	^{836}TGACTCTCA^{844}	5.55%	^{3061}GGCGG^{3065}	59.31	--	
	^{973}CGATAGTCA^{981}	14.23%	^{1381}GTTGAGTCA^{1389}	0.05%	--		--	
	^{1425}ATGGAGTCA^{1433}	4.96%	^{1505}TGACTTACC^{1513}	8.57%	--		--	
	^{2503}TCTCAGTCA^{2511}	9.29%	^{3086}ATTCAGTCA^{3094}	9.26%	--		--	
	^{3090}AGTCAGTCA^{3098}	9.26%	^{5157}TGACTGTCT^{5165}	14.32%	--		--	
	^{4268}GAGAAGTCA^{4276}	13.07%	^{4950}TGACTTATC^{4958}	8.51%	--		--	
	^{6221}TGACTTGGC^{6229}	14.33%	^{6890}TGACTTGTA^{6898}	14.77	--		--	
	^{7554}GAAAAGTCA^{7562}	13.57%	^{7855}TGAGAGTCA^{7863}	5.55%	--		--	
	^{8503}CCCAAGTCA^{8511}	14.59%	^{8801}GGTGAGTCA^{8809}	0.05%	--		--	
	^{9956}TGACTATCT^{9964}	14.32%						

4.4 Functional miR-494 binding sites in the SP1 and STAT5B 3'UTRs

Section 4.3.3 showed reduced mRNA levels of SP1 and STAT5B following miR-494 transfection. To determine the direct interaction between the miR-494 and the 3'UTR sequences of affected transcription factors, luciferase reporter constructs containing *PROS1*, *JUN, SP1* and *STAT5B*-3'UTR were produced. Functional miR-494 binding sites were identified in the previous study by Tay *et. al.* (2013), therefore, *PROS1*-3'UTR luciferase reporter construct was used as a positive control for this study. Dual luciferase reporter assay showed that the luciferase activity of *SP1* and *STAT5B*-3'UTR was significantly decreased, by ~12% and ~23% respectively ($p < 0.05$), with increasing miR-494 concentration. No significant changes was observed in the luciferase activity of the *JUN*-3'UTR reporter construct. Therefore, dual luciferase reporter assay results suggested that a functional miR-494 binding site was present in the 3'UTR sequence of *SP1* and *STAT5B.* The dual luciferase reporter assay results were concordant with the RT-qPCR results analysing the mRNA levels of *JUN, SP1* and *STAT5B* following miR-494 transfection.

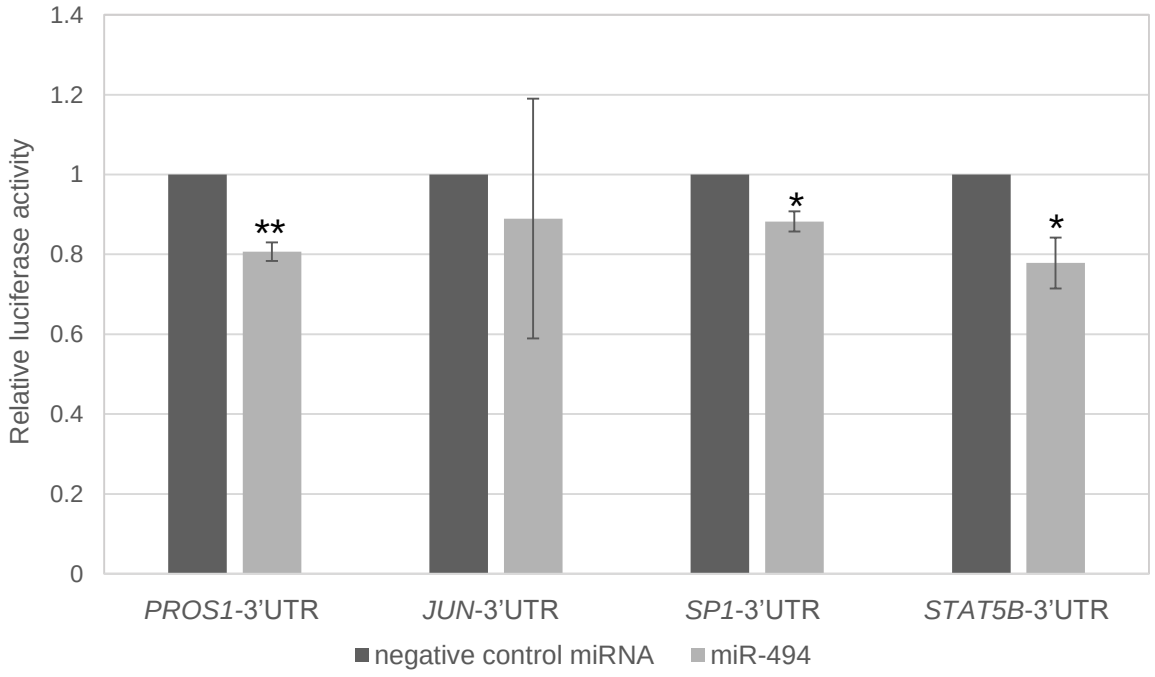

Figure 4.5 Direct interaction between the miR-494 and the transcription factors 3'UTRs. HuH-7 cells were cotransfected with pmiR-*PROS1, JUN, SP1* and *STAT5B*-3'UTRs luciferase reporter and 50nM negative control miRNA or 50nM miR-494. The luciferase activity were analysed at 24h post-transfection. Relative luciferase activity were determined by the ratio of Firefly and Renilla counts.

Chapter 5: Discussion

The roles of miRNAs have been identified in the regulation of key cellular processes and pathophysiology of various cancers. Recently, a number of miRNAs has been ascribed roles in regulating the coagulation cascade and haemostasis. Several miRNAs regulate the expression of microparticles in platelet aggregation or the development of megakaryocytes through targeting different transcription factors (Garzon *et. al.*, 2006; Landry *et. al.*, 2009). Moreover, multiple miRNAs regulate the expression of two major procoagulants, fibrinogen and TF (Fort *et. al.*, 2010; Li *et. al.*, 2014b). However, the role of miRNAs in coagulation and haemostasis is still poorly characterised. A recent study by Tay *et al.* (2013) reported that miR-494 directly downregulates the PS mRNA levels by binding to the *PROS1* mRNA-3'UTR. Further investigations on the miR-494 functions in coagulation demonstrated that overexpression of miR-494 in HuH-7 cells resulted in significant changes in the mRNA levels of multiple coagulation factors, including those lacking miR-494 binding sites in their 3'UTR sequences (Dr. Jasmine Tay, personal communication). These results strongly suggested that miR-494 plays an important role in coagulation and haemostasis, and may also be important in the development of thrombotic diseases. The present study demonstrated that miR-494 can directly or indirectly regulate multiple coagulation factors to promote thrombosis.

Seven untested primary antibodies required optimisation for immunoblotting experiments. Four of the seven primary antibodies (PS, PLG, C4BPA and TF) were optimised with the optimum dilutions, determined to be 1:1000, 1:500, 1:200 and 1:1000 respectively. The optimisation blot of PS and PLG primary antibodies showed that these two protein sizes were came out as expected. However, the observed protein size of C4BPA and TF was larger than the expected size possibly due to difference in SDS-PAGE resolution and/or post-translational modifications of these proteins.

SDS-PAGE migration is one of the explanation that observed C4BPA and TF protein sizes are not the same as their formula molecular weights. Rath *et al*. (2009) reported that the observed protein size of membrane proteins does not always correlate with calculated molecular weights. They suggested that altered SDS binding is mainly caused by abnormal protein-detergent contacts, such as incomplete denaturation. However, in some cases, SDS-PAGE migration can be caused by protein-protein contacts, suggesting that the protein folding may be involved in SDS-PAGE migration (Rath *et. al.*, 2009).

Post-translational modification (PTM), such as phosphorylation, sumoylation and ubiquitination, is an enzymatic modification of protein to increase functional diversity of a protein. Protein phosphorylation is one example of PTM which allows activation or inhibition of proteins by cleaving regulatory subunits or protein degradation. Several studies on phosphorylation of TF demonstrated that the cytoplasmic domain of TF, containing two phosphorylation sites, and is rapidly phosphorylated by the activation of protein C kinase α (Zioncheck *et. al.*, 1992; Dorfleutner and Ruf, 2003). Moreover, online prediction tools, NetPhosK 1.0 (http://www.cbs.dtu.dk/services/NetPhosK/), SUMOplot™ Analysis Program (http://www.abgent.com/sumoplot) and UbPred (http://www.ubpred.org/) were used for identifying protein phosphorylation, sumoylation, and ubiquitination sites in the peptide sequences. The results showed that multiple protein C kinase phosphorylation sites were identified in the TF and C4BPA proteins. Three predicted sumoylation sites and three predicted ubiquitination sites were found in the TF protein. In contrast, five predicted ubiquitination sites and eight sumoylation sites were found in the C4BPA protein. These suggested that PTM could explain the larger TF and C4BPA protein size shown in the optimisation blot. Moreover, PTM of coagulation factors is not only restricted in the TF and C4BPA proteins. Vitamin K-dependent plasma proteins, including Protein C (PC) and PS, are also modified during or after protein biosynthesis. The PTM of PC and PS is often through γ-carboxylation, undertaken by a vitamin K-dependent carboxylase to convert glutamate to carboxyglutamate; and N-linked

glycosylation (Walsh and Jefferis, 2006). Both γ-carboxylation and N-linked glycosylation are processed in the endoplasmic reticulum.

The TFPI, ADAMTS13 and THBS1 primary antibodies optimisation could not be completed in this study due to time constraints. The TFPI antibody optimisation blot showed that the protein of interest was presented in the MCF-7 cells but not in the HuH-7 cells. Under normal physiological condition, TFPI is primarily expressed in megakaryocytes and microvascular endothelial cells but not highly synthesised by hepatocytes (Osterud *et. al.*, 1995). Therefore, the HuH-7 cell line was not the best cell line for optimising the TFPI primary antibody. TFPI, ADATMS13 and THBS1 primary antibodies were blotted with two different blocking conditions, 3% and 5% (w/v) skim milk/TBST blotto blocking solution. Moreover, the SDS-PAGE gels for optimising the ADATMS13 and THBS1 primary antibodies were electrophoresed for 2.5 hours at a low constant amps (25mA). Therefore, the presence of multiple non-specific bands maybe caused by low quality primary or secondary antibodies. Further optimisation of the ADATMS13 and THBS1 primary antibodies is required for analysing their protein levels in miR-494 transfected HuH-7 cells.

The mRNA and protein levels of the four coagulation factors were determined in HuH-7 cells with the miR-494 transfection. According to the pervious results obtained in our laboratory, the mRNA expression of two anticoagulants, *PROS1* and *PLG,* was significantly decreased with increasing concentration of miR-494. Conversely, the mRNA level of multiple procoagulants, including *C4BPA* and *F3*, was significantly increased at 48h post-transfection (Tay *et al*. unpublished results). In this study, the results showed that only *PROS1* and *PLG* mRNA levels were significantly decreased at 48h post-transfection, which supported the previous results performed in the laboratory. There is a considerable trend towards significant change in

upregulation of *C4BPA* mRNA level at 48h miR-494 post-transfection. No changes in the *F3* mRNA levels were detected in miR-494 transfected HuH-7 cells.

In this study, the protein levels of PS, PLG, C4BPA and TF was determined at 48h and 72h miR-494 post-transfection in HuH-7 cells. Western blot results showed that exogenous miR-494 significantly downregulates the protein expression of PS and PLG, and upregulates the C4BPA protein level, which is concordant with the RT-qPCR results analysing their mRNA levels. Moreover, the RT-qPCR results showed that the *F3* mRNA levels were upregulated at 72h miR-494 post-transfection and no change was identified at 48h post-transfection. However, western blot results showed TF protein expression was downregulated at 72h miR-494 72h post-transfection, which did not correlate with its mRNA level. One explanation is that the western blot detected intracellular protein, whereas TF is naturally transported to the cell surface and secreted (Drake *et. al.*, 1989). This may be a possible explanation of negative correlation between TF mRNA and protein levels. Further investigations on the miR-494 effects of TF protein expression in the media are required. Taken together, the prothrombotic effect of miR-494 can be achieved through repressed PS and PLG expression, and enhanced C4BPA expression.

The results showed that functional miR-494 binding sites are present in the 3'UTR sequences of *SP1* and *STAT5B*, and the mRNA levels of *SP1* and *STAT5B* were significantly downregulated with miR-494 transfection. These suggested that miR-494 downregulates *SP1* and *STAT5B* mRNA levels by binding to the 3'UTR sequence of *SP1* and *STAT5B* mRNA transcripts. Moreover, the expression of PLG, which lacks a miR-494 binding sites in its 3'UTR sequence, was significantly downregulated with miR-494 transfection. Computational analysis showed that a predicted Sp1 binding site was found in the promoter region of human *PLG*

gene, which suggested that Sp1 may be a transcriptional activator or repressor of *PLG* gene. Taken together, miR-494 may downregulate the PLG expression indirectly by targeting SP1.

The results suggested that miR-494 directly downregulates *SP1* mRNA expression by binding to the *SP1* mRNA-3'UTR sequence. Sp1 is an important transcription factor in other cell signalling pathways (Figure 5.1), therefore, miR-494 may indirectly regulate multiple gene expression, such as p53 and p21, to inhibit tumourigenesis or regulate the cell cycle through Sp1 downregulation (Kavurma and Khachigian, 2004; Knappskog *et. al.*, 2011). In addition, miR-494 may regulate PLG expression through downregulating Sp1 expression because a predicted Sp1 transcription factor binding site was found in the promoter region of human PLG gene.

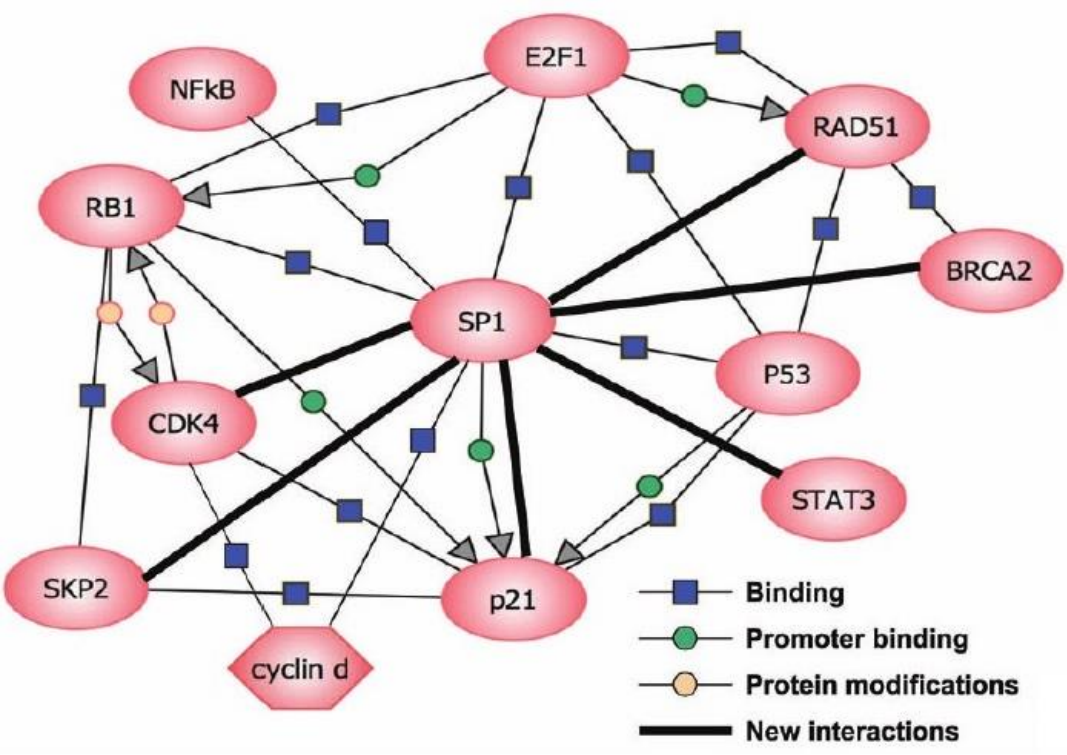

Figure 5.1 The interaction between Sp1 and different proteins (Tapias *et. al.*, 2008).

Sp1 regulates the expression of important transcription factors, such as p53, to inhibit tumourigenesis. Sp1 enhances the gene expression of E3 ubiquitin-protein ligase (MDM2), a key regulator of p53, via binding to the *MDM2* promoter region (Knappskog *et. al.*, 2011; Knappskog and Lonning, 2011). Increased expression of MDM2 results in the repression of p53 expression and the development of cancer. These suggested that miR-494 may enhance p53 expression via Sp1-mediated transcriptional regulation of MDM2, leading to the inhibition of tumourigenesis.

Sp1 can acts as both transcriptional activators and repressors to activate or repress the gene expression of *p21*, a cyclin-dependent kinase (CDK) inhibitor, through two different mechanism. Biggs *et al.* (1996) reported that Sp1 binding sites were identified in two major regions of the *p21* promoter. These Sp1 binding sites were essential for activating the *p21* transcription. Moreover, five Sp1-binding elements were identified in the promoter region of *p21* (Kavurma and Khachigian, 2004). Further studies on these Sp1-binding elements showed that mutations of two specific elements result in the activation of *p21* promoter, interestingly, mutations of three specific elements inactivate the *p21* promoter, which suggested that Sp1 regulates *p21* transcription via cis-acting positive and negative regulatory elements in the *p21* promoter (Kavurma and Khachigian, 2004). These two studies suggested that SP1 activates or represses the expression of p21. According to these studies, miR-494 can activate or repress the expression *p21* via the downregulation of Sp1 to regulate the cell cycle. Two studies on miR-494 functions in the regulation of cell cycle showed that miR-494 can inhibit or accelerate the G_1/S transition in the cell cycle. Olaru *et al.* (2011) suggested that miR-494 arrests the cell cycle at G_1/S transition through downregulation of CDK4, CDK6, CCND1, CCNE2 and HDAC1. However, Lim *et al* (2014) argued that miR-494 indirectly decreased the expression of p27 and p21 through directly inhibiting MCC expression, leading to accelerating G_1/S transition. Therefore, miR-494-mediated downregulation of Sp1 supported these two studies that miR-494 can inhibit and accelerate the G_1/S transition to regulate cell cycle. Taken

together, Sp1 decreases cancer susceptibility and regulates cell cycle through *MDM2* and *p21* genes.

Oestrogen responsive transcription factor, Sp1, regulates gene expression through the interaction between estrogen receptor alpha (ERα) and Sp1. Several gene expressions, including *KiSS1* and *TNFα*, are upregulated or downregulated via the interaction between ERα and Sp1 (Li *et. al.*, 2007). The Sp1 and Sp3 directly bind to the GC-rich motif in the promoter region of KiSS1. The expression of *KiSS1* gene is stably stimulated by the regulation of Sp1 and Sp3 without the presence of oestrogen (E_2). However, ERα is activated with the exposure of E_2 and binds to the Sp1/Sp3 binding sites to allow the activation or repression of *KiSS1* gene expression, which depends on the binding of a coactivator or corepressor to ERα (Li *et. al.*, 2007). Another study on the ERα-Sp1 interaction showed that high E_2 level enhances the *TNFα* gene transcription to induce apoptosis. Activated ERα interacts with the two Sp1 binding sites in the promoter region of *TNFα* to increase the expression of TNFα, leading to increased caspase-3 expression and induction of apoptosis (Tu *et. al.*, 2013). Therefore, these studies suggested that Sp1 can act as both transcriptional activators and repressors in different genes through the ERα-Sp1 interaction.

Moreover, several recent studies reported that high E_2 levels may cause thrombosis due to the downregulation of PS expression. Suzuki *et al.* (2010) reported that high E_2 concentration in $HepG_2$ cells results in suppression of *PROS1* gene expression through the interaction of Sp1 and ERα in the promoter region of *PROS1*. They suggested that, without E_2 stimulation, Sp1 and Sp3 upregulate the *PROS1* gene expression through other transcriptional coactivators. However, with the exposure of E_2, ERα interacts with the Sp1 binding sites in the promoter region of *PROS1*. These results in suppression of *PROS1* gene expression due to histone deacetylation of *PROS1* gene. Another study by Tay *et al.* (2013) further confirmed

that increased E_2 concentration in HuH-7 cells downregulates *PROS1* mRNA expression via a direct interaction between miR-494 and the 3'UTR sequence of *PROS1* mRNA transcript. In this study, the results showed that miR-494 downregulates *SP1* mRNA expression through the direct interaction of miR-494 and the *SP1* mRNA-3'UTR. At least four functional Sp1 binding sites are identified in the promoter region of *PROS1*, with two binding sites are essential for trans-activating the *PROS1* promoter (de Wolf *et. al.*, 2006). These studies confirmed that high E_2 levels in human liver cells downregulate PS expression through the upregulation of miR-494 or the ERα-Sp1 interaction in the *PROS1* promoter region. In addition, a study by deGraffenired *et al.* (2002) demonstrated that the expression of Sp1 is critical for the ERα gene transcription. They reported that two Sp1 binding sites are identified in the three essential elements for full ERα promoter activity. Increased expression of Sp1 and Sp3 leads to elevated ERα promoter activity, which suggested that these two transcription factors are able to enhance the ERα expression (deGraffenried *et. al.*, 2002). These suggested that the downregulation of Sp1 may reduce the repressive effects on the *PROS1* promoter region via ERα-Sp1 interaction (Figure 5.2). Overall, high E_2 concentration results in decreased *PROS1* expression because the Sp1 effects on the ERα promoter region is relatively small.

The Sp1 transcription factor targets the *PLG* promoter region to enhance its promoter activity. In this study, computational analyses suggested that a predicted Sp1 binding site is present in the promoter region of *PLG* (section 4.4.2). Furthermore, a study on Sp1 binding sites in murine *PLG* promoter suggested that two Sp1 binding sites are identified in the promoter region of murine *PLG* gene, and are required for the full response of *PLG* promoter activity. The presence of these Sp1 binding sites increased the *PLG* promoter activity, which suggests Sp1 acts as a transcriptional activator in the promoter region of *PLG* (Gutierrez-Fernandez *et. al.*, 2007). This study may explain the downregulation of PLG with the presence of miR-494. miR-494 directly represses the mRNA levels of *SP1* by binding to the 3'UTR sequence of *SP1*

mRNA transcript, which results in decreased mRNA and protein expression of PLG. However, this report studied the promoter region of murine *PLG* gene in neuroendocrine tissue rather than human *PLG* gene. Therefore, a further study on the interaction between Sp1 and the human *PLG* promoter region is required to confirm miR-494-mediated Sp1 downregulation could cause PLG downregulation.

Taken together, we hypothesise oestrogen overexpression results in increased miR-494 expression. Upregulation of miR-494 downregulates the mRNA expression of Sp1 by directly binding to *SP1* mRNA-3'UTR sequences, and the Sp1 downregulation results in reduction of PLG expression and further downregulated PS expression (Figure 5.2).

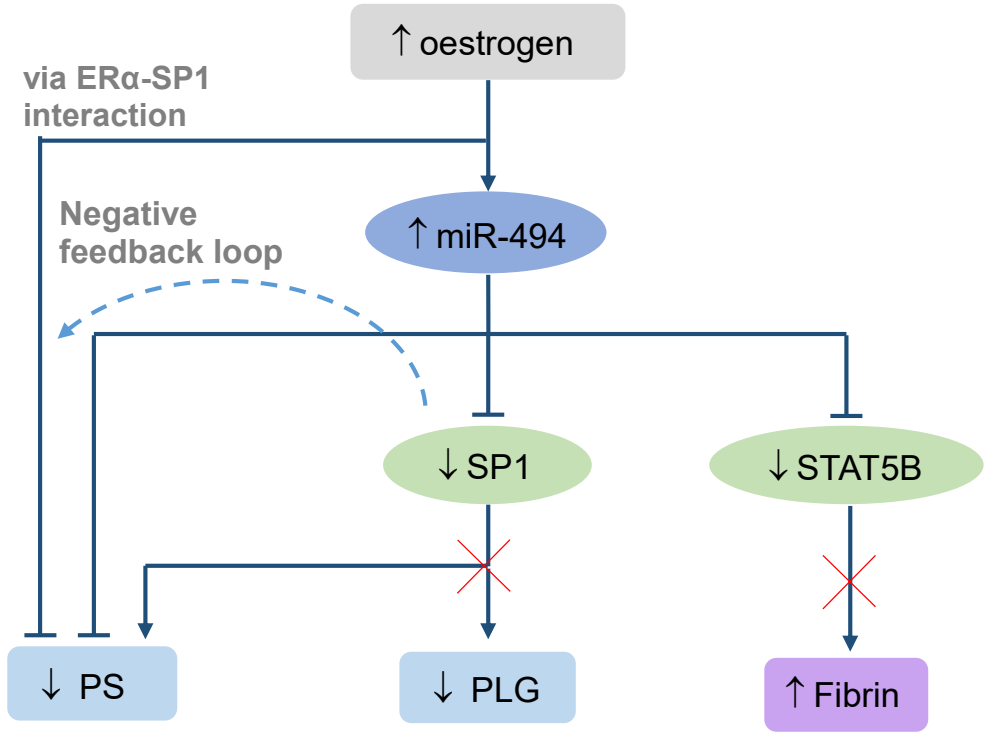

Figure 5.2 The effects of overexpressed miR-494 by increasing circulating oestrogen levels in coagulation and haemostasis.

The results showed that miR-494 directly downregulates STAT5B mRNA levels by binding to the 3'UTR sequence of *STAT5B* mRNA transcript. STAT5B is an important transcription factor in the kinase signalling and various cell signalling pathways, such as the JAK-STAT and the Protein kinase B (AKT) signalling pathways (Nyga *et. al.*, 2005; Bibi *et. al.*, 2014; Dalgic *et. al.*, 2015). Therefore, miR-494 may indirectly regulate these cell signalling pathways through STAT5B repression. Moreover, the STAT5-knockdown mouse model showed increase thrombotic susceptibility through accelerating the formation of fibrin, which suggested that miR-494 may cause acceleration of fibrin formation through STAT5B downregulation (Nordstrom *et. al.*, 2010).

STAT5B may have an important role in coagulation and haemostasis. The absence of STAT5B induces fibrin clot formation and increases thrombosis susceptibility. Nordstrom *et. al.* (2010) demonstrated that the mice deficient in STAT5A and STAT5B have a higher risk in developing thrombotic diseases. The clotting time is shorter with the absence of STAT5A and STAT5B. Moreover, the rate of fibrin polymerisation is significantly increased in the plasma of STAT5-deficient mice. However, no changes are found in the thrombin generation (Nordstrom *et. al.*, 2010). They suggested that the fibrin clot formation in the STAT5-deficient mice is due to the reduction of an unknown circulating inhibitor concentration, rather than the activation of intrinsic or extrinsic pathway or increased numbers of thrombin in the plasma (Nordstrom *et. al.*, 2010). They also demonstrated that this circulating inhibitor cleaves fibrinopeptide B (FpB) through the regulation of thrombin. Another studies on specific deletion of STAT5A and STAT5B in hepatocyte causes increased thrombosis susceptibility through significantly shortened clotting times (Nordstrom *et. al.*, 2010). Therefore, miR-494 may induce fibrin clot formation and increase the thrombosis susceptibility through downregulating STAT5B (Figure 5.2). Moreover, we believed that one or more hidden STAT5B binding site(s) may reside in the *PLG* promoter to cause the acceleration of fibrin formation through the fibrinolytic pathway,

however, further investigations are required for explaining the mechanism of accelerating fibrin formation with the absence of STAT5B.

Future directions

The results of the project provided insight into the potential role(s) of miR-494 in haemostasis and thrombosis. The exact roles of miR-494 in coagulation and haemostasis, however, warrants further investigation.

The results showed that TF protein expression does not correlated with its mRNA levels (chapter 4.2). The discrepancy is possibly caused by measuring the intracellular fraction of a naturally secreted protein. The methodology used in this study focused on the intracellular protein levels but not the extracellular protein levels. TF is an important coagulation factor in the coagulation cascade and haemostasis, therefore, answering the question over the negative correlation between TF mRNA and protein expression is necessary. Therefore, the TF protein expression at the cell surface, as well as secreted forms, requires further investigation.

Apart from regulating *PROS1, PLG* and *C4BPA* gene expression, miR-494 may regulate other coagulation factors expression. Several studies suggested that Sp1 targets the promoter region of multiple coagulation factors to enhance their gene expression. Functional Sp1 binding sites are identified in the promoter region of several coagulation factors, including tissue factor pathway inhibitor 2 (TFPI2), Protein C inhibitor (PCI) and plasminogen activator inhibitor-1 (PAI-1). Zerrouqi *et al.* (2014) reported that functional Sp1 binding sites are found in the promoter region of human *TFPI2* gene. The expression of TFPI2 is upregulated with the presence of Sp1. In addition, Hayashi *et al.* (1998) suggested that another Sp1 binding site

is identified in the promoter region of human *PCI* gene, which is an inhibitor of the anticoagulant, Protein C. These studies showed that multiple functional Sp1 binding sites were identified in the promoter region of several anticoagulant genes, which suggested that miR-494 may indirectly downregulate these coagulation factors by targeting Sp1. However, Sp1 binding sites are found in one of the procoagulants, PAI-1, promoter region. The function of PAI-1 is to inhibit fibrinolysis via inhibiting t-PA and u-PA. Two adjacent Sp1 binding sites are identified in the promoter region of human PAI-1, and Sp1 acts as a transcriptional activator in the promoter region of PAI-1 (Chen *et. al.*, 1998). These studies suggested that the effects of miR-494 may not be restricted in PS, PLG and C4BPA, and further studies on miR-494 effects in these coagulation factors are required.

In this study, computational analysis was used for predicting miR-494 binding sites in the 3'UTR sequence of *JUN, SP1* and *STAT5B*, however, these prediction tools are limited to analysing canonical sequences. Novel miR-494 binding sites may still exist in the 3'UTR sequences of *SP1* and *STAT5B* mRNA transcripts. Therefore, RNA sequencing may be a better methodology to determine the direct interaction between miR-494 and the 3'UTR sequence of multiple transcription factors. Moreover, this study focused on determining the miR-494 effects on different coagulation factors in HuH-7 cells. The biological activities in human cell lines sometimes are different to normal cells. Future studies may also focus on the endogenous miR-494 effects in other biologically relevant cell types.

Evidence suggested that miR-223 regulates the coagulation cascade and platelet aggregation. miR-223 directly downregulates TF expression to regulate the coagulation cascade (Li *et. al.*, 2014b). In platelet aggregation, miR-223 has been shown to target different genes that involved in platelets and regulate platelet aggregation, including $P2Y_{12}$ (Landry *et. al.*, 2009). $P2Y_{12}$ is a seven transmembrane G_i-coupled receptor involved in haemostasis, for

example, platelet aggregation and platelet granule secretion. The formation of Ago2-miR-223 complex negatively regulates mRNA and protein expression of $P2Y_{12}$ via direct targeting its 3'UTR sequence. Landry *et al.* (2009) also suggested that, due to the lack of nuclear components, Drosha and DGCR8, in platelets, the pre-miRNAs in platelets are produced and processed in megakaryocyte precursor cells and transferred into platelets. Therefore, the roles of miRNAs is not only restricted in regulating of the coagulation cascade. The results in this study showed that miR-494 regulates multiple coagulation factors expression to promote thrombosis, however, it may also have a role in regulating platelet aggregation. Future study on the miR-494 effects in platelet aggregation will be investigated in human plasma samples and megakaryocytic cell lines.

To conclude, the role of miRNAs in coagulation and haemostasis is still poorly characterised. A recent study suggested that miR-494 directly downregulates *PROS1* mRNA expression by binding to the 3'UTR sequence of its mRNA transcript, which suggested that it may have a role in coagulation. This study demonstrated that miR-494 regulates multiple coagulation factors and transcription factors expression. miR-494 significantly downregulates the expression of PS and PLG, and upregulates the C4BPA expression. Moreover, miR-494 directly downregulates the Sp1 and STAT5B expression through binding to the *SP1* and *STAT5B* mRNA-3'UTR sequences. These suggested that miR-494 may indirectly downregulate PLG through repressing Sp1 expression. Taken together, these results suggested that miR-494 may have a prothrombotic effect in human liver cells.

Chapter 6: References

Adams, R. L. & Bird, J. B. 2009. Review article: Coagulation cascade and therapeutics update: Relevance to nephrology. Part 1: Overview of coagulation, thrombophilias and history of anticoagulants. *Nephrology,* 14(5): 462-470.

Ahmad, S. S., Rawala-Sheikh, R. & Walsh, P. N. 1992. Components and assembly of the factor X activating complex. *Seminars in Thrombosis and Hemostasis,* 18(3): 311323.

Anbazhagan, A. N., Priyamvada, S., Kumar, A., Maher, D. B., Borthakur, A., Alrefai, W. A., Malakooti, J., Kwon, J. H. & Dudeja, P. K. 2014. Translational repression of SLC26A3 by miR-494 in intestinal epithelial cells. *American Journal of Physiology - Gastrointestinal and Liver Physiology,* 306(2): 123-131.

Asuthkar, S., Velpula, K. K., Nalla, A. K., Gogineni, V. R., Gondi, C. S. & Rao, J. S. 2014. Irradiation-induced angiogenesis is associated with an MMP-9-miR-494-syndecan-1 regulatory loop in medulloblastoma cells. *Oncogene,* 33(15): 1922-1933.

Bai, Y., Sun, Y., Peng, J., Liao, H., Gao, H., Guo, Y. & Guo, L. 2014. Overexpression of secretagogin inhibits cell apoptosis and induces chemoresistance in small cell lung cancer under the regulation of miR-494. *Oncotarget,* 5(17): 7760-7775.

Bennett, J. S. 2005. Structure and function of the platelet integrin alphaIIbbeta3. *The Journal of Clinical Investigation,* 115(12): 3363-3369.

Bertina, R. M. Nomenclature proposal for Protein S deficiency. XXXVI Annual meeting of the Scientific and Standardization Committee of the International Society for Thrombosis and Haemostasis, June 1990 Barcelona, Spain.

Betel, D., Wilson, M., Gabow, A., Marks, D. S. & Sander, C. 2008. The microRNA.org resource: targets and expression. *Nucleic Acids Research,* 36(Database issue): D149-153.

Bibi, S., Arslanhan, M. D., Langenfeld, F., Jeanningros, S., Cerny-Reiterer, S., Hadzijusufovic, E., Tchertanov, L., Moriggl, R., Valent, P. & Arock, M. 2014. Cooperating STAT5 and AKT signaling pathways in chronic myeloid leukemia and mastocytosis: possible new targets of therapy. *Haematologica,* 99(3): 417-429.

Biggs, J. R., Kudlow, J. E. & Kraft, A. S. 1996. The role of the transcription factor Sp1 in regulating the expression of the WAF1/CIP1 gene in U937 leukemic cells. *The Journal of Biological Chemistry,* 271(2): 901-906.

Camerer, E., Kolsto, A. B. & Prydz, H. 1996. Cell biology of tissue factor, the principal initiator of blood coagulation. *Thrombosis Research,* 81(1): 1-41.

Carmell, M. A. & Hannon, G. J. 2004. RNase III enzymes and the initiation of gene silencing. *Nature Structural & Molecular Biology,* 11(3): 214-218.

Carroll, A. P., Goodall, G. J. & Liu, B. 2014. Understanding principles of miRNA target recognition and function through integrated biological and bioinformatics approaches. *Wiley Interdiscip Rev RNA,* 5(3): 361-379.

Castoldi, E., Maurissen, L. F. A., Tormene, D., Spiezia, L., Gavasso, S., Radu, C., Hackeng, T. M., Rosing, J. & Simioni, P. 2010. Similar hypercoagulable state and thrombosis risk in type I and type III protein S-deficient individuals from families with mixed type I/III protein S deficiency. *Haematologica,* 95(9): 1563-1571.

Cattaneo, M., Gachet, C., Cazenave, J.-P. & Packham, M. A. 2002. Adenosine diphosphate (ADP) does not induce thromboxane A2 generation in human platelets. *Blood,* 99(10): 3868-3870.

Chai, J., Dong, W., Xie, C., Wang, L., Han, D. L., Wang, S., Guo, H. L. & Zhang, Z. L. 2015. MicroRNA-494 sensitizes colon cancer cells to fluorouracil through regulation of DPYD. *IUBMB Life,* 67(3): 191-201.

Chang, T.-H., Huang, H.-Y., Hsu, J. B.-K., Weng, S.-L., Horng, J.-T. & Huang, H.-D. 2013. An enhanced computational platform for investigating the roles of regulatory RNA and for identifying functional RNA motifs. *BMC Bioinformatics,* 14(Suppl 2): S4.

Chapin, J. C. & Hajjar, K. A. 2015. Fibrinolysis and the control of blood coagulation. *Blood Reviews,* 29(1): 17-24.

Chen, B., Hou, Z., Li, C. & Tong, Y. 2015a. MiRNA-494 inhibits metastasis of cervical cancer through Pttg1. *Tumour Biology*: [Epub ahead of print].

Chen, H. H., Huang, W. T., Yang, L. W. & Lin, C. W. 2015b. The PTEN-AKT-mTOR/RICTOR pathway in nasal natural killer cell lymphoma is activated by miR-494-3p via PTEN but inhibited by miR-142-3p via RICTOR. *The American Journal of Pathology,* 185(5): 1487-1499.

Chen, S., Zhao, G., Miao, H., Tang, R., Song, Y., Hu, Y., Wang, Z. & Hou, Y. 2015c. MicroRNA-494 inhibits the growth and angiogenesis-regulating potential of mesenchymal stem cells. *FEBS Letters,* 589(6): 710-717.

Chen, Y. Q., Su, M., Walia, R. R., Hao, Q., Covington, J. W. & Vaughan, D. E. 1998. Sp1 sites mediate activation of the plasminogen activator inhibitor-1 promoter by glucose in vascular smooth muscle cells. *The Journal of Biological Chemistry,* 273(14): 82258231.

Cho, E. J., Kim, Y. C., Hwang, J. H., Lee, H., Park, S. S., Kim, S. Y., Kim, S. & Chin, H. J. 2012. Inherited protein S deficiency due to a novel nonsense mutation in the PROS1 gene in the patient with recurrent vascular access thrombosis: A case report. *Kidney Research and Clinical Practice,* 31(1): 72-75.

Chuang, K. H., Whitney-Miller, C. L., Chu, C. Y., Zhou, Z., Dokus, M. K., Schmit, S. & Barry, C. T. 2015. MicroRNA-494 is a master epigenetic regulator of multiple invasionsuppressor microRNAs by targeting ten eleven translocation 1 in invasive human hepatocellular carcinoma tumors. *Hepatology*: [Epub ahead of print].

Clemetson, K. J. 2012. Platelets and primary haemostasis. *Thrombosis Research,* 129(3): 220-224.

Dahlback, B. 1991. Protein S and C4b-binding protein: Components involved in the regulation of the protein C anticoagulant system. *Thrombosis and Haemostasis,* 66(1): 49-61.

Dahlback, B. & Villoutreix, B. O. 2005. Regulation of blood coagulation by the protein C anticoagulant pathway: novel insights into structure-function relationships and molecular recognition. *Arteriosclerosis, Thrombosis, and Vascular Biology,* 25(7): 1311-1320.

Dalgic, C. T., Kaymaz, B. T., Ozkan, M. C., Dalmizrak, A., Sahin, F. & Saydam, G. 2015. Investigating the Role of JAK/STAT Pathway on Dasatinib-Induced Apoptosis for CML Cell Model K562. *Clinical Lymphoma Myeloma and Leukemia,* 15 Suppl: S161166.

Davie, E. W. & Ratnoff, O. D. 1964. Waterfall sequence for intrinsic blood clotting. *Science,* 145(3638): 1310-1312.

De Wolf, C. J., Cupers, R. M., Bertina, R. M. & Vos, H. L. 2006. The constitutive expression of anticoagulant protein S is regulated through multiple binding sites for Sp1 and Sp3 transcription factors in the protein S gene promoter. *The Journal of Biological Chemistry,* 281(26): 17635-17643.

Degraffenried, L. A., Hilsenbeck, S. G. & Fuqua, S. A. 2002. Sp1 is essential for estrogen receptor alpha gene transcription. *The Journal of Steroid Biochemistry and Molecular Biology,* 82(1): 7-18.

Dorfleutner, A. & Ruf, W. 2003. Regulation of tissue factor cytoplasmic domain phosphorylation by palmitoylation. *Blood,* 102(12): 3998-4005.

Drake, T. A., Morrissey, J. H. & Edgington, T. S. 1989. Selective cellular expression of tissue factor in human tissues. Implications for disorders of hemostasis and thrombosis. *American Journal of Pathology,* 134(5): 1087-1097.

Duan, H., Jiang, Y., Zhang, H. & Wu, Y. 2010. MiR-320 and miR-494 affect cell cycles of primary murine bronchial epithelial cells exposed to benzo[a]pyrene. *Toxicology in Vitro,* 24(3): 928-935.

Duan, H. F., Li, X. Q., Hu, H. Y., Li, Y. C., Cai, Z., Mei, X. S., Yu, P., Nie, L. P., Zhang, W., Yu, Z. D. & Nie, G. H. 2015a. Functional elucidation of miR-494 in the tumorigenesis of nasopharyngeal carcinoma. *Tumor Biology*: [Epub ahead of print].

Duan, Q., Yang, L., Gong, W., Chaugai, S., Wang, F., Chen, C., Wang, P., Zou, M. H. & Wang, D. W. 2015b. MicroRNA-214 Is Upregulated in Heart Failure Patients and Suppresses XBP1-Mediated Endothelial Cells Angiogenesis. *Journal of Cellular Physiology,* 230(8): 1964-1973.

Eulalio, A., Huntzinger, E., Nishihara, T., Rehwinkel, J., Fauser, M. & Izaurralde, E. 2009. Deadenylation is a widespread effect of miRNA regulation. *RNA,* 15(1): 21-32.

Evenas, P., Dahlback, B. & Garcia De Frutos, P. 2000. The first laminin G-type domain in the SHBG-like region of protein S contains residues essential for activation of the receptor tyrosine kinase sky. *The Journal of Biological Chemistry,* 381(3): 199-209.

Fair, D. S. & Marlar, R. A. 1986. Biosynthesis and secretion of factor VII, protein C, protein S, and the Protein C inhibitor from a human hepatoma cell line. *Blood,* 67(1): 64-70.

Fay, P. J. & Walker, F. J. 1989. Inactivation of human factor VIII by activated protein C: evidence that the factor VIII light chain contains the activated protein C binding site. *Biochim Biophys Acta,* 994(2): 142-148.

Fish, R. J. & Neerman-Arbez, M. 2012. A novel regulatory element between the human FGA and FGG genes. *Thrombosis and Haemostasis,* 108(3): 427-434.

Fort, A., Borel, C., Migliavacca, E., Antonarakis, S. E., Fish, R. J. & Neerman-Arbez, M. 2010. Regulation of fibrinogen production by microRNAs. *Blood,* 116(14): 2608-2615.

Garcia De Frutos, P., Fuentes-Prior, P., Hurtado, B. & Sala, N. 2007. Molecular basis of protein S deficiency. *Thrombosis and Haemostasis,* 98(3): 543-556.

Garzon, R., Liu, S., Fabbri, M., Liu, Z., Heaphy, C. E., Callegari, E., Schwind, S., Pang, J., Yu, J., Muthusamy, N., Havelange, V., Volinia, S., Blum, W., Rush, L. J., Perrotti, D., Andreeff, M., Bloomfield, C. D., Byrd, J. C., Chan, K., Wu, L. C., Croce, C. M. & Marcucci, G. 2009. MicroRNA-29b induces global DNA hypomethylation and tumor suppressor gene reexpression in acute myeloid leukemia by targeting directly DNMT3A and 3B and indirectly DNMT1. *Blood,* 113(25): 6411-6418.

Garzon, R., Pichiorri, F., Palumbo, T., Iuliano, R., Cimmino, A., Aqeilan, R., Volinia, S., Bhatt, D., Alder, H., Marcucci, G., Calin, G. A., Liu, C. G., Bloomfield, C. D., Andreeff, M. & Croce, C. M. 2006. MicroRNA fingerprints during human megakaryocytopoiesis. *Proceedings of the National Academy of Sciences,* 103(13): 5078-5083.

Gbd 2013 Mortality and Causes of Death Collaborators 2015. Global, regional, and national age-sex specific all-cause and cause-specific mortality for 240 causes of death, 1990-2013: a systematic analysis for the Global Burden of Disease Study 2013. *The Lancet,* 385(9963): 117-171.

Goldsby, R. A., Kindt, T. J., Osbourne, B. A. & Kuby, J. 2000. *Kuby immunology,* New York, W.H. Freeman.

Gutierrez-Fernandez, A., Parmer, R. J. & Miles, L. A. 2007. Plasminogen gene expression is regulated by nerve growth factor. *Journal of Thrombosis and Haemostasis,* 5(8): 1715-1725.

Hamberg, M., Svensson, J. & Samuelsson, B. 1975. Thromboxanes: a new group of biologically active compounds derived from prostaglandin endoperoxides. *Proceedings of the National Academy of Sciences,* 72(8): 2994-2998.

Han, J., Lee, Y., Yeom, K. H., Kim, Y. K., Jin, H. & Kim, V. N. 2004. The Drosha-DGCR8 complex in primary microRNA processing. *Genes & Development,* 18(24): 30163027.

Harrison, P. & Cramer, E. M. 1993. Platelet alpha-granules. *Blood Reviews,* 7(1): 52-62.

Hatziapostolou, M., Polytarchou, C., Aggelidou, E., Drakaki, A., Poultsides, G. A., Jaeger, S. A., Ogata, H., Karin, M., Struhl, K., Hadzopoulou-Cladaras, M. & Iliopoulos, D. 2011. An HNF4alpha-miRNA inflammatory feedback circuit regulates hepatocellular oncogenesis. *Cell,* 147(6): 1233-1247.

Hayashi, T., Usui, M., Nishioka, J., Zhang, Z. X. & Suzuki, K. 1998. Regulation of the human protein C inhibitor gene expression in HepG2 cells: role of Sp1 and AP2. *Biochemical Journal,* 332(2): 573-582.

He, W., Li, Y., Chen, X., Lu, L., Tang, B., Wang, Z., Pan, Y., Cai, S., He, Y. & Ke, Z. 2014. miR-494 acts as an anti-oncogene in gastric carcinoma by targeting c-myc. *Journal of Gastroenterology and Hepatology,* 29(7): 1427-1434.

Hoffbrand, A. V. & Pettit, J. E. 1993. Coagulation disoreders. *Essential haemoatology* Oxford, UK: Blackwell Science Ltd.

Hoylaerts, M., Rijken, D. C., Lijnen, H. R. & Collen, D. 1982. Kinetics of the activation of plasminogen by human tissue plasminogen activator. Role of fibrin. *Journal of Biological Chemistry,* 257(6): 2912-2919.

Hunter, D. J. & Fineberg, H. V. 2014. Convergence to common purpose in global health. *The New England Journal of Medicine,* 370(18): 1753-1755.

Iwawaki, Y., Mizusawa, N., Iwata, T., Higaki, N., Goto, T., Watanabe, M., Tomotake, Y., Ichikawa, T. & Yoshimoto, K. 2015. MiR-494-3p induced by compressive force inhibits cell proliferation in MC3T3-E1 cells. *Journal of Bioscience and Bioengineering*: [Epub ahead of print].

Jacobs-Helber, S. M., Wickrema, A., Birrer, M. J. & Sawyer, S. T. 1998. AP1 Regulation of Proliferation and Initiation of Apoptosis in Erythropoietin-Dependent Erythroid Cells. *Molecular and Cellular Biology,* 18(7): 3699-3707.

John, B., Enright, A. J., Aravin, A., Tuschl, T., Sander, C. & Marks, D. S. 2004. Human microRNA targets. *PLOS Biology,* 2(11): 1862-1879.

Kapinas, K. & Delany, A. M. 2011. MicroRNA biogenesis and regulation of bone remodeling. *Arthritis Research & Therapy,* 13(3): 220.

Kavurma, M. M. & Khachigian, L. M. 2004. Vascular smooth muscle cell-specific regulation of cyclin-dependent kinase inhibitor p21(WAF1/Cip1) transcription by Sp1 is mediated via distinct cis-acting positive and negative regulatory elements in the proximal p21(WAF1/Cip1) promoter. *Journal of Cellular Biochemistry,* 93(5): 904916.

Kim, W. K., Park, M., Kim, Y. K., Tae, Y. K., Yang, H. K., Lee, J. M. & Kim, H. 2011. MicroRNA-494 downregulates KIT and inhibits gastrointestinal stromal tumor cell proliferation. *Clinical Cancer Research,* 17(24): 7584-7594.

Knappskog, S., Bjornslett, M., Myklebust, L. M., Huijts, P. E., Vreeswijk, M. P., Edvardsen, H., Guo, Y., Zhang, X., Yang, M., Ylisaukko-Oja, S. K., Alhopuro, P., Arola, J., Tollenaar, R. A., Van Asperen, C. J., Seynaeve, C., Staalesen, V., Chrisanthar, R., Lokkevik, E., Salvesen, H. B., Evans, D. G., Newman, W. G., Lin, D., Aaltonen, L. A., Borresen-Dale, A. L., Tell, G. S., Stoltenberg, C., Romundstad, P., Hveem, K., Lillehaug, J. R., Vatten, L., Devilee, P., Dorum, A. & Lonning, P. E. 2011. The MDM2 promoter SNP285C/309G haplotype diminishes Sp1 transcription factor binding and reduces risk for breast and ovarian cancer in Caucasians. *Cancer Cell,* 19(2): 273282.

Knappskog, S. & Lonning, P. E. 2011. Effects of the MDM2 promoter SNP285 and SNP309 on Sp1 transcription factor binding and cancer risk. *Transcription,* 2(5): 207-210.

Krek, A., Grun, D., Poy, M. N., Wolf, R., Rosenberg, L., Epstein, E. J., Macmenamin, P., Da Piedade, I., Gunsalus, K. C., Stoffel, M. & Rajewsky, N. 2005. Combinatorial microRNA target predictions. *Nature Genetics,* 37(5): 495-500.

Kwak, S. Y., Yang, J. S., Kim, B. Y., Bae, I. H. & Han, Y. H. 2014. Ionizing radiationinducible miR-494 promotes glioma cell invasion through EGFR stabilization by targeting p190B rhoGAP. *Biochimica et Biophysica Acta,* 1843(3): 508-516.

Lan, Y. F., Chen, H. H., Lai, P. F., Cheng, C. F., Huang, Y. T., Lee, Y. C., Chen, T. W. & Lin, H. 2012. MicroRNA-494 reduces ATF3 expression and promotes AKI. *Journal of the American Society of Nephrology,* 23(12): 2012-2023.

Landry, P., Plante, I., Ouellet, D. L., Perron, M. P., Rousseau, G. & Provost, P. 2009. Existence of a microRNA pathway in anucleate platelets. *Nature Structural & Molecular Biology,* 16(9): 961-966.

Landthaler, M., Gaidatzis, D., Rothballer, A., Chen, P. Y., Soll, S. J., Dinic, L., Ojo, T., Hafner, M., Zavolan, M. & Tuschl, T. 2008. Molecular characterization of human Argonaute-containing ribonucleoprotein complexes and their bound target mRNAs. *RNA,* 14(12): 2580-2596.

Lawson, J. H. & Mann, K. G. 1991. Cooperative activation of human factor IX by the human extrinsic pathway of blood coagulation. *The Journal of Biological Chemistry,* 266(17): 11317-11327.

Lee, R. C., Feinbaum, R. L. & Ambros, V. 1993. The C. elegans heterochronic gene lin-4 encodes small RNAs with antisense complementarity to lin-14. *Cell,* 75(5): 843-854.

Lee, Y., Ahn, C., Han, J., Choi, H., Kim, J., Yim, J., Lee, J., Provost, P., Radmark, O., Kim, S. & Kim, V. N. 2003. The nuclear RNase III Drosha initiates microRNA processing. *Nature,* 425(6956): 415-419.

Lee, Y., Jeon, K., Lee, J. T., Kim, S. & Kim, V. N. 2002. MicroRNA maturation: stepwise processing and subcellular localization. *EMBO Journal,* 21(17): 4663-4670.

Lee, Y., Kim, M., Han, J., Yeom, K.-H., Lee, S., Baek, S. H. & Kim, V. N. 2004. MicroRNA genes are transcribed by RNA polymerase II. *The EMBO Journal,* 23(20): 40514060.

Lewis, B. P., Burge, C. B. & Bartel, D. P. 2005. Conserved seed pairing, often flanked by adenosines, indicates that thousands of human genes are microRNA targets. *Cell,* 120(1): 15-20.

Li, D., Mitchell, D., Luo, J., Yi, Z., Cho, S.-G., Guo, J., Li, X., Ning, G., Wu, X. & Liu, M. 2007. Estrogen regulates KiSS1 gene expression through estrogen receptor alpha and SP protein complexes. *Endocrinology,* 148(10): 4821-4828.

Li, L., Li, Z., Kong, X., Xie, D., Jia, Z., Jiang, W., Cui, J., Du, Y., Wei, D., Huang, S. & Xie, K. 2014a. Down-regulation of microRNA-494 via loss of SMAD4 increases FOXM1 and beta-catenin signaling in pancreatic ductal adenocarcinoma cells. *Gastroenterology,* 147(2): 485-497.e418.

Li, S., Chen, H., Ren, J., Geng, Q., Song, J., Lee, C., Cao, C., Zhang, J. & Xu, N. 2014b. MicroRNA-223 inhibits tissue factor expression in vascular endothelial cells. *Atherosclerosis,* 237(2): 514-520.

Li, S., Ren, J., Xu, N., Zhang, J., Geng, Q., Cao, C., Lee, C., Song, J., Li, J. & Chen, H. 2014c. MicroRNA-19b functions as potential anti-thrombotic protector in patients with unstable angina by targeting tissue factor. *Journal of Molecular and Cellular Cardiology,* 75: 49-57.

Li, X. T., Wang, H. Z., Wu, Z. W., Yang, T. Q., Zhao, Z. H., Chen, G. L., Xie, X. S., Li, B., Wei, Y. X., Huang, Y. L., Zhou, Y. X. & Du, Z. W. 2015. miR-494-3p Regulates Cellular Proliferation, Invasion, Migration, and Apoptosis by PTEN/AKT Signaling in Human Glioblastoma Cells. *Cellular and Molecular Neurobiology*: [Epub ahead of print].

Liborio-Kimura, T. N., Jung, H. M. & Chan, E. K. 2015. miR-494 represses HOXA10 expression and inhibits cell proliferation in oral cancer. *Oral Oncology,* 51(2): 151157.

Lim, L., Balakrishnan, A., Huskey, N., Jones, K. D., Jodari, M., Ng, R., Song, G., Riordan, J., Anderton, B., Cheung, S. T., Willenbring, H., Dupuy, A., Chen, X., Brown, D., Chang, A. N. & Goga, A. 2014. MicroRNA-494 within an oncogenic microRNA megacluster regulates G1/S transition in liver tumorigenesis through suppression of mutated in colorectal cancer. *Hepatology,* 59(1): 202-215.

Linse, S., Härdig, Y., Schultz, D. A. & Dahlbäck, B. 1997. A Region of Vitamin K-dependent Protein S That Binds to C4b Binding Protein (C4BP) Identified Using Bacteriophage Peptide Display Libraries. *The Journal of Biological Chemistry,* 272(23): 14658414665.

Liu, B., Li, J. & Cairns, M. J. 2014. Identifying miRNAs, targets and functions. *Briefings in Bioinformatics,* 15(1): 1-19.

Liu, L., Jiang, Y., Zhang, H., Greenlee, A. R. & Han, Z. 2010. Overexpressed miR-494 downregulates PTEN gene expression in cells transformed by anti-benzo(a)pyrene-trans7,8-dihydrodiol-9,10-epoxide. *Life Science,* 86(5-6): 192-198.

Liu, Y., Lai, L., Chen, Q., Song, Y., Xu, S., Ma, F., Wang, X., Wang, J., Yu, H., Cao, X. & Wang, Q. 2012. MicroRNA-494 is required for the accumulation and functions of tumor-expanded myeloid-derived suppressor cells via targeting of PTEN. *The Journal of Immunology,* 188(11): 5500-5510.

Liu, Y., Li, X., Zhu, S., Zhang, J. G., Yang, M., Qin, Q., Deng, S. C., Wang, B., Tian, K., Liu, L., Niu, Y., Wang, C. Y. & Zhao, G. 2015. Ectopic expression of miR-494 inhibited the proliferation, invasion and chemoresistance of pancreatic cancer by regulating SIRT1 and c-Myc. *Gene Therapy*: [Epub ahead of print].

Long Road Graphics Inc. 2012. *Activated Partial Thromboplastin Time* [Online]. Available: http://practical-haemostasis.com/Screening%20Tests/aptt.html [Accessed 08 July 2015.

Macfarlane, R. G. 1964. An enzyme cascade in the blood clotting mechanism, and its function as a biochemical amplifier. *Nature,* 202: 498-499.

Manchester, T. U. O. 2015. *miRBase* [Online]. Available: http://www.mirbase.org/ [Accessed 13 July, 2015.

Mann, K. G., Krishnaswamy, S. & Lawson, J. H. 1992. Surface-dependent hemostasis. *Seminars in Hematology,* 29(3): 213-226.

Martini, F. H. & Nath, J. L. 2009. *Fundamentals of anatomy and physiology,* San Francisco, CA, Pearson Benjamin Cummings.

Megiorni, F., Cialfi, S., Dominici, C., Quattrucci, S. & Pizzuti, A. 2011. Synergistic posttranscriptional regulation of the Cystic Fibrosis Transmembrane conductance Regulator (CFTR) by miR-101 and miR-494 specific binding. *PLOS One,* 6(10): e26601.

Mohnle, P., Schutz, S. V., Schmidt, M., Hinske, C., Hubner, M., Heyn, J., Beiras-Fernandez, A. & Kreth, S. 2014. MicroRNA-665 is involved in the regulation of the expression of the cardioprotective cannabinoid receptor CB2 in patients with severe heart failure. *Biochemical and Biophysical Research Communications,* 451(4): 516-521.

Monkovict, D. D. & Tracy, P. B. 1990. Activation of human Factor V by Factor Xa and thrombin. *Biochemistry,* 29(5): 1118-1128.

Nordstrom, S. M., Holliday, B. A., Sos, B. C., Smyth, J. W., Levy, R. E., Dukes, J. W., Lord, S. T. & Weiss, E. J. 2010. Increased thrombosis susceptibility and altered fibrin formation in STAT5-deficient mice. *Blood,* 116(25): 5724-5733.

Nyga, R., Pecquet, C., Harir, N., Gu, H., Dhennin-Duthille, I., Regnier, A., Gouilleux-Gruart, V. E., Lassoued, K. ı. & Gouilleux, F. 2005. Activated STAT5 proteins induce activation of the PI 3-kinase/Akt and Ras/MAPK pathways via the Gab2 scaffolding adapter. *Biochemical Journal,* 390(1): 359-366.

Oeth, P., Parry, G. C. & Mackman, N. 1997. Regulation of the tissue factor gene in human monocytic cells. Role of AP-1, NF-kappa B/Rel, and Sp1 proteins in uninduced and lipopolysaccharide-induced expression. *Arteriosclerosis, Thrombosis, and Vascular Biology,* 17(2): 365-374.

Oglesby, I. K., Chotirmall, S. H., Mcelvaney, N. G. & Greene, C. M. 2013. Regulation of cystic fibrosis transmembrane conductance regulator by microRNA-145, -223, and 494 is altered in DeltaF508 cystic fibrosis airway epithelium. *The Journal of Immunology,* 190(7): 3354-3362.

Ohdaira, H., Sekiguchi, M., Miyata, K. & Yoshida, K. 2012. MicroRNA-494 suppresses cell proliferation and induces senescence in A549 lung cancer cells. *Cell Proliferation,* 45(1): 32-38.

Olaru, A. V., Ghiaur, G., Yamanaka, S., Luvsanjav, D., An, F., Popescu, I., Alexandrescu, S., Allen, S., Pawlik, T. M., Torbenson, M., Georgiades, C., Roberts, L. R., Gores, G. J., Ferguson-Smith, A., Almeida, M. I., Calin, G. A., Mezey, E. & Selaru, F. M. 2011. MicroRNA down-regulated in human cholangiocarcinoma control cell cycle through multiple targets involved in the G1/S checkpoint. *Hepatology,* 54(6): 2089-2098.

Osterud, B., Bajaj, M. S. & Bajaj, S. P. 1995. Sites of tissue factor pathway inhibitor (TFPI) and tissue factor expression under physiologic and pathologic conditions. On behalf of the subcommittee on tissue factor pathway inhibitor (TFPI) of the scientific and standardization committee of the ISTH. *Thrombosis and haemostasis,* 73(5): 873.

Østerud, B. & Rapaport, S. I. 1977. Activation of factor IX by the reaction product of tissue factor and factor VII: additional pathway for initiating blood coagulation. *Proceedings of the National Academy of Sciences of the United States of America,* 74(12): 52605264.

Pignone, M. & Williams, C. D. 2010. Aspirin for primary prevention of cardiovascular disease in diabetes mellitus. *Nature Reviews Endocrinology,* 6(11): 619-628.

Pintao, M. C., Garcia, A. A., Borgel, D., Alhenc-Gelas, M., Spek, C. A., De Visser, M. C., Gandrille, S. & Reitsma, P. H. 2009. Gross deletions/duplications in PROS1 are relatively common in point mutation-negative hereditary protein S deficiency. *Hum Genet,* 126(3): 449-456.

Ramachandran, S., Karp, P. H., Osterhaus, S. R., Jiang, P., Wohlford-Lenane, C., Lennox, K. A., Jacobi, A. M., Praekh, K., Rose, S. D., Behlke, M. A., Xing, Y., Welsh, M. J. & Mccray, P. B., Jr. 2013. Post-transcriptional regulation of cystic fibrosis transmembrane conductance regulator expression and function by microRNAs. *American Journal of Respiratory Cell and Molecular Biology,* 49(4): 544-551.

Ramakrishnan, V., Deguzman, F., Bao, M., Hall, S. W., Leung, L. L. & Phillips, D. R. 2001. A thrombin receptor function for platelet glycoprotein Ib-IX unmasked by cleavage of glycoprotein V. *Proceedings of the National Academy of Sciences,* 98(4): 1823-1828.

Rath, A., Glibowicka, M., Nadeau, V. G., Chen, G. & Deber, C. M. 2009. Detergent binding explains anomalous SDS-PAGE migration of membrane proteins. *Proceedings of the National Academy of Sciences,* 106(6): 1760-1765.

Romano, G., Acunzo, M., Garofalo, M., Di Leva, G., Cascione, L., Zanca, C., Bolon, B., Condorelli, G. & Croce, C. M. 2012. MiR-494 is regulated by ERK1/2 and modulates TRAIL-induced apoptosis in non-small-cell lung cancer through BIM down-regulation. *Proceedings of the National Academy of Sciences,* 109(41): 16570-16575.

Ruggeri, Z. M. 1997. Mechanisms initiating platelet thrombus formation. *Thrombosis and Haemostasis,* 78(1): 611-616.

Ruggeri, Z. M. 2003. Von Willebrand factor, platelets and endothelial cell interactions. *Journal of Thrombosis and Haemostasis,* 1(7): 1335-1342.

Rui Yi, Yi Qin, Macara, I. G. & Cullen, B. R. 2003. Exportin-5 mediates the nuclear export of pre-microRNAs and short hairpin RNAs. *Genes & Development,* 17(24): 3011-3016.

Sadler, J. E. 1998. Biochemistry and genetics of von Willebrand factor. *Annual Review of Biochemistry,* 67: 395-424.

Salloum-Asfar, S., Teruel-Montoya, R., Arroyo, A. B., Garcia-Barbera, N., Chaudhry, A., Schuetz, E., Luengo-Gil, G., Vicente, V., Gonzalez-Conejero, R. & Martinez, C. 2014. Regulation of coagulation factor XI expression by microRNAs in the human liver. *PLOS One,* 9(11): e111713.

Sandset, P. M. & Abildgaard, U. 1991. Extrinsic pathway inhibitor - the key to feedback control of blood coagulation initiated by tissue thromboplastin. *Haemostasis,* 21(4): 219-239.

Schuijt, T. J., Bakhtiari, K., Daffre, S., Deponte, K., Wielders, S. J., Marquart, J. A., Hovius, J. W., Van Der Poll, T., Fikrig, E., Bunce, M. W., Camire, R. M., Nicolaes, G. A., Meijers, J. C. & Van 'T Veer, C. 2013. Factor Xa activation of factor V is of paramount importance in initiating the coagulation system: lessons from a tick salivary protein. *Circulation,* 128(3): 254-266.

Shen, P. F., Chen, X. Q., Liao, Y. C., Chen, N., Zhou, Q., Wei, Q., Li, X., Wang, J. & Zeng, H. 2014. MicroRNA-494-3p targets CXCR4 to suppress the proliferation, invasion, and migration of prostate cancer. *The Prostate Journal,* 74(7): 756-767.

Sugiyama, T., Okuma, M., Ushikubi, F., Sensaki, S., Kanaji, K. & Uchino, H. 1987. A novel platelet aggregating factor found in a patient with defective collagen-induced platelet aggregation and autoimmune thrombocytopenia. *Blood,* 69(6): 1712-1720.

Sun, G., Zhou, Y., Li, H., Guo, Y., Shan, J., Xia, M., Li, Y., Li, S., Long, D. & Feng, L. 2013. Over-expression of microRNA-494 up-regulates hypoxia-inducible factor-1 alpha expression via PI3K/Akt pathway and protects against hypoxia-induced apoptosis. *Journal of Biomedical Science,* 20: 100.

Sun, H. B., Chen, X., Ji, H., Wu, T., Lu, H. W., Zhang, Y., Li, H. & Li, Y. M. 2014. miR494 is an independent prognostic factor and promotes cell migration and invasion in colorectal cancer by directly targeting PTEN. *International Journal of Oncology,* 45(6): 2486-2494.

Suzuki, A., Sanda, N., Miyawaki, Y., Fujimori, Y., Yamada, T., Takagi, A., Murate, T., Saito, H. & Kojima, T. 2010. Down-regulation of PROS1 gene expression by 17betaestradiol via estrogen receptor alpha (ERalpha)-Sp1 interaction recruiting receptorinteracting protein 140 and the corepressor-HDAC3 complex. *The Journal of Biological Chemistry,* 285(18): 13444-13453.

Tapias, A., Ciudad, C. J., Roninson, I. B. & Noe, V. 2008. Regulation of Sp1 by cell cycle related proteins. *Cell Cycle,* 7(18): 2856-2867.

Tay, J. W., Romeo, G., Hughes, Q. W. & Baker, R. I. 2013. Micro-ribonucleic Acid 494 regulation of protein S expression. *Journal of Thrombosis and Haemostasis,* 11(8): 1547-1555.

Taylor, F. B., Dahlback, B., Chang, A. C. K., Lockhart, M., Hatanaka, K., Peer, G. & Esmon, C. T. 1995. Role of Free Protein S and C4b Binding Protein in Regulating the Coagulant Response to Escherichia coli. *Blood,* 86(7): 2642-2652.

Ten Kate, M. K. & Van Der Meer, J. 2008. Protein S deficiency: a clinical perspective. *Haemophilia,* 14(6): 1222-1228.

Teruel-Montoya, R., Rosendaal, F. R. & Martinez, C. 2015. MicroRNAs in hemostasis. *Journal of Thrombosis and Haemostasis,* 13(2): 170-181.

Teruel, R., Perez-Sanchez, C., Corral, J., Herranz, M. T., Perez-Andreu, V., Saiz, E., GarciaBarbera, N., Martinez-Martinez, I., Roldan, V., Vicente, V., Lopez-Pedrera, C. & Martinez, C. 2011. Identification of miRNAs as potential modulators of tissue factor expression in patients with systemic lupus erythematosus and antiphospholipid syndrome. *Journal of Thrombosis and Haemostasis,* 9(10): 1985-1992.

Tominaga, K., Srikantan, S., Lee, E. K., Subaran, S. S., Martindale, J. L., Abdelmohsen, K. & Gorospe, M. 2011. Competitive regulation of nucleolin expression by HuR and miR494. *Molecular and Cellular Biology,* 31(20): 4219-4231.

Tu, C. C., Kumar, V. B., Day, C. H., Kuo, W. W., Yeh, S. P., Chen, R. J., Liao, C. R., Chen, H. Y., Tsai, F. J., Wu, W. J. & Huang, C. Y. 2013. Estrogen receptor alpha (ESR1) over-expression mediated apoptosis in Hep3B cells by binding with SP1 proteins. *Journal of Molecular Endocrinology,* 51(1): 203-212.

Vehar, G. A. & Davie, E. W. 1980. Preparation and properties of bovine factor VIII (antihemophilic factor). *Biochemistry,* 19(3): 401-410.

Walsh, G. & Jefferis, R. 2006. Post-translational modifications in the context of therapeutic proteins. *Nature Biotechnology,* 24(10): 1241-1252.

Wang, J., Chen, H., Liao, Y., Chen, N., Liu, T., Zhang, H. & Zhang, H. 2015a. Expression and clinical evidence of miR-494 and PTEN in non-small cell lung cancer. *Tumor Biology*: [Epub ahead of print].

Wang, T., Li, P., Ma, X., Tian, P., Han, C., Zang, J., Kong, J. & Yan, H. 2015b. MicroRNA494 inhibition protects nucleus pulposus cells from TNF-alpha-induced apoptosis by targeting JunD. *Biochimie*: [Epub ahead of print].

Wang, X., Zhang, X., Ren, X. P., Chen, J., Liu, H., Yang, J., Medvedovic, M., Hu, Z. & Fan, G. C. 2010. MicroRNA-494 targeting both proapoptotic and antiapoptotic proteins protects against ischemia/reperfusion-induced cardiac injury. *Circulation,* 122(13): 1308-1318.

Weiss, H. J. 1975. Platelet physiology and abnormalities of platelet function *The New England Journal of Medicine,* 293(11): 531-541.

Williams, K. C., Renthal, N. E., Condon, J. C., Gerard, R. D. & Mendelson, C. R. 2012. MicroRNA-200a serves a key role in the decline of progesterone receptor function leading to term and preterm labor. *Proceedings of the National Academy of Sciences,* 109(19): 7529-7534.

Xiong, R., Wang, Z., Zhao, Z., Li, H., Chen, W., Zhang, B., Wang, L., Wu, L., Li, W., Ding, J. & Chen, S. 2014. MicroRNA-494 reduces DJ-1 expression and exacerbates neurodegeneration. *Neurobiology of Aging,* 35(3): 705-714.

Yamamoto, H., Morino, K., Nishio, Y., Ugi, S., Yoshizaki, T., Kashiwagi, A. & Maegawa, H. 2012. MicroRNA-494 regulates mitochondrial biogenesis in skeletal muscle through mitochondrial transcription factor A and Forkhead box j3. *American Journal of Physiology - Endocrinology and Metabolism,* 303(12): E1419-1427.

Yamanaka, S., Campbell, N. R., An, F., Kuo, S. C., Potter, J. J., Mezey, E., Maitra, A. & Selaru, F. M. 2012. Coordinated effects of microRNA-494 induce G(2)/M arrest in human cholangiocarcinoma. *Cell Cycle,* 11(14): 2729-2738.

Yu, G., Li, H., Wang, X., Wu, T., Zhu, J., Huang, S., Wan, Y. & Tang, J. 2013a. MicroRNA19a targets tissue factor to inhibit colon cancer cells migration and invasion. *Molecular and Cellular Biochemistry,* 380(1-2): 239-247.

Yu, Y. H., Wu, D. S., Huang, F. F., Zhang, Z., Liu, L. X., Zhang, J., Zhan, H. E., Peng, M. Y., Zeng, H. & Chen, F. P. 2013b. MicroRNA-20b and ERK1/2 pathway independently regulate the expression of tissue factor in hematopoietic and trophoblastic differentiation of human embryonic stem cells. *Stem Cell Research & Therapy,* 4(5): 121.

Yuan, J., Benway, C. J., Bagley, J. & Iacomini, J. 2015. MicroRNA-494 Promotes Cyclosporine-Induced Nephrotoxicity and Epithelial to Mesenchymal Transition by Inhibiting PTEN. *American Journal of Transplantation,* 15(6): 1682-1691.

Zerrouqi, A., Pyrzynska, B., Brat, D. J. & Van Meir, E. G. 2014. P14ARF suppresses tumorinduced thrombosis by regulating the tissue factor pathway. *Cancer Research,* 74(5): 1371-1378.

Zhang, R., Chen, X., Zhang, S., Zhang, X., Li, T., Liu, Z., Wang, J., Zang, W., Wang, Y., Du, Y. & Zhao, G. 2015. Upregulation of miR-494 Inhibits Cell Growth and Invasion and Induces Cell Apoptosis by Targeting Cleft Lip and Palate Transmembrane 1-Like in Esophageal Squamous Cell Carcinoma. *Digestive Diseases and Sciences,* 60(5): 1247-1255.

Zhang, X., Yu, H., Lou, J. R., Zheng, J., Zhu, H., Popescu, N. I., Lupu, F., Lind, S. E. & Ding, W. Q. 2011. MicroRNA-19 (miR-19) regulates tissue factor expression in breast cancer cells. *The Journal of Biological Chemistry,* 286(2): 1429-1435.

Zhou, R. P., Chen, G., Shen, Z. L. & Pan, L. Q. 2014. Cinobufacin suppresses cell proliferation via miR-494 in BGC- 823 gastric cancer cells. *Asian Pacific journal of cancer prevention,* 15(3): 1241-1245.

Zioncheck, T. F., Roy, S. & Vehar, G. A. 1992. The cytoplasmic domain of tissue factor is phosphorylated by a protein kinase C-dependent mechanism. *The Journal of Biological Chemistry,* 267(6): 3561-3564.

Appendix I: Buffers & Solutions

1. DMEM medium

500mL	Bottle of DMEM medium
50mL	fetal calf serum
5mL	Penicillin/streptomycin
5mL	Non-essential amino acid solution
5mL	Sodium pyruvate

The medium was stored at 4°C.

2. RMPI-1640 medium

500mL	Bottle of RMPI-1640 medium
50mL	fetal calf serum
5mL	Penicillin/streptomycin
5mL	Sodium pyruvate

The medium was stored at 4°C.

3. Phosphate buffered saline (PBS)

10	Phosphate buffer saline tablets
2L	Deionised water

Ten phosphate buffered saline (PBS) tablets from Sigma-Aldrich Co., USA were dissolved in 2L deionised water. After it fully dissolved, 2L of PBS were aliquotted into 6 bottles. The pH were checked by using pH meter. All the 6 bottles were autoclaved.

4. 2x denaturing solution

375µL	2-mercaptoethanol
1	2x denaturing solution

Add 375µL 2-mercaptoethanol into the 2x denaturing solution and mix well. The solution was stored at 4°C and warm it before use.

5. miRNA wash solution 1

21mL	100% ethanol
1	miRNA washing solution 1

Add 21mL 100% ethanol into the miRNA washing solution 1 and mix well. The solution was stored at room temperature.

6. miRNA wash solution 2/3

40mL	100% ethanol
1	miRNA washing solution 2/3

Add 40mL 100% ethanol into miRNA washing solution 2/3 and mix well. The solution was stored at room temperature.

7. 20% sucrose

4g	Sucrose
20mL	ddH_2O

Sucrose was dissolved in ddH_2O to a final volume of 20mL. The solution was stored at room temperature

8. 4M sodium chloride (NaCl)

11.69g	NaCl
100mL	ddH_2O

NaCl was dissolved in ddH_2O to a final volume of 100mL. The solution was autoclaved and stored at room temperature.

9. 10% sodium dodecyl sulphate (SDS)

10g	SDS
100mL	ddH_2O

SDS was dissolved in ddH_2O to a final volume of 100 mL. (Face mask was required while handling SDS powder.)

10. 1M Tris-HCl

121.1g	Tris-Base
1L	ddH_2O

Tris-Base was dissolved in approximately 800 ddH_2O. The pH of the solution (pH 6.8 or 7.4) is required to adjust with 10M HCl, the add ddH_2O to a final volume of 1L. The solution was autoclaved and stored at room temperature.

11. 10x Running Buffer

144g	Glycine
30g	Tris-Base
10g	SDS
1L	ddH_2O

Tris, glycine and SDS were dissolved in 1L ddH_2O. (Face mask was required while handling SDS powder.) The solution was stored at room temperature.

12. Western Transfer Buffer

3.03g	Tris-Base
14.4g	Glycine
800mL	ddH_2O
200mL	Methanol

Tris-Base and glycine was dissolved in 800mL of ddH_2O. 200mL of methanol was added and stored at 4°C. Transfer buffer was made fresh every time.

13. Tris buffered saline with Tween 20 (TBST)

37.5mL	4M NaCl[8]
50mL	1M Tris-HCl[10]
	ddH_2O
0.5mL	Tween 20

37.5mL of NaCl and 50mL Tris-HCL were mixed and added ddH_2O to a final volume of 1L. Tween 20 was added and mix well. The solution was stored at room temperature.

14. Blotto blocking solution (3%)

1.2g	Skim milk powder
40mL	TBST[14]

Skim milk powder was dissolved in TBST[14] and mixed on a shaker before use.

15. Western 10x loading dye

12.5mL	Glycerol
2.5mL	1M Tris-HCl pH6.8[10]
2.5mL	20% SDS[17]
2.5mL	B-Mercaptoethanol
0.25g	Bromophenol blue
25mL	ddH_2O

Glycerol, Tris-HCl[10], 20% SDS[17], bromophenol blue and ddH_2O were mixed together in a 50mL tube. B-mercaptoethanol was then added to the mixture in a fume hood. The dye was stored as 1mL aliquots at -20°C.

16. Whole cell lysis buffer

2mL	ddH_2O
2mL	10% SDS[9]
5mL	20% Sucrose[7]
0.5mL	1M Tris-HCl[10]
0.5mL	B-Mercaptoethanol

All the solution were combined. The tube was wrapped with foil to protect it from light.

17. 20% sodium dodecyl sulphate (SDS)

20g	SDS
100mL	ddH_2O

SDS was dissolved in ddH_2O to a final volume of 100 mL. (Face mask was required while handling SDS powder.)

18. Blotto blocking solution (5%)

2g	Skim milk powder
40mL	TBST[14]

Skim milk powder was dissolved in TBST[14] and mixed on a shaker before use.

Appendix II: pmiR-Report Luciferase plasmid

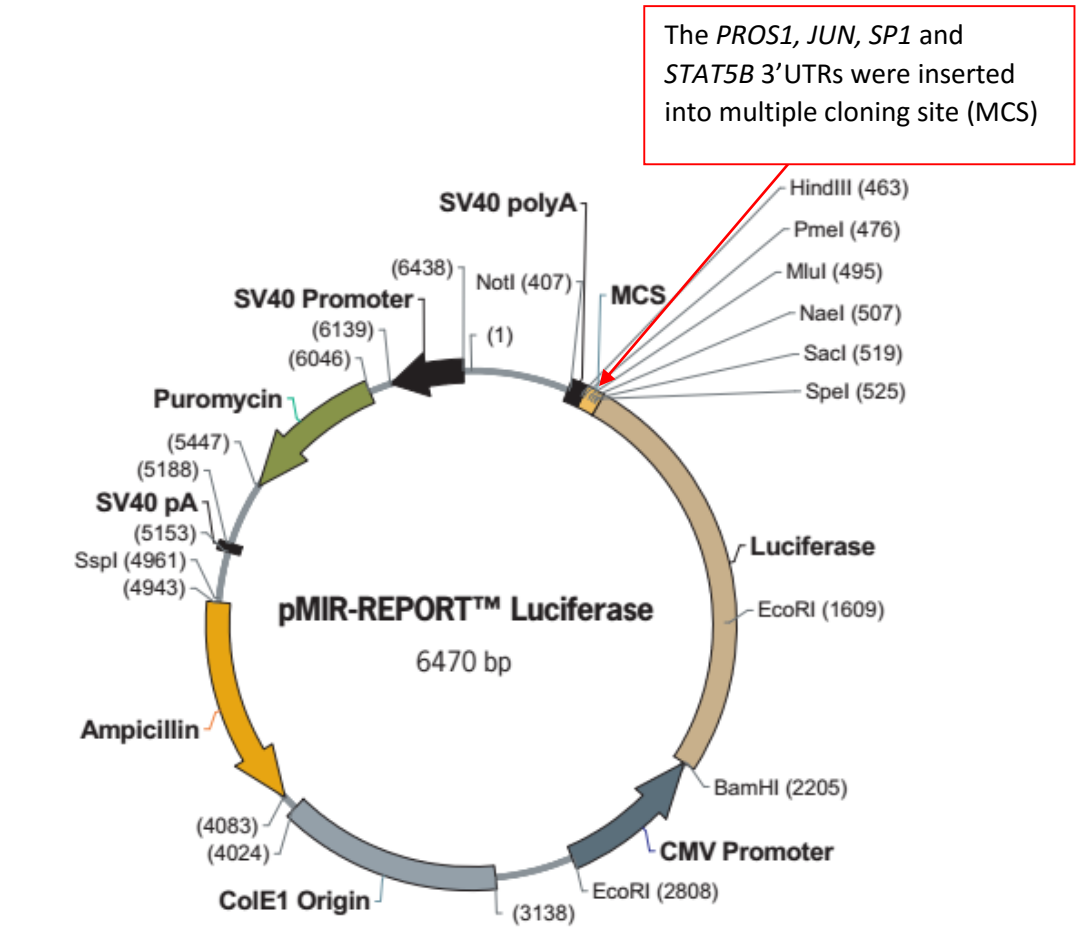

Figure 1. pMIR-REPORT Luciferase

CMV Promoter: 2210–2813
Firefly luciferase: 540–2210
MCS: 467–539
SV40 Poly(A): 404–467
SV40 Promoter: 6139–6438
Puromycin: 5447–6046
SV40 pA signal: 5153–5188
Ampicillin: 4083–4943
ColE1 Origin: 3138–4024

Appendix IIa. Map of pmiR-Report luciferase plasmid. The site of 3'UTRs insertion is highlighted as red.

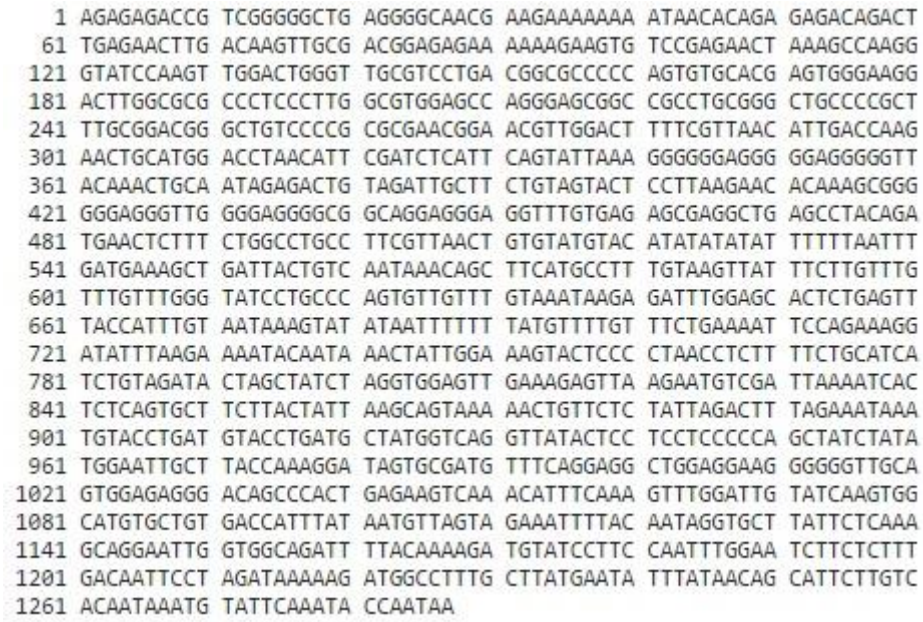

Appendix IIb. The 3'UTR sequence of *JUN* inserted into pmiR-Report Luciferase plasmid.

```
   1 GATCAGGCAC CCGGGGCCAG AGACATATGG GCCATACCCC TTAACCCCGG GATGCAAGGT
  61 AGCATGGGTC CAAGAGACAT GGAAGAGAGA GCCATGAAGC ATTAAAATGC ATGGTGTTGA
 121 GAAGAATCAG GAGAGGGATA CAAGAGAGGA GATGGGGTCC CGGCACCCAT CTGTATCATC
 181 AGTGCCTCTT TGAAGGTGGG AAACATTAGT GAAAATTCTG TTGGTGCCAC GCTTTGATGA
 241 GCATTTGTTT GACCCCAGTT TCTTCTTACA CTTCTTACCC CAGCCTACCC TTCCTGCATT
 301 TCTCTTCTCA GCTCTTCCAT GATGGATTCC CCCCCCTTTC CTAAAGCCAT CATGCCTTGA
 361 TAAATATATA TGATCATTGA AATACTTTTT AACAAAAAAC AGATTCTATA TTATTATATA
 421 TATATATATA TATATAAAGA TATATAGAGA TGCATTCACA GGGGTTGGCT GGGAGGAGGA
 481 AGACCATTCT GTGACCAAAA TACCTTGGTC ATTTTTTTTA TATTGCCTTA TTTCCCTATG
 541 GCTGAGCCTT GTTGTGACAC ATCAAGCTTT TCTGTAGATG TTGTCTTGGC TTCCCACCAG
 601 CTTAAGCGTT CATATGCTCT GCTTTTAGTT CATATATACA TACATAATGT TTTTCCTTTC
 661 TTAATTTTGT CTTTTTGTTT GGGATCAGCT TCTTGCACTC CTTCCCTAAC TCAACTGTTG
 721 CCGTCTCATC TTCTCTCATC TGATCACTTC ATGTTTTGTT TTTGTTACTG CCTGGATGAG
 781 GCACTTCTGT CAATTTTTTC AGGACCTTAG TTCCAGCAGC AGAATGGAAA AATCCTTGAA
 841 GCCCAGGCTG ATGCTTGAAG TAACTGTGGA GGGAGTGTTC AAAATACTAC TGACGCAGGC
 901 ACCTTCTTGG CGCTGGAGAG TCAAAGGCAT CTCCCTTCAT TAGCTGCTCT GAGCATCAAG
 961 AATTAGAAGT CTTTCAGTGG AATTGTACAA GAGTCCCTTT GAAGATAATA ATCTTGGCTC
1021 AGTTTGTATA AACTGTCAAA TTTTCAAATA ATAGGTAGGG GGCTTTCACT AGGAAAATCA
1081 TGTGCTCAGA AGAGGAAATG ACTCGTAGTC AGGTTCAGGA GTTAGTGGAG TATTTGGACT
1141 TTGGTACTGC TGTCTTCCAA GGTAGCTCTA AGTTTTGATG TGTGGGCTTC TGAGTTTATA
1201 TTCTGAAAGG AAATACACTT CTTTTGAACA TCCCCACTAG GTTCTTTTCC ATTGTCAATA
1261 AGGAGCATCA GCCAGTGAAT CTGTTTCAGG TTTCCATTCT GCAGAACTCC TCCAAAGCAT
1321 GTGCTAGTGG CAAGACAGTG GTTCTTATGA TGTTTTCCCT TAACTTTTCC TTGTATGTTC
1381 TTGGGTGGTT CCTAAGGGAA AGGGAAGCAC ATGATCATGG GAATGATAGC CCAGAACAAA
1441 AAGAAATCTT GTCTTACCAC AGTGTTTTAT AGGAGAGATT GGGAGAAATC ATCCTGTTTT
1501 CTCTGTGACC TGATTTCAGA AGAGACTGAT CCAAAAATTA TAACGGCAGG GAACCTAGTG
1561 CATTTGGCAC TGAGATTTAA ATGCAACCAG AATTGTCCTC AAGGCCCAGC CATAAAAGCA
1621 TTGTCTCTCT CGACCTTCTG GTATCTTGTT AGAGAGCTTT TCACTGTGAG GAAGTGTGGA
1681 AAAATAGCTC TGTGTGTGTG TGTGTGTGTG TGTGTGTGTG TGTGTGTAAT CTGTTAGGTT
1741 GGGGATAGGT TTTCTGCTAG CCAATATTAA AAGAGACCTG CAATAAAAAA ATTACCCTGA
1801 TCTGATAGAA AGCAAGTGTT TTTGTATGTG TGGGTGAATG TGTGTTCATG CCCGTATATG
1861 TCTACACACA GATGACAAAT TATATTTGAA ATCGTTGGAA AATAAATTCA GATCAAAATG
1921 CCTTTCAGGC CCATTACCTA GAAATCTATC TTAAAACCTG GGTATGTTCC TAAGGTCATT
1981 TCTTTGCTTA TGCTAAATTA ATTACAATTA TGAATGGAGG ATATTCTACT GTACTTTTTT
2041 AAAAAGAAAC TATTTTTGTG TTTGAAAGTG AAACCAACAT CCAGATCTAT AGCAGAGTCC
2101 TTATTCTTCT CATAAATCTT TTTACTTTGG CTACAAATAG ATGATGGTAT GATTCTATTA
2161 TATATTTTAT ATAAAATCCA TCCAAATTAA GTTTTGGGTA AGTGTGTTGT TTAATCTGAA
2221 CTATAGTAAC TTAATACTCT AAACAATAGT TCACTCCATT TGGTCCTTTC TCCACAGATG
2281 TAATTATGTT TTCAACTCAG GAACTATGGC AAGGAACTTT CCCCAGATCA AATTCTATTA
2341 ACGCTGAGAT ACAAGTCATC CATGCACAGC CACTATCATA CCCTTTATTC TCACTGAAAG
2401 GCAGAACTCA GAACCTGTTA TTTTATGTCT GTAATCATGT ACTTTGGCAT CTTTTGGAGG
2461 AAAGGGGCAG GATAACTCAC TGGAATGTAC AGTATTTTGC TAGTGCATTT CAAGGAATGG
2521 AATCTTCTCC AGTATGAAAT TACCAGATAT AAAATAATGT AATGATGCTG AGGATATAAG
2581 CTTTTAGAAG GTAATTTGAT GGTATTTCTT TCTCGAATGA AAAGCTGCTG GTTTACCCTC
2641 AACCCTATTC ATTAGCATTA CCATGAGTGA ATTTATATCT AATTATTTCC ACTTGCCCTG
2701 TTCTCTTCAC ACCAAGGAAG CTCCAGATCC AGTATCTTGT TTGGCCTCAA AACAGAAGCA
2761 GCTTCTTTTG TCTCCCAGCA GTAGTGAGCC ACTCAGTCTC TTCCACAGGA AGTTTGGAGC
2821 CTACATTCCT TGAGTCAGGA GCTTATTACA GAAAAACCCC GTTTCCCTGA ACTTTTGGCT
2881 AACAGAAATT AATTTAACTG ACATGCATAT TGATTCTGAA ATTTTTTTCC TAAGTTTTTT
2941 TCATTTTTTT GAATGAGTTT TTTAAATTTT TTAGATGACC AAAACTTGCA GGGCAGGGGA
3001 TGCCCAGAAG AGTGGTGAGA TAGTAAAACA CTTATTCCCT CATCCTTTCA GGTTTTCAGG
3061 TTGCCCATTT ATATTCATTT ACATGTCATT TGACTGTCTC ACTTTTTACC CAGAACAGTA
3121 ACAACCCACA CCGTCTTCCT TCAGGGATTT CCAACTGGCA CTCTGTGGGT GCTACACAGA
3181 ATGCAATTTA ATGGATATTT CTCAGCCTGG TTCAGAATAA ATTGATCCTT TGATCCCAGA
3241 AAGTATATAC TGAAGTGTGG GATAAAGATT ATGATTAGGG GAGGGTTGGA GACAAAAGCT
3301 GTAAATTACT ATGGCTGATT TATTTCTACT ATATACATAT ATATTTTTTG CTTTTGTATA
3361 TCCTATATAG GAAACTAAGC ATTGTATTTT TTTTAACAAA TCTAAAAAAG CACTATGAAC
3421 TACAGGTGTT TGACTTTCAA AATATATTTT GTATTGTTAA TATCTTCACA TTGTGTGAAT
3481 ACTGGAAGCT GCAGATCTTT GCTAGGACGC AATAAATTTA TATACTTTTT GAGGGGTTCT
3541 TCTGGGGTGC TAATCAGGCC CCTGTTATGC TTAGGGGGAG CCCTGGTGCT ACTTGCTTGA
3601 AGTTTTCAGT GTAAGTACCC TGATGCCTTT TGGACCTTGG GATCAGATCA AGAGTTTTGG
3661 AGATCAGGTA CCAAGGAAAT AAGGACAGTC TAGCTGCCTC AAGTGAGGGG CCCTTTGCAT
3721 AGCTCTCCTT CCCCCTCACT GAAGCTGGGT AGCCTATTGG GGTTGAGAGG GAAAATGTGA
3781 AATCTCAGAA TTTATCTCCC TTAGAAGAGA GCCAGTAACT TATGTACAAG GATGAAAGAA
3841 AGGTCGCAGC AGTAGCTTTG GGGAAAGGGA GGAAGATATG GCACTTCTCC AACCCCGGAA
3901 AACATTGCTT TTGAAAACTG CTGATAAAAT ATGAGCCGGT TATTACTTCT GTTTGGGAGA
3961 CTGTGCTCTC TGTGGTGCCT CTCTTGGCTC TACTCCACAG ATACCAGACC TCTTCTAAGA
4021 GGATGAGCAG ACCAGCTTTG AGGTTGACCT GTTTCTCTTT GTCTGCCTTC CCAAAACACC
```

```
4081 AGCCCCCAGG AAGACATTAA GCAGCCTTAA GCTTAAATTC CTACTCCCTC TTCCAAATTT
4141 GGCTCACTTG CCTTAGATCC AAGGCAGGGA AAGGAAAAGA AGGGGGGTCT CTGGCTTTAT
4201 TACTCCCCTA AGTCTTTACT CTGACTTCCC CAAACCCAGA AAGATTTTCT CCACAGTGTT
4261 CATTTGAAAG AGGAGTATTT TGTCCCATTT TCCCCTTCCT CATTATCAAA CAGCCCCAGT
4321 CTTCCTTGTC TCTGCTAAGA AAGTAGAGGC ATGATGATCT GCCTCTCAAC TGCCCTAAGT
4381 CCTAGCTAAG TATCAGGGGA AAAAAAAAAA AAAAAAGCCT AACAAATGGG ATTAGACTAG
4441 GGCTGCAAGT AGTGAGGATT TTGTTGATAC CTCTGCTGGG ATGTGTGCTT TCCCATATCT
4501 TGCCTTCAGG AATTACACTG TGCCTTTTCC CCAGGGATAT GGGCTCTGTC TACCCAGTGC
4561 TCCAGTTTCC CGGTAACTGC TCTTGAACAT TGTGGACAAG GGCAGGTCTT CATATTTTTG
4621 ATCATCCCTT TCTCCCAGTG AAATCCCATA GCCCTTACCT AGAGTCTAGG GCACAAAGAC
4681 TTCGGGGAAG ATACACTGAG ATTGACCTGA GGAGACATCT ACACACACCA GTGGCAGCTG
4741 CCCCAGGGCC TGCTTCCCCT TCCTAAGTCT GTCATCCTCT GGAAGGGATG GGTGGTGCTC
4801 CAATCTCTGG TGCCTAAAAA CCCAAGTTTA TTTCTCTCTT AACACTGGCA ATAACCAGTC
4861 CACACCACTG TTGCCTTTTA AAACCTCTTA ATAATCTCAT GCTGTGTTTG TTTTGATTCC
4921 AATCCAATTA TCACCAGGGC TGTGTGGGTA AATGCTTTTA AATGCTCTCT CATCTTGTTC
4981 TTCCCCCTCA CCCCCCACTC TTAGGTATGT ATGATGCTAA TCTTGTCCCT AAGTAAGTTT
5041 CTTCCTGCTC CTTTTGTATC TTCCTTTCTT GTCTTTCCTC CTACCTTTTG TCTCTTGGTG
5101 TTTTGGGACT TTTTTTTTTT TTTTTTTGGC CTTTTGTACA AAGATTAGTT TCAATGTAGT
5161 CTGTAGCCTC CTTTGTAAAC CAATTAAAAA GTTTTTTAAT AAAAAA
```

Appendix IIc. The 3'UTR sequence of *SP1* inserted into pmiR-Report Luciferase plasmid.

```
   1 CCCCGCGACC TCTCCATCTT CAGCTTCTTC ATCTTCACCA GAGGAATCAC TCTTGTGGAT
  61 GTTTTAATTC CATGAATCGC TTCTCTTTTG AAACAATACT CATAATGTGA AGTGTTAATA
 121 CTAGTTGTGA CCTTAGTGTT TCTGTGCATG GTGGCACCAG CGAAGGGAGT GCGAGTATGT
 181 GTTTGTGTGT GTGTGTGTGT GTGTGTGTGT GTGCGTGTTT GCACGTTATG GTGTTTCTCC
 241 CTCTCACTGT CTGAGAGTTT AGTTGTAGCA GAGGGGCCAC AGACAGAAGC TGTGGTGGTT
 301 TTTACTTTGT GCAAAAAGGC AGTGAGTTTC GTGAAGCCTG GAAGTTGGCC ATGTGTCTTA
 361 AGAGTGGCTG GACTTTGACA TGTGGCTGTT TGAATAAGAG AAGGACAAAG GGAGGAGAAA
 421 GCACATGTGC TCCAGTGAGT CTTCGTCACT CTGTCTGCCA AGCAATTGAT ATATAACCGT
 481 GATTGTCTCT GCTTTTCTTC TGAAATGTAG ATAACTGCTT TTTGACAAAG AGAGCCTTCC
 541 CTCTCCCCCA CCCCTGTGTT CTTGGGTAGG AATGGGAAAA GGGGCAACCT ACAAAGATTG
 601 TTGGGGCAAG GGAAGTCACA AGCTTTCGGA TGGGCGGTGG CTTTTCACAA AACATTTAGC
 661 TCATCTTATT CTCTCTTTGT CCTCTCTCCC CTCCTGCCCG CCCGCACCCT GGAATTGCCA
 721 CTCAGTTCCT CTGGGTGTGC ACATATGTTT GGAGAAATAG AGGAGAGAAA AGAGGGCCAC
 781 GTAACTGAGA GCTTACAGTG CCAATGCCGT TTGTGTTCTG GCCAGAGTGG AGTGCGCAGC
 841 CCTGACTCCC AGGCGCTGAG ATTGTTGCCT GGTTACCCAG GAAGCTGCTG TTCCGGCTGC
 901 CCAGCCTTTC TCTGAGCCAG CGGATGCACA GTCCGTGGCC TTCTTCAGGC TTATTGATGA
 961 TGCTTTTTGC AAATGTTGAA TCATGGTTCT GTTTCTAAGT TGGATCTTTT TTGTTTTCTC
1021 CTTGCCACCC TAATTTGACA TCAAAATTCT CTCTTGTGCA TTGGGCCCTG GGTCATTCAA
1081 ACCCAGGTCA CCTCATTCCC CTTCTCTGTT CACACCTAAT GTCTTGAAGA GTAGGTAGCA
1141 GCAGTGTGGG CTGAACCTAG GCCAGCTTGC TTAGCGGGTC ACCCTGCTGT GAAGTCCTGG
1201 CAGGTGTTGG TAATGTGTGG AAATGCAGTC AGCAAGTTTG CTGGGGAGTT TGATAAAAGT
1261 ATAAAACAAA ACAAAAAAAG CCTCGGTATA ATTTTGTTCC ACGACTTCTT CTGTAGCTTT
1321 ACACCAGAAG GAAGGAATGG GCTACAGCAG GTAGTGGAGG AAGAGGGGGG TGAGCAGGTG
1381 TATTAAAATA GCTTACGGGT AAGGCCTAAA AGGTCACCCC TCGGCCCCCT CTCCAAAAGA
1441 AGGGCATGGG CACCCCCAGG AGAGGATGGC CCCAAAAACC TTATTTTTAT ACATGAGAGT
1501 AAATAAACAT ATTTTTTTTA CAAAAATAAC TTCTGAATTT ATCAGTGTTT TGCCGTTAAA
1561 AATATTCCTC TATAGTAAAT TATTTATTGG AAGATGACTT TTTTAAAGCT GCCGTTTGCC
1621 TTGGCTTGGT TTCATACACT GATTTATTTT TCTATGCCAG GCAGTAGAGT CTCTCTGCCT
1681 CTGAGGAGCA GGCTACCCGC ATCCCACTCA GCCCCTCCCT ACCCCTCAAG ATTTGATGAA
1741 AATTCCAACC ATGAGGATGG GTGCATCGGG GAAGGGTGAG AAGGAGAGCC TGCCTGCTCA
1801 GGGATCCAGG CTCGTAGAGT CACTCCCTGC CCGTCTCCCA GAGATGCTTC ACCAGCACCT
1861 GCCTCTGAGA CCTCGCTCTC TGTTCCAGCA ACCCTGGTTG GGGGGTCAGA CTTGATACAC
1921 TTTCAGGTTG GGAGTGGACC CACCCCAGGG CCTGCTGAGG ACAGAGCAGC CAGGCCGTCC
1981 TGGCTCACTT TGCAGTTGGC ACTGGGTTGG GGAGGAAGAG AGCTGATGAG TGTGGCTTCC
2041 CTGAGCTGGG GTTTCCCTGC TTGTCCAGTT GTGAGCTGTC CTCGGTGTTA CCGAGGCTGT
2101 GCCTAGAGAG TGGAGATTTT TGATGAAAGG TGTGCTCGCT CTCTGCGTTC TATCTTCTCT
2161 CTCCTCCTTG TTCCTGCAAA CCACAAGATA AAGGTAGTGG TGTGTCTCGA CCCCATCAGC
2221 CTCTCACCCA CTCCCAGACA CACACAAGTC CTCAAAAGTT TCAGCTCCGT GTGTGAGATG
2281 TGCAGGTTTT TTCTAGGGGG TAGGGGGAGA CTAAAATCGA ATATAACTTA AAATGAAAGT
2341 ATACTTTTTA TAATTTTTCT TTTTAAAACT TGGTGAAATT ATTTCAGATA CATATTTTAG
2401 TGTCAAGGCA GATTAGTTAT TTAGCCACCA AAAAAAAGTA TTGTGTACAA TTTGGGGCCT
2461 CAAATTTGAC TCTGCCTCAA AAAAAAGAAA TATATCCTAT GCAGAGTTAC AGTCACAAAG
2521 TTGTGTATTT TATGTTACAA TAAAGCCTTC CTCTGAAGGG ATGGTATTGA
```

Appendix IId. The 3'UTR sequence of *STAT5B* inserted into pmiR-Report Luciferase plasmid.